WITTSTEIN, MATTHEW W., Ph. D. Characteristics And Coupling Of Cardiac And Locomotor Rhythms During Treadmill Walking Tasks (2016).
Directed by Dr. Christopher K. Rhea. 141 pp.

Studying the variability of physiological subsystems (e.g., cardiac and locomotor control systems) has been insightful in understanding how functional and dysfunctional patterns emerge within their behaviors. The coupling of these subsystems (termed cardiolocomotor coupling) is believed to be important to maintain healthy functioning in the diverse conditions in which individuals must operate. Aging and pathology result in alterations to both the patterns of individual systems, as well as to how those systems couple to each other. By examining cardiac and locomotor rhythms concurrently during treadmill walking, it is possible to ascertain how these two rhythms relate to each other in different populations (i.e., younger and older adults) and with varying task constraints (i.e., a gait synchronization task or fast walking task). The purpose of this research was to simultaneously document the characteristics of cardiac and gait rhythms in younger (18-35 yrs) and older (63-80 yrs) healthy adults while walking and to establish the extent to which changes in these systems are coupled when gait is constrained. This study consisted of two repeated-measures experiments that participants completed on two separate days. Both experiments consisted of three 15-minute phases. During the first (baseline) and third (retention) phases of both experiments, participants walked with no cues or specific instructions at their preferred walking speed. During the second phase, participants were asked to synchronize their step falls to the timing of a visual cue (experiment 1) or to walk at 125% of their preferred walking speed (experiment 2). Fifty-one healthy adults (26 older, 67.67±4.70 yrs, 1.72±0.09 m, 70.13±14.30 kg; 25 younger, 24.57±4.29 yrs, 1.76±0.09 m, 73.34±15.35 kg) participated in this study. Participants' cardiac rhythms (R-R interval time series) and locomotor rhythms (stride interval, step

width, and step length time series) were measured while walking on a treadmill. Characteristics of variability in cardiac and locomotor rhythms and the coupling between cardiac and gait rhythms were measured. Results revealed that younger and older healthy adults alter gait patterns similarly when presented with a gait synchronization or fast walking task and that these tasks also alter cardiac patterns. Likewise, both groups exhibited enhanced cardiolocomotor coupling when tasked with a step timing constraint or increased speed during treadmill walking. Combined, these findings suggest that walking tasks likely alter both locomotor and cardiac dynamics and the coupling of physiological subsystems could be insightful in understanding the diverse effects aging and pathology have on individuals.

CHARACTERISTICS AND COUPLING OF CARDIAC AND LOCOMOTOR RHYTHMS DURING TREADMILL WALKING TASKS

by

Matthew W. Wittstein

A Dissertation Submitted to
the Faculty of The Graduate School at
The University of North Carolina at Greensboro
in Partial Fulfillment
of the Requirements for the Degree
Doctor of Philosophy

Greensboro
2016

Approved by

_____
Committee Co-Chair

_____
Committee Co-Chair

APPROVAL PAGE

This dissertation written by Matthew W. Wittstein has been approved by the following committee of the Faculty of The Graduate School at The University of North Carolina at Greensboro.

Committee Co-Chair_____

_____

Committee Members_____

_____

_____

_____
Date of Acceptance by Committee

_____
Date of Final Oral Examination

TABLE OF CONTENTS

LIST OF TABLES

LIST OF FIGURES

CHAPTER I

INTRODUCTION

Statement of Problem

Physiology is a branch of biology that examines the function of organisms and their parts. While there are many parts of a physiological system, cardiac behavior and motor behavior are two of the most commonly assessed components. Research on the behavior of these two subsystems has led to advancements in knowledge about how healthy behavior emerges, as well as what occurs when aging or pathology affects one or both subsystems. Specifically, the study of the variability in patterns of behavior has been particularly useful in understanding a subsystem's functional ability (Goldberger, Peng, & Lipsitz, 2002; Stergiou & Decker, 2011).

Variability of cardiac and gait patterns, individually, is indicative of the quality of function of the underlying control systems (Berntson et al., 1997; Davids, Bennett, & Newell, 2006; Kleiger, Miller, Bigger Jr, & Moss, 1987; Winter, 1991). These systems have been well studied on their own, but less often examined together. Structural and functional connections between the cardiac and motor systems innately link these two fundamental physiological subsystems. As individuals age or experience pathology, several changes occur within and between physiological subsystems. Thus, by examining the individual and shared patterns of variability of cardiac and motor behavior, we will better understand fundamentally how physiological systems work together to form

functional (or sometimes dysfunctional) behaviors, provide new insight for the assessment of dynamical diseases and aging that affect multiple physiological systems, and provide additional information to help guide rehabilitation and treatment associated with dysfunction.

The electrocardiogram (ECG) is among the most studied biological signals. Through years of research, it has become accepted that cardiac behavior does not follow a perfectly repetitive rhythm. Instead, variability in heart rate patterns is an integral part of normal cardiac function (Acharya, Joseph, Kannathal, Lim, & Suri, 2006). Through this understanding, the field of Heart Rate Variability (HRV) developed and provided several new insights into the characteristics of normal and abnormal cardiac rhythms. Not only are normal cardiac rhythms variable, but they also exhibit fractal characteristics. That is, the fluctuations of heart beat intervals exhibit similar patterns whether they are observed on a large time scale (several hundred beats) or a small time scale (tens of beats). Fractal patterns can appear highly complex, however the patterns are not merely random, but contain a level of determinism (albeit, often nonlinear). Fractal patterns can be quantified using numerous metrics that essentially provide information as to a signal's complexity. Detrended fluctuation analysis (DFA), sample entropy (SE), and recurrence quantification analysis (RQA) are among the more prominent methods to assess the complexity of physiological signals with fractal patterns (e.g., cardiac and gait rhythms). Interestingly, aging and pathology have been associated with a change in complexity – often a loss – that is demonstrated by decreased DFA scaling exponent alpha (DFA α),

decreased SE, and changes in the metrics derived from RQA. These metrics were first used to study HRV, but have now been applied to study other physiological subsystems.

As HRV became more commonplace and insightful into cardiac rhythms, researchers began to extend this variability framework to the study of human movement. Similar to cardiac behavior, healthy gait rhythms exhibit inherent variability. The temporal (stride time interval) and spatial (step length and step width) kinematics of gait are variable and exhibit fractal characteristics. Thus, algorithms used to assess HRV became equally useful in studying the control of human gait. Some have contended that variability in gait patterns is a functional component related to the adaptability or flexibility of the motor system (Hausdorff, 2007; Rhea & Kiefer, 2014; Stergiou & Decker, 2011). Logically, variability would afford the ability to make small (or large) adjustments when presented with an obstacle, perturbation, or alteration in the task or environment. On the other hand, gait patterns locked into a set rhythm may be less able to handle more complex tasks such as climbing stairs or recovering from catching a toe on the curb. Changes in the magnitude and structure of variability of gait rhythms, like cardiac rhythms, are also indicative of dysfunction in the underlying control networks (Brach, Berlin, VanSwearingen, Newman, & Studenski, 2005; Brach, Studenski, Perera, VanSwearingen, & Newman, 2008; Gabell & Nayak, 1984; Hausdorff, 2005). Specifically, reduced standard deviation (SD) or coefficient of variation (CV) of stride time and step width have been associated with higher risk of falls (Hausdorff, Rios, & Edelberg, 2001; Hausdorff, 2007). Similarly, a change in complexity appears to be indicative of the motor system losing fine-tune control (decreased complexity) or

becoming overly constrained and rigid (increased complexity). Therefore, it has been proposed that there are optimal levels of both magnitude and structure of variability within and between gait cycles (Stergiou & Decker, 2011).

While cardiac and gait function have been widely examined independently, less attention has been focused on understanding the coupling of these interconnected subsystems. Following the path and role of blood through the cardiovascular system, it is easy to see that cardiac function affects the transport of oxygen and nutrients to muscles for motion. Likewise, movement facilitates the return of blood to the heart and therefore may influence cardiac patterns.

It has been contended that cardiolocomotor synchronization may be a more metabolically efficient during exercise (Phillips & Jin, 2013). However, the need for coupling, or improved efficiency, could be a due to either task goals (i.e., performance improvements) or health quality (i.e., aging or pathology). Thus, coupling may be a marker of improved efficiency or of a decline in health. We would expect, therefore, that aging and disease would increase the coupling of physiological subsystems to allow them to operate more efficiency. From an adaptability perspective, however, this may make those subsystems less robust to perturbations created by the environment or task. Thus, examining the coupling of physiological subsystems will provide new insight into both physiological efficiency and the processes associated with aging and pathology.

Novak, Hu, Vyas, & Lipsitz (2007) observed greater cardiolocomotor coupling in elderly individuals relative to younger individuals during treadmill walking. Specifically, cardiac beat-to-beat intervals were positively associated with step intervals and

normalized foot pressure. Thus, muscle contractures may serve as a rhythmic pump returning venous blood to the heart and act as a possible mechanism for this coupling phenomenon (Novak et al., 2007). Cardiolocomotor coupling has also been observed during bicycling, a task which does not involve impact events or significant changes in vertical acceleration (Kirby, Nugent, Marlow, MacLeod, & Marble, 1989). Therefore, muscle contracture, as opposed to heel impact or vertical acceleration of the heart, may play a larger role in this coupling behavior. Cardiolocomotor synchronization has been observed both spontaneously and voluntarily; both cases resulting in a dissociation of both cardiorespiratory and respirolocomotor coupling (Niizeki, Kawahara, & Miyamoto, 1993). Combined, coupling may be a result of two independent constraints – changes in physiological demands, such as during exercise, or due to processes specific to aging or pathology.

Individual characteristics of cardiac and motor patterns, as well as how those patterns couple with each other provide information about the extent to which physiological function is healthy and normal. Thus, the purpose of this dissertation is to examine the variability characteristics of the cardiac and gait rhythms individually and as they relate to each other. Younger and older healthy adults will participate in this study to allow observation of effects relating to normal aging processes. By specifying constraints in a gait task, it is possible to observe the concurrent changes in cardiac and motor patterns, and assess the relationship of the output of these two physiological subsystems. The characteristics of cardiac rhythms, gait rhythms, and cardiolocomotor coupling will be quantified in two experimental conditions: (1) before, during, and after a gait

synchronization task during treadmill walking at a self-selected pace and (2) before, during, and after walking faster than preferred speed. Both experimental conditions have been previously shown to alter the fractal characteristics in gait of young healthy adults (Jordan, Challis, & Newell, 2007b; Rhea, Kiefer, D'Andrea, Warren, & Aaron, 2014), so this study will extend our previous knowledge by (1) determining if similar changes in gait characteristics are observed in older adults, (2) quantifying cardiac characteristics when gait characteristics are modulated in a specific manner in both age groups, and (3) characterizing the coupling between the cardiac and motor systems during these physically challenging tasks in both age groups.

Objective and Hypothesis

The objective is to simultaneously document the characteristics of cardiac and gait rhythms during walking and to establish the extent to which changes in these systems are coupled when the gait is constrained via (1) a gait synchronization task or (2) walking faster than preferred speed. A necessary step to accomplish this will be to test and expand on a technique used to quantify coupling specifically for cardiac and locomotor signals.

Hypothesis 1: As a group, young healthy adults will exhibit different variability characteristics of gait rhythms compared to older adults. Specifically, we hypothesize that the younger group will have greater mean, smaller SD and CV, greater DFA α, and greater SE of stride time, step length, and step width time series. We expect these predictions to persist through each phase of both experiments.

Hypothesis 2: As a group, young healthy adults will exhibit different variability characteristics of cardiac rhythms compared to older adults. Specifically, we hypothesize

that the younger group will have greater mean, greater SD and CV, greater DFA α, and greater SE of R-R intervals. We expect these predictions to persist through each phase of both experiments.

Hypothesis 3: We hypothesize that cardiolocomotor coupling during the pre-test phase will be similar between the younger and older groups. When gait is constrained via the gait synchronization task or increased walking speed (experimental phase), we predict the older group will demonstrate a larger increase in the coupling index. During the post-test phase, we predict the younger group will return to pre-test phase values of the coupling index, while the older group will exhibit residual effects of the experimental phase.

Limitations and Assumptions

1. The results from this dissertation will be unable to be generalized to populations other than younger and older healthy adults, as will be examined in the study.
2. All participants will attenuate to the task (gait synchronization or 125% of preferred walking speed) to the best of their ability throughout the entire experimental phase.
3. The sampling frequency of 100 Hz for the motion capture system (Qualisys AB, Göteborg, Sweden) is adequate to accurately track and calculate the kinematics of lower limb body segments during walking.
4. The sampling frequency of 1000 Hz for the electrocardiogram (Biopac Systems, Inc., Goleta, CA, USA) is adequate to accurately observe cardiac signals and identify timing of R-peaks.

5. This work will not account for all possible pre-existing pathologies of the cardiac or motor subsystems, especially if not yet diagnosed by a physician.
6. Walking on a treadmill may be different than overground walking, which may include variable surface conditions in addition to the inherent variability of human gait.
7. Participants will be able to select a preferred walking speed similar to that of overground walking.

Delimitations

1. Kinematic measurements will be made for both legs. However, variability measures will only calculated for the right limb. In cases where the right limb is unable to be used, such as marker drop-out, the left limb will be used.
2. Only healthy adults, either 18-35 or 63-80 years of age will participate in this study.
3. Events will be automatically identified. False-positives and false-negatives will be removed or manually replaced, respectively, as appropriate.

Operational Definitions

Healthy: No diagnosis of cardiac, neuromuscular, or movement dysfunction; no acute injury or illness that would prevent participants from exhibiting normal cardiac or movement behaviors; self-reported ability to walk for 45 consecutive minutes on a treadmill at a self-selected pace; normal or corrected to normal vision.

Coupling: Concurrent changes in the behavioral state of two separate physiological signals. In this research, the signals being examined are cardiac R-R interval and stride

interval time series. Using ordered recurrence plot analysis, the coupling index quantifies the extent to which these two signals are coupled.

Variability: Variability is defined here to refer to both linear and nonlinear assessments of signal distributions, fluctuations, and patterns. The SD and CV of a time series will be used to describe the magnitude of variability. The structure of variability will be measured using DFA αand SE. RQA will be used to quantify the coupling strength between the structure of variability in cardiac and gait behavior.

Time series: A time series consists of a collection of events or measurements in the order in which they occurred.

Young: Between 18 and 35 years old.

Older: Between 63 and 80 years old.

Gait synchronization task: Walking on a treadmill while matching step timing with the timing of a visual cue – in this case blinking left and right footprints.

Preferred walking speed: Self-selected pace on the treadmill described as a walk with a dog or through the park. A detailed description of this selection process is described in the Chapter 3.

Variables

Independent Variables

Sex – Sex will be recorded for each participant.

Age (Group) – Age will be calculated in years from the participant's birthdate to the date of starting participation.

Resting HRV – 8-minutes of ECG will be recorded during sitting at the beginning of each testing session. HRV characteristics (mean, SD, DFA α, and SE) will be calculated from the beat-to-beat time series.

Blood pressure – Systolic and diastolic blood pressure (mmHg) will be recorded following 8-minutes of sitting at the beginning of each testing session.

Preferred walking speed – Preferred walking speed will be found for each participant on their first day of participation using an iterative process in which the participant begins very slow or very quickly on the treadmill and informs the researchers to speed up or slow down the treadmill, respectively, until they are at a comfortable walking pace similar to walking through a park. The process will be repeated until consecutive attempts are within 0.2 m/s. The last two speeds selected by the participant will be averaged and used as the preferred walking speed for the rest of the study.

Dependent Variables

μ_{RR}, μ_{ST}, μ_{SW}, μ_{SL}– The average heart beat interval (**μ_{RR}**), average stride interval (**μ_{ST}**), average step width (**μ_{SW}**), and average step length (**μ_{SL}**) will be calculated from each signal's time series as:

$$\mu = [\sum_{i=1 \rightarrow N}(x_i])]/N,$$

the sum of each datum of the time series, divided by the total number of observations.

σ_{RR}, σ_{ST}, σ_{SW}, σ_{SL} – The standard deviation will be calculated from each time series as:

$$\sigma = \sqrt{\{[\sum_{i=1 \rightarrow N}(x_i - \mu)^2]/N\}}$$

where x_i is each value in the time series, μ is the mean of the appropriate time series, and N is the total number of observations in the time series.

α_{RR}, α_{ST}, α_{SW}, α_{SL} – Detrended fluctuation analysis scaling exponent alpha will be calculated from each time series using custom written Matlab scripts. The algorithm is discussed in Chapter 2. Values approaching 0.5 are considered to be associated with randomness, and values approaching or exceeding 1.0 are associated with more scale invariant long-range correlations (or increased fractality).

SE_{RR}, SE_{ST}, SE_{SW}, SE_{SL} – Sample entropy will be calculated from each time series using custom written Matlab scripts. The algorithm is discussed in Chapter 2. Values approaching 0 are considered to be highly regularly, and values approaching 2.0 are considered to be highly complex.

Coupling index – The coupling index will be calculated from order pattern recurrence plots of the R-R interval and stride interval time series. The algorithm is discussed in Chapter 2. No clear standards are in place for the value of the coupling index, however, they will serve as a metric on a comparative basis. Higher values are associated with stronger coupling between two signals. Theoretically values can range from 0 (no coupling) to 1 (complete coupling), but physiological data have been previously reported on the scale of 10^{-2} (Groth, 2005).

CHAPTER II

REVIEW OF THE LITERATURE

Variability in Human Physiology

Variability of physiological systems is becoming a vastly studied phenomenon. Beat-to-beat variability in cardiac behavior was first formally identified by Reverend Stephen Hales over 250 years ago (Hales, 2000). Not until the invention of the electrocardiogram (ECG), however, did the study of cardiac rhythms evolve into a more quantifiable behavior. Similarly, it has been established for over a century that human gait exhibits variability from stride-to-stride (von Vierordt, 1881). Through these observations, and advances in mathematics and statistics, numerous ways to quantify variability in human physiology have been developed. Herein, the topic of magnitude of variability will be used to refer to the standard deviation (SD) and coefficient of variation (CV), both of which provide a summary statistic of the overall behavior. Alternatively, the manner in which the variability unfolds over time (or space) will be quantified by examining the structure of variability. While there are many metrics available for the assessment of the structure of variability (Bravi, Longtin, & Seely, 2011), this proposal only utilizes the most common and clinically valuable metrics to date, which includes detrended fluctuation analysis (DFA), sample entropy (SE), and recurrence quantification analysis (RQA).

Cardiac Rhythms

The electrocardiogram (ECG) is one of the most studied physiological signals. Cardiac rhythms, similar to gait rhythms, are controlled through a number of mechanisms and could be considered as a dynamical system. The study of heart rate variability (HRV) has become a heavily studied field and informative of the physiological factors controlling cardiac rhythms, especially autonomic activity (Acharya et al., 2006; Camm et al., 1996).

The plethora of measures to quantify variability are discussed in detail by Bravi, Longtin, and Seely (2011). This review highlights that many of these measures originate from the study of heart rate times series. In fact, Jeffrey Hausdorff, a leading researcher who studies the clinical importance of gait dynamics, explains that his foray into gait dynamics stemmed from wanting to understand the relationship between heart rate variability (HRV) and gait dynamics on a beat-to-beat and stride-to-stride basis (Hausdorff, 2007).

HRV refers to the analysis of the beat-to-beat variations in cardiac rhythms. It is believed that HRV is associated with the ability of the cardiac system to adapt to changes in environment, task, or the heart itself. Both linear and nonlinear measures have been employed to study this phenomenon. The prevailing theory is that autonomic neural regulation of the cardiovascular system causes the normal variations observed in cardiac rhythms (Saul, 1990). The sympathetic and parasympathetic nervous systems are able to respond to perturbations and allow healthy heart function to occur in a wide variety of

environments and during changing tasks. The next sections outline some of the most commonly used linear and nonlinear analyses to analyze HRV.

Linear Analyses

Linear analyses of HRV are predominantly in the time and frequency domains. This section provides a summary of the metrics recommended by the Task Force of the European Society of Cardiology and the North American Society of Pacing and Electrophysiology (Camm et al., 1996) to assess HRV clinically. Measurements in the time domain include standard deviation of normal-normal beats (SDNN), HRV triangular index, standard deviation of average normal-normal beats (SDANN), and root mean square of squared differences (RMSSD). SDNN summarizes the overall magnitude of variability within a single recording (typically 24-hours). Similarly, the triangular index is a geometric assessment of the distribution of R-R intervals and represents another overall measure of HRV. SDANN assesses the long-term variability of heart rate by calculating the SD of the means of consecutive 5-minute windows of ECG data. RMSSD takes the root mean square of the differences of consecutive heart beat intervals and quantifies the short-term variability and accounts for the order of heart beats. Linear measures of HRV have been shown to decrease with aging and in association with pathology (Guzzetti, Magatelli, Borroni, & Mezzetti, 2001; Kleiger et al., 1987).

Power spectral density (PSD) analysis has been employed to assess the contributions of specific frequency bands on the cardiac signal. Using a Fast Fourier Transform (FFT), a continuous ECG recording is converted to its frequency components. The power of frequencies are then reported as a histogram with bins that define ultra-low

frequency (ULF) (< .003 Hz), very low frequency (VLF) (.003 - .04 Hz), low frequency (LF) (.04 - .15 Hz), and high frequency (HF) (.15 - .4 Hz) components. ULF measurements are only reliable in long-term recordings (24-hours) because they occur on such a slow scale. Additionally, the ratio of LF to HF components (LF/HF) is often reported. LF and HF are also often expressed as normalized units as the ratio of power to total power minus VLF components. It is believed that vagal activity is primarily responsible for the HF component. The LF component, when expressed as normalized units, is believed to be associated with sympathetic modulations. Finally, the LF/HF ratio measures the balance between sympathetic and vagal modulations. The physiological interpretations of ULF and VLF components are still unclear and warrant continued study (Camm et al., 1996). Table 1 summarizes time and frequency domain measurements of HRV recommended by the Task Force.

Table 1. Linear Measures of Heart Rate Variability in the Time and Frequency Domains. Task Force recommendation of linear metrics to assess heart rate variability in the frequency and time domains. * and † denotes metrics used only for short (5 min) and long (24 h) ECG recordings, respectively. (Adapted from Camm et al., 1996).

Linear measures of Heart Rate Variability in the Time and Frequency Domains		
Metric	Units	Description
Time Domain Measures		
Statistical Measures		
SDNN	ms	Standard deviation of all NN intervals
SDANN	ms	Standard deviation of the averages of NN intervals in all 5-minute segments of the entire recording
RMSSD	ms	The square root of the mean of the sum of the squares of differences between adjacent NN intervals
Geometric Measures		
HRV triangular index		Total number of all NN intervals divided by the height of the histogram of all NN intervals measured on a discrete scale with bins of 7.8125 ms (1/128 seconds)
Frequency Domain Measures		
5-min total power	ms^2	The variance of NN intervals over the temporal segment (≈≤0.4 Hz)*
Total power	ms^2	Variance of all NN intervals (≈≤0.4 Hz)†
ULF	ms^2	Power in the ULF range (≤0.003 Hz)
VLF	ms^2	Power in VLF range (≤0.04 Hz)
LF	ms^2	Power in LF range (0.04-0.15 Hz)
LF norm	nu	LF power in normalized units LF/(total power−VLF)×100
HF	ms^2	Power in HF range (0.15-0.4 Hz)
HF norm	nu	HF power in normalized units HF/(total power−VLF)×100
LF/HF	na	Ratio LF [ms^2]/HF[ms^2]

Nonlinear Analyses

As previously discussed, the advent of nonlinear metrics to assess time series has led to a number of alternative measurements to quantify the rhythms in a cardiac signal. The Task Force recommendations suggest that nonlinear tools are only promising and have not yet led to major breakthroughs in understanding of HRV (Camm et al., 1996). Therefore, they should continue to be studied but are not yet appropriate for clinical assessment. However, more recent research has begun to describe the clinical utility of nonlinear analyses (Manor & Lipsitz, 2013; Schumacher, 2004). The next few paragraphs describe two of the most commonly used nonlinear analyses for physiological signals: (1) detrended fluctuation analysis and (2) sample entropy.

Detrended Fluctuation Analysis

DFA was originally presented by Peng et al. (1994) to assess the long-range correlations in DNA sequences. This work originated from fluctuation analysis and introduced a detrending process to help deal with nonstationary signals. A very clear explanation of the DFA process is described in Peng, Havlin, Stanley, & Goldberger (1995) and is paraphrased below.

The detrended fluctuation analysis process follows these steps: (1) integrate the time series, (2) divide the time series into windows of equal length, *n*, (3) within each box, fit a least-squares linear fit, (4) detrend the integrated time series by subtracting the local trend (least-square linear fit line) from the time series data, and (5) calculate the root mean square fluctuation, $F(n)$, of the integrated and detrended time series (eq. 1).

$$F(n) = \sqrt{\{1/N \cdot \sum_{k=1 \rightarrow N}[y(k)-y_n(k)]^2\}} \text{ (eq. 1)}$$

In eq. 1, *N* and *n* are the total number of data points within each window (*n* is used as a description for the box size, and N for the number of data points, but these values are equal in this case), $y(k)$ is the current data point being evaluated, and $y_n(k)$ is the local trend value for the current data point being evaluated. This process is repeated for several time scales (box sizes), resulting in a relationship between box size (n) and the average fluctuations for that box size $F(n)$. The typical range for box sizes is from 4 data points to ¼ the length of the time series. When plotting the relationship of $F(n)$ and *n* on a double-log plot, a linear relationship indicates self-similar scaling. The slope of this linear relationship is termed DFA scaling exponent alpha (DFA α), and quantifies the scaling characteristic of a time series (Figure 1).

For a completely random, uncorrelated time series, DFA α is equal to 0.5. Values of DFA α larger than 0.5 and less than 1.0 indicate that large fluctuations are more likely to be followed by large fluctuations, and small fluctuations by small. This characteristic is termed persistence. Values of DFA α less than 0.5 are indicative of antipersistence, or large fluctuations being followed by small fluctuations and vice versa.

Figure 1. Illustration of the DFA Process. The stride interval time series is demeaned using the y(k) function (a). Next, the time series is partitioned into a series of box sizes. For visual clarity, a subset of the time series (minutes 7-9) have been zoomed in on and two of the box sizes are shown (b). A trend line is fitted within each box and the residual variability above and below the trend line is calculated using the F_n function. The residual variability within each box size is then plotted on a log-log plot and a least squares line is fit to the data. The slope of the least squares line is the DFA α metric. (Adapted from Rhea & Kiefer, 2014).

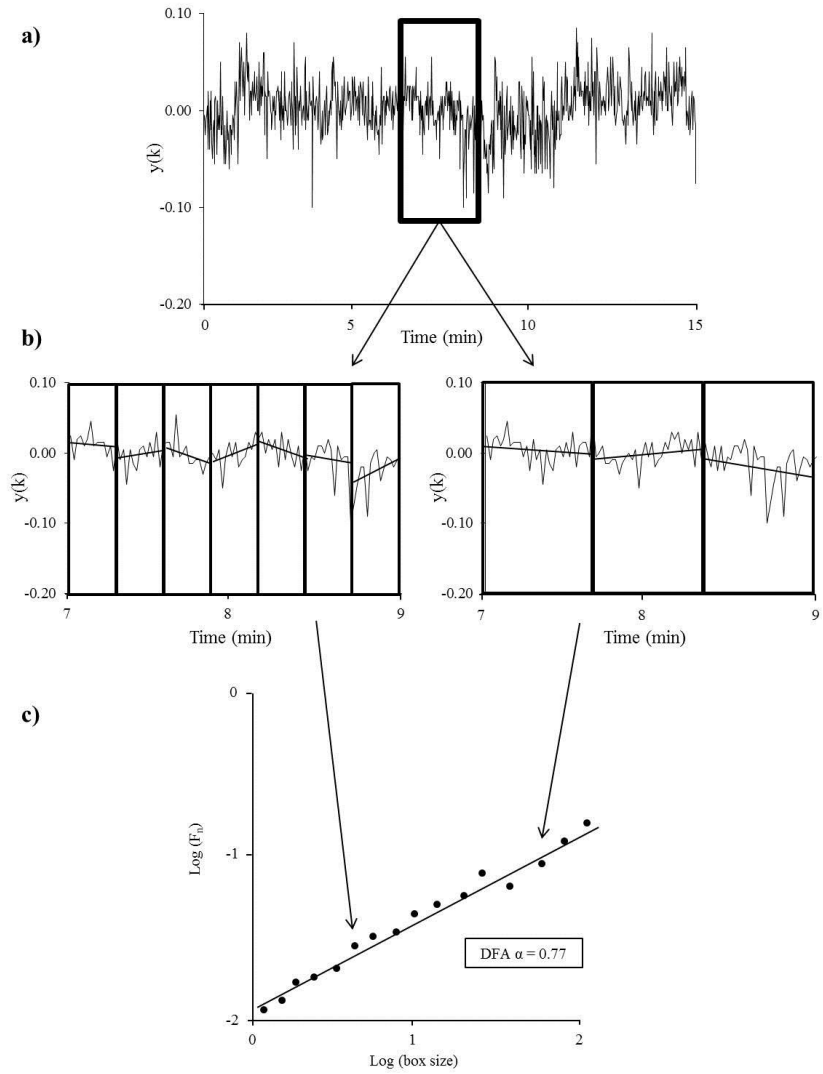

Persistence is typically observed in healthy physiological signals (Diniz et al., 2011; Van Orden, Kloos, & Wallot, 2009) and DFA α values of healthy cardiac beat-to-beat intervals during rest are near 1.0 (Acharya, Lim, & Joseph, 2002). More importantly, DFA α has been identified as a potential indicator of healthy (or unhealthy) neural function for the cardiac system (Acharya et al., 2002). The DFA α can be partitioned into separate values by quantifying different parts of the log-log plot slope line, which is informative about the variability patterns at smaller and larger time scales. Box sizes of 4 to 16 are used to quantify α_1, while box sizes of 16 to 64 are used to calculate α_2.Using the α_1 and α_2 values in a HRV analysis, distinction can be made between normal heart patterns, complete heart block, and ectopic (abnormal) heart rhythms (Acharya et al., 2002; Mourot, 2014). The specific α values have been associated with the relative contribution of sympathetic and vagal control of heart beat dynamics (α_1) and changes in sympathetic modulation (α_2) (Willson, Francis, Wensel, Coats, & Parker, 2002). This also has the potential to provide predictive and prognostic value to clinicians (Goldberger, Amaral, et al., 2002; Manor & Lipsitz, 2013).

Sample Entropy

Sample entropy evolved from information theory and ultimately quantifies the regularity (inverse of complexity) of time series data (Richman & Moorman, 2000). Similar to DFA, this work evolved from a comparable analysis, approximate entropy (ApEn), which was developed by Pincus, Gladstone, & Ehrenkranz (1991) to provide a computationally efficient way to measure the entropy of time-series data. Intuitively, SE quantifies the complexity (high SE values) or regularity (low SE values) of a time series.

Both ApEn and SE use a template matching algorithm to compare the number of matches at template size m to the number of matches at template size $m+1$. ApEn counts a self-match in this process and, therefore, may overestimate the regularity of a time-series. SE was developed to ignore self-matches and provide a more accurate assessment of regularity. The mathematical process to measure sample entropy is paraphrased below from Richman & Moorman (2000).

Calculating sample entropy requires setting the template length (m) and the radius (r) that defines the maximum distance between the template and vector being evaluated to be considered a match. The value r is often expressed in terms of the SD of the time-series to allow for comparison of time-series with different magnitudes of variability.

The calculation of sample entropy follows the following steps: (1) create a set of vectors (x_m) each consisting of all the sets of consecutive points of length m, (2) calculate the scalar distance as defined in eq. 2 between each vector in x_m, (3) count the number of vector pairs (of length m) with a distance (d) less than r (this count of matches will be called B), and (4) repeat steps 1 through 3 using a template of size m+1 to find the number of vector pairs (of length $m+1$) with a distance less than r (this count of matches will be called A).

$$d[x(i),x(j)] = max\{|u)i+k)-u(j+k)|: 0 \leq k \leq m-1\} \quad \text{(eq. 2)}$$

In the preceding steps, self-matches are not counted, and only the first $N - m$ templates are used to ensure that all vectors used are defined. The conditional probabilities of B and A are then calculated as the sum of the conditional probabilities for each vector matching each template of size m and $m+1$, respectively. Finally, the negative natural logarithm of the conditional probability of A divided the conditional probability of B is calculated and defined as SE. Because the conditional probabilities for both A and B are based on the same number of templates, this can be simplified to just use the counts of A and B (eq. 3).

$$SE(m,r,N)=-ln(A/B) \quad \text{(eq. 3)}$$

Therefore, SE(m,r,N) is equal to the negative natural logarithm of total matches of size $m+1$ per matches of size m, accounting for every possible template of size $m+1$ and m.

Setting the parameters m and r is especially important, as they both will greatly influence the number of matches identified. Lake, Richman, Griffin, & Moorman (2002) defined a process to optimize these parameters. This method suggests identifying acceptable values for m based on a priori reasoning, then using this to select an acceptable value of r such that the 95% confidence interval is approximately 10% of the SE estimate.

Several additional measures of entropy exist, but the utility of SE and ApEn in the analysis of physiological time series makes them the most important to discuss. In general, entropy has been used to measure the regularity of several types of systems (e.g., chaotic, mechanical, physiological). Yet, ApEn and SE have become the most

prominently reported entropy metrics for physiological time series. Pincus et al. (1991) originally developed ApEn to study heart beat rhythms, endocrine hormone pulsatility, and respiratory data as a relative measure that had strong potential to identify differences between healthy and clinical groups. The work by Richman & Moorman (2000) and Lake et al. (2002) built upon this and primarily focused on cardiac rhythms.

Cardiac rhythms tend to show higher levels of complexity associated with improved health status. Entropy has been used to quantify the regularity of cardiac rhythms in healthy, elderly, pathological, and neonates, among other populations. Even with healthy aging, entropy tends to decrease as an indicator of a loss of complexity of the cardiac control system (Pikkujämsä et al., 1999). Multiscale entropy has been used to show that healthy cardiac patterns have more complexity than the cardiac behavior in clinical populations with congestive heart failure or atrial fibrillation (Costa, Peng, & Goldberger, 2008; Eduardo Virgilio Silva & Otavio Murta, 2012). Interestingly, these two pathologies come about in different ways – loss of variability and increased regularity (i.e., congestive heart failure) and more random cardiac patterns (i.e., atrial fibrillation). Recently, Mourot (2014) demonstrated the ability of short cardiac time series (only 256 beat-to-beat intervals) and entropy (i.e., ApEn and SE) to distinguish between coronary artery disease and healthy heart function. Use of these metrics with shorter data sets is valuable because it will allow clinicians to collect data during a visit and not rely on other methods, such as 24-hour monitoring for data collection.

In general, it is believed that an appropriate level of entropy – or irregularity – of rhythmic physiological patterns is a marker of the inherent flexibility and adaptability of

the observed physiological system. In contrast, decreased entropy, or regularity, may make a physiological system rigid and unable to adapt to stressors when needed. However, it should be noted that an overly irregular system, such as that observed from atrial fibrillation, will likely also lead to dysfunctional behavior. Thus, there is a "sweet spot" between regular and irregular behavior that allows flexible and adaptive behavior to emerge. These behaviors emerge from, among other things, the neural connectivity of the underlying control system, to which SE has been proposed to be sensitive enough to pick up (Lipsitz, 2002; Pincus, 1994). Specifically, as SE decreases, cardiac output becomes more regular because the underlying control mechanisms become less complex with aging and pathology. Mechanistically, this has been suggested to be related to vagal control of cardiac function (Beckers, Ramaekers, & Aubert, 2001). Additionally, it has been shown consistently that aging and pathology result in a loss of complexity as measured by entropy (i.e., SE, ApEn, and Multiscale SE) in both movement patterns and cardiac patterns.

The preceding sections have detailed the mathematics and utility of detrended fluctuation analysis and sample entropy. While these are only two of the myriad of metrics that can be used to quantify the dynamics of physiological time series (Bravi et al., 2011), they are presented because they quantify unique characteristics of time series and can be plausibly linked to mechanistic explanations and functional outcomes. DFA α appears most likely associated with vagal control of heart rate dynamics, while SE may be associated with the health and connectivity of neural networks and feedback mechanisms within the cardiac control systems. Using the loss of (or change in)

complexity theory as a theoretical basis, aging and pathology lead to a loss of neural connectivity throughout the body. This leads to a loss of complexity in the control mechanisms for both autonomic function (i.e., cardiac patterns) and voluntary movement (i.e., gait rhythms). DFA α allows us to assess the fractal scaling of the output of these systems, while SE provides a measure of complexity. Thus, DFA α and SE act as global indices of physiological function with plausibly different mechanisms. Together, these two metrics have the potential to elucidate characteristics of cardiac control that are not obvious from linear methodologies or even alone.

Loss of (or Change in) 'Complexity' as a Theoretical Construct

Lipsitz and Goldberger (1992) proposed the loss of 'complexity' theory as a plausible explanation of the outcomes related to aging and pathology. They hypothesized that aging is due to "a progressive loss of complexity in the dynamics of all physiological systems" (p. 1808). Lipsitz and Goldberger describe (1) loss or impairment of components and (2) altered coupling between components as the likely mechanisms for loss of physiological complexity. At the entire system level, we can think of this as either dysfunction of an individual subsystem (e.g., cardiac and motor behavior) or changes in how subsystems work together to produce healthy function.

Complexity is a quality of a signal or a behavior that is difficult to define (Grassberger, 2012). Existing somewhere between order and chaos, complexity should not be confused with randomness. Hallmarks of complex biological systems are self-organization, emergence of features not implicit in the systems, and inherent feedback within and between component systems (Diniz et al., 2011; Grassberger, 2012). Thus,

there have been numerous metrics to quantify complexity of physiological time series, and a consensus on definition and quantification has not been reached. Yet, there are several examples of research that demonstrate loss of complexity as a characteristic of aging or pathology. Definitions and measurement of complexity is often varied between researchers. Thus, caution should be taken when assessing these research findings. What has generally been reported, however, is that complexity of heart rate dynamics and locomotor behavior decline with age, independent of pathological changes in physiological function (Manor & Lipsitz, 2013). Some recent research in motor behavior suggests that in certain circumstances complexity could also increase due to aging or pathology (Morrison & Newell, 2012). Differences in tremor signal in different tasks, specifically, highlights the importance of accounting for the effect of task on behavior complexity. In this light, loss of complexity theory should be considered a subset of dynamical disease theory proposed by Glass and Mackey (1988), in which changes in the dynamic characteristics (i.e., either increases or decreases in complexity) are due to changes in the underlying function of the systems observed.

Changes in Cardiovascular Complexity

With the growth of heart rate variability as a field and advances in applying dynamic systems tools to physiology, several recent studies have improved our understanding of complexity in the cardiovascular system. Through the loss of neural connectivity or other mechanisms, aging results in a loss of complexity of the cardiac patterns. Kaplan et al. (1991) identified decreased entropy and dimension of cardiac dynamics (i.e., heart rate time series and continuous blood pressure) in older adults

compared to younger adults during supine paced breathing, supine spontaneous breathing, and 60° tilt spontaneous breathing. Both of these findings are indicative of less complex cardiac dynamics and therefore a loss of complexity in the control mechanisms of heart rate. Similarly, Pikkujämsä et al. (1999) identified a decrease in ApEn and increase in DFA α associated with aging, indicative of loss of complexity of the cardiac control systems. This study examined healthy participants throughout the lifespan (age 1 to 82).

Pathology of the cardiovascular system has also been shown to relate to changes in complexity of heart rate patterns. Interestingly, the connection between entropy and critical care indices (i.e., disease severity and mortality) has recently come to light for several cardiovascular pathologies (Angelini et al., 2007; Costa, Goldberger, & Peng, 2002; Gomez-Garcia, Martinez-Vargas, & Castellanos-Dominguez, 2011; K. K. L. Ho et al., 1997; Y.-L. Ho, Lin, Lin, & Lo, 2011; Norris, Stein, & Morris Jr, 2008). Loss of complexity is more prominent in patients presenting pathological cardiac function and is also associated with reduced survival rates. These findings support the added value of examining nonlinear measures of complexity along with traditional HRV characteristics.

Gait Rhythms

Gait is a fundamental motor skill performed by nearly every human being. It has been studied throughout the years and its quality is often indicative of the health and mobility capacity of a person. Historically, movement variability has been viewed as an indication that the motor system lacks the necessary control to perform a task in a repeatable manner. As such, increases in variability were viewed as indications of a

poorly functioning system, whereas minimizing variability demonstrated the control needed to be a skilled performer (Bryan & Harter, 1897; Thorndike, Lay, & Dean, 1909; Thorndike, 1927).

Traditionally, gait is assessed by examining summary metrics, such as mean stride time, during short bouts of walking. However, it has become widely accepted that the stride times of both healthy and unhealthy adults exhibit fluctuations (Gabell & Nayak, 1984; Hausdorff et al., 1996; West & Griffin, 1998). Variability in human movement is no longer thought of as noise or error, but instead it is considered an intrinsic and deterministic property of the dynamical systems that control movement (Davids, Glazier, Araújo, & Bartlett, 2003; Glazier, Davids, & Bartlett, 2003; Stergiou, Harbourne, & Cavanaugh, 2006). Moreover, studies examining the magnitude (i.e., standard deviation) and structure (i.e., nonlinear assessments) of variability in gait rhythms have identified utility in the variety of metrics used in the assessment of gait (Bravi et al., 2011).

Human gait is a repetitive, cyclic activity that can be characterized in several ways. Often, specific features of a stride cycle (e.g., stance or swing phase time, peak knee flexion angle, gait asymmetry) are used to assess the quality of an individual's movements. Because of the cyclical nature of human gait, summary measures for these features have been developed for young, elderly, as well as some pathological populations and are often used as a comparative basis when assessing an individual's movement quality (Oberg, Karsznia, & Öberg, 1994; Öberg, Karsznia, & Öberg, 1993; Winter, 1991). These normative data have provided clinicians with a simple measurement to characterize different impairments in gait and to determine an appropriate course of

action. Yet, as our fundamental understanding of different motor deficits has continued to grow, new tools have emerged that provide additional insight into the variability present in gait rhythms. The following sections outline the linear and nonlinear analyses commonly used in gait and what has been learned from this research.

Linear Analyses

As previously described, linear measures such as SD and CV measure the magnitude of variability present in a time series. Jordan, Challis, & Newell (2007) identified that increasing walking speed, from 80% to 120% of preferred walking speed incrementally decreased stride time while increasing step length. This study also revealed that CV of both stride interval and step length decrease with increasing gait speed. An increase in the magnitude of variability has been shown to relate to increased fall-risk (Hausdorff et al., 2001). Rosano et al. (2007) observed increases in the SD of step width associated with a "greater burden of subclinical [sic] abnormalities" (p.193). However, the relationship between gait variability and dysfunction has not been completely one-sided. Brach et al. (2005) showed that either too much or too little variability in step width was associated with fall history in elderly adults exhibiting normal healthy gait speeds. In another study, Brach et al. (2008) identified that variability in different characteristics of gait may have different underlying mechanisms. Specifically, central nervous system impairment was associated with increased stance time variability while sensory impairment (i.e., visual or proprioceptive) was associated with increased step width variability. The consensus of research in gait variability is that there is an optimal magnitude of variability, and too much or too little can be detrimental to function or

performance (Stergiou et al., 2006). This optimal range is likely dependent on the task, environment, and individual – a key characteristic of dynamical systems.

Nonlinear Analyses

In addition to quantifying the magnitude of variability, researchers have used nonlinear analyses to quantify the structure of variability, which defines how the variability unfolds over time. The structure of variability allows for the identification of patterns of variability over short and long time scales. Specifically, DFA SE have become popular nonlinear analyses and are well-suited for the study of gait time series.

As discussed previously, DFA quantifies the fractal scaling of a time series, and SE quantifies the degree of irregularity (i.e., complexity) of a time series by using a pattern matching algorithm. DFA and SE have been selected because they quantify the structure of variability and some have argued that they relate to the adaptability or healthy function of physiological systems (Goldberger, 1990; Manor & Lipsitz, 2013; Rhea et al., 2011; Vaillancourt & Newell, 2002). DFA values in physiological systems typically range between 0.5 to 1.0, with the lower numbers indicating more random patterns and the higher number representing more organized patterns. Stride-to-stride intervals are typically around 0.75 for normal healthy gait (Hausdorff et al., 1996). Step width and step length patterns are less published, but some research suggests that these gait characteristics exhibit DFA values closer to 0.5 (Stergiou & Decker, 2011; Wittstein et al., under review).

In walking and running on a treadmill, DFA α has been shown to observe a U-shaped curve, with increasing values of DFA α as speed moves away from a participant's

self-selected pace (Jordan, Challis, & Newell, 2007a; Jordan et al., 2007b). Hausdorff et al. (1997) identified that DFA α in both healthy aging and Huntington's disease patients exhibit lower values (though still persistent) than healthy young and age-matched controls, respectively. Gates & Dingwell (2007) identified no difference between peripheral neuropathy patients and age-matched controls. Hausdorff (2007) suggests that these findings, together, suggest that there may be a specific neural locus responsible for the generation of stride interval fractality. The observation of decreased fractal scaling in Huntington's disease patients suggest that the striatal pathology in the basil ganglia associated with loss of fine motor may be this specific locus. Moreover, other deficits or differences in this region of the brain could explain some of the variation observed across even healthy young adults.

In gait, entropy – in its many forms – has been useful to associate the irregularity of walking patterns with clinical changes in walking. In the flexion-extension time series during walking, ACL deficient knees exhibit a lower entropy than healthy knees (Georgoulis, Moraiti, Ristanis, & Stergiou, 2006). Similarly, OA patients had significantly lower SE values of shank accelerations than age-matched healthy participants (Tochigi, Segal, Vaseenon, & Brown, 2012). Buzzi and Ulrich (2004) demonstrated that sagittal plane accelerations of the thigh, shank, and foot tended to be more regular (lower ApEn) in children with down syndrome compared to healthy controls. For stride interval time series, normal walking speed has been shown to be more complex than fast, slow, or walking paced by a metronome (Costa, Goldberger, & Peng, 2005).

In general, it has been shown that both DFA α and entropy of gait characteristics tend to be different in aging or pathological populations, or when the system is stressed (walking faster or slower than the preferred speed). It is reasonable, then, to assume that a change in these characteristics, even in healthy individuals, is suggestive of changes in the underlying neural control process that maintains gait patterns. For this reason, Stergiou et al. (2006) have suggested an optimal variability hypothesis which applies to both linear and nonlinear measurements of variability. In application, a change in DFA α or entropy could potentially be used to assess the quality with which the motor system is functioning, and whether or not the motor system is able to change its control mechanisms to changing environmental and task constraints.

Changes in Locomotor Complexity

Redundancy in the neural control of movement results in complex patterns of locomotor behavior. While there have been a few studies that relate complexity in gait to ability to overcome physical (Hausdorff, 2007; Jordan, Challis, Cusumano, & Newell, 2009) and cognitive (Grubaugh & Rhea, 2014) stress (such as a trip or dual-tasking, respectively), there have been several studies examining the changes in complexity of gait patterns associated with aging and illness, as well as when participants are asked to alter their walking speed or patterns. Aging has consistently shown a loss of complexity in movement patterns as indicated by lower DFA α (Hausdorff et al., 1997; Scafetta, Marchi, & West, 2009), SE (Tochigi et al., 2012), and ApEn (Buzzi & Ulrich, 2004). Similarly, distinct pathologies with differing mechanisms have also demonstrated evidence of loss of complexity. Herman et al. (2005) demonstrated that fractal scaling

exponent (DFA α) is lower in fallers than non-fallers with higher-level gait disorders (i.e., not due to structural or peripheral neural deficits and without clearly identified pathology). Similarly, the fractal scaling of gait rhythms of individuals with Huntington's disease (Hausdorff et al., 1997) or Parkinson's disease (Frenkel-Toledo et al., 2005) is lower than healthy controls.

While some authors contend that lower fractal scaling actually represents more complexity (Vaillancourt & Newell, 2002), it is important to note that complexity and randomness are not synonymous. A completely random gait pattern lacks any predictability and therefore it is not complex. A healthy gait pattern exhibits some low level of predictability, but its complexity is more colloquially defined as the ease with which we can accurately model the gait behavior. Thus, it is important to consider the context of the research and metrics before assessing the directionality of the relationship between a metric and complexity.

As has been discussed, loss of complexity theory is a framework within which to study aging and pathological processes. Changes in both structure (e.g., loss of neurons) and function (e.g., reduced muscle strength) of the physiological system and it subsystems, as well as alterations in how components couple with each other, provide a plausible explanation for loss of complexity theory. Thus, examining the complexity of the cardiac and locomotor subsystems individually, as well as the coupling between these subsystems, advances our understanding of how physiological function emerges. These findings may then lead to improved assessments of health and provide health-relevant dynamical characteristics to drive the development of new rehabilitation techniques.

Manor and Lipsitz (2013) reviewed several examples of how complexity has been used as a sensitive measure to test the effectiveness of interventions for both cardiac dynamics and postural control. Hausdorff (2007) has also demonstrated the utility of gait dynamics to understand quality of the motor control system and the relationship of gait variability to health and injury. These papers outline the potential of using complexity to understand the alterations in gait and cardiac function through normal aging and pathological mechanisms.

Physiological Coupling

The coupling of physiological subsystems is not a new topic of research. Yet, breakthroughs in understanding the mechanisms and effects of coupling have been few and far between. As reviewed above, research in physiological variability has primarily been observed in one subsystem at a time. There are competing theories as to whether coupling of physiological subsystems, broadly defined, is beneficial or detrimental to healthy human functioning. Logically, it makes sense that a highly synchronized and coupled system could have the benefit of more efficient function, such as the synchronized rowing of an elite crew team. In this light, Godin & Buchman (1996) suggest that the decoupling of organ function may signal the onset of multiple organ dysfunction syndrome. Similarly, cardiolocomotor coupling may be more energetically efficient (Niizeki & Saitoh, 2014). However, contrary to this hypothesis, several researchers contend that coupling is a sign of loss of complexity, simplifying the control mechanisms for physiological function, and therefore a potential marker of dysfunction (Kyriazis, 2003; Novak et al., 2007).

It is plausible that both of these postulates in regard to the role of physiological coupling are accurate. That is, a healthy physiological system may consist of a series of subsystems (e.g., cardiac and motor) that have the ability to couple and uncouple based on the particular task demands. For example, when the task becomes physically challenging, the subsystems may couple to conserve energy. However, there may also be situations when it is either energetically or functionally more efficient to have each subsystem work independently. For example, it is desirable for the heart to keep beating in the absence of gait (i.e., sitting in a chair). That adaptive ability of the physiological system to transition the mode of subsystem synchronization best utilized for a particular task is a hallmark of a healthy system. Alternatively, aging and pathology have consequences that affect the capacity of several physiological subsystems, which may preclude the ability to couple or uncouple as freely as a healthy system. Thus, these systems may lock into a mode of synchronization or independency as a way to maintain some, yet not optimally adaptive, behavior. Therefore, it is important to understand how physiological subsystems interact to more confidently identify when physiological healthy has been compromised.

To begin to understand how the cardiac and locomotor systems are linked, we conducted a pilot study examining the dynamics of both systems during a gait synchronization task in young, healthy adults (Wittstein & Rhea, 2015). The task consisted of synchronizing the gait cycle to a set of flashing footprints on a projection screen in front of the treadmill. In this population, the cardiac and locomotor dynamics exhibited independent changes through each phase (pre-test, exp, and post-test) of the

study. The mean R-R interval increased during the synchronization phase (likely due to the faster stride times requiring higher cardiac output), while no significant differences were exhibited by CV and DFA α across phases. Meanwhile, the locomotor dynamics exhibited changes associated with the specific phase of the experiment. In a loosely coupled system, as we would expect in young healthy adults, the cardiac function and motor tasks can function nearly independently. However, in an older population, we would expect to see similar shifts in dynamics across phases in these two systems because they are likely more strongly coupled. Data from our pilot study are presented in Figure 2, as well as what we hypothesize to observe in an older population that likely have increased coupling of their cardiac and locomotor systems.

Figure 2. Pilot Data and Hypothetical Data for Cardiac and Stride Time Rhythms. Mean, CV, and DFA α (top to bottom) of stride time (blue solid) and R-R interval (red solid). Hypothesized data is also presented (dashed lines) to demonstrate how increased cardiolocomotor coupling may potentially be observed through individual physiological subsystems.

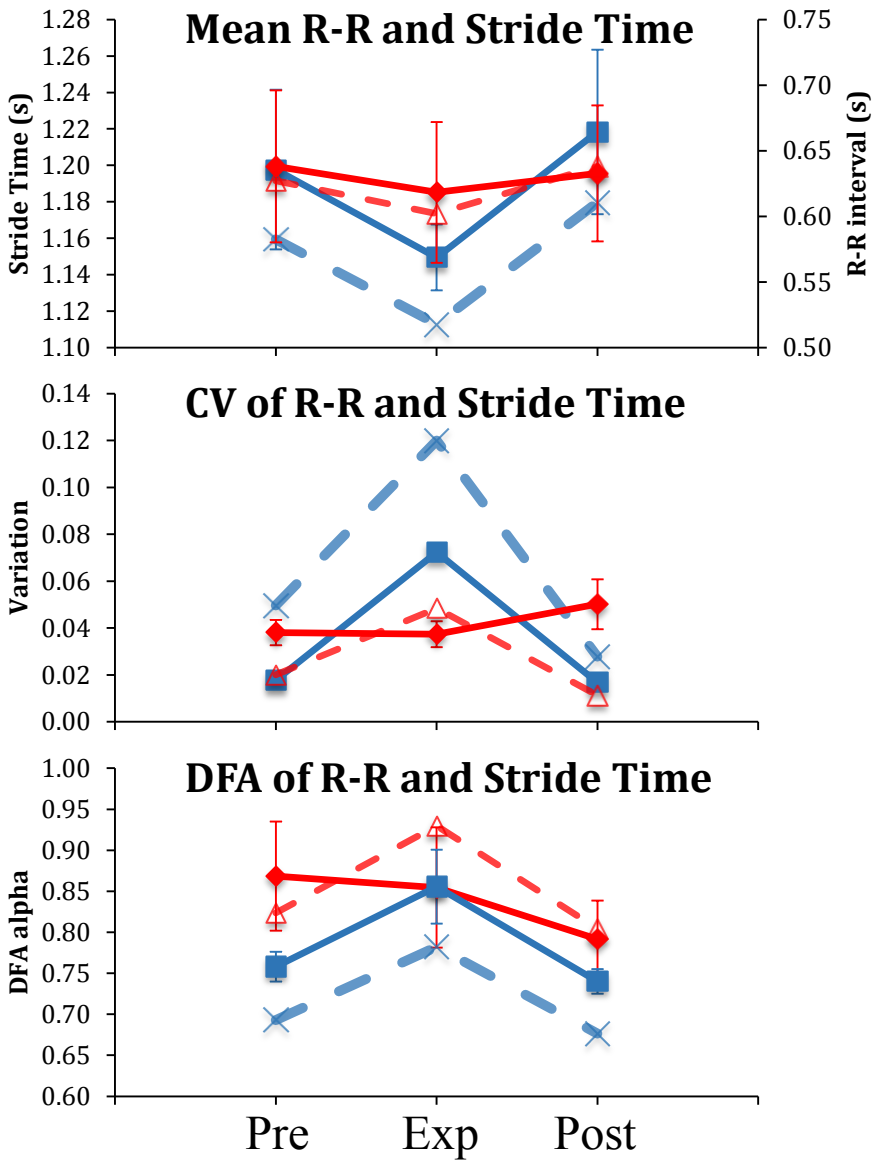

There have been several practical and theoretical challenges in directly quantifying the coupling characteristic of mathematical systems and physiological systems. Thus, coupling has been defined and measured in several ways, often dependent on the field in which it is being observed. From a mechanical systems perspective, coupling is most often defined as a physical link between two mechanical bodies. Thus, the two bodies' motions must be linked. If this link is rigid, the two bodies will be perfectly coupled. If the link consists of multiple segments, springs, or is otherwise not rigid, the relationship between the two bodies becomes more complex and potentially nonlinear. In computer programming, coupling refers to the extent to which one routine relies on another. For example, if one program requires information from another program to operate, those systems are coupled. We can apply these definitions to physiological subsystems because they share neural connections, physical connections, and resources. Additionally, the ultimate goal of each subsystem is to allow the individual to function (i.e., maintain life). By measuring the coupling, or the extent of synchronization, of two physiological subsystems we are able to identify how closely those subsystems can affect each other.

Given these definitions, researchers have used varying mathematical methods to define and describe coupling of physiological subsystems. Kreuz et al. (2007) discuss several different types of synchronization and used coupled mathematical models to test and compare six measurements of synchronization. Their ultimate findings were that measurements of synchronization should be chosen "pragmatically as the measure which most reliably yields valuable information [sic] in test applications" (p. 36). This

demonstrates the challenges associated with quantifying coupling or synchronization of complex systems (e.g., physiological subsystems).

Numerous methodologies have been employed to describe and quantify the coupling of two time series. Rosenberg and colleagues (1989) demonstrated the value of using both time- and frequency-domain (i.e. Fourier transformations) techniques in identifying coupling between neural pathways that activate the same muscle spindle. In this method, it was possible to remove the influence of one input by filtering specific frequency regions of a signal and ultimately demonstrated that the response changes of the muscle spindles were additive of its inputs (two separate static fusimotor axons). However, the Fourier approach is limited because it does not account for the temporal localization of events. The use of phase angles (or relationships) has also been used to quantify the coupling of time series (Mrowka, Cimponeriu, Patzak, & Rosenblum, 2003; Niizeki & Saitoh, 2014). The advantage to this technique is that it potentially allows for some description of directionality of coupling (i.e., the phase angle could be positive or negative between two signals). However, this method examines the relative timing of events and does not account for the impact that past events may have on future events.

Information theory has provided many tools and into the measurement of dynamic characteristics of time series, including the coupling between time series (Grassberger, 1991; Richman & Moorman, 2000; Schreiber, 2000; Schulz et al., 2013; Xie, Zheng, Guo, & Chen, 2010). This technique is the basis of the aforementioned SE and ApEn, along with Cross-SE and Cross-ApEn, with the latter two quantifying the coupling between two time series. The basic foundation of this method is to measure how much

information is contained within a series of data (Shannon, 1948) can be applied to examine the shared information (or unique information) between two separate time series (Richman & Moorman, 2000). Using a template matching technique, it is possible to examine if patterns repeat within a time series or between two separate time series. In practice, this has been used to measure the asynchrony of various types of time series, including economic data (Lin, Shang, & Zhong, 2014; Liu, Qian, & Lu, 2010) and physiological time series (Fabris, De Colle, & Sparacino, 2013; Richman & Moorman, 2000; T. Zhang, Yang, & Coote, 2007). An advantage of using entropy measures is that it is used across several fields and is easily modifiable to varying data types, having been widely used for physiological time series, among others. On the other hand, the interpretation of entropy measures is still debated and entropy may be highly sensitive to signal infidelity (i.e., spikes in data) (Aboy, Cuesta-Frau, Austin, & Micó-Tormos, 2007; Molina-Picó et al., 2011).

Lastly, linear techniques have been used to examine the coupling between physiological time series. Kirby et al. (1989) defined cardiolocomotor coupling as present when the heart and step rates were within 1% of each other. In this example, synchronization is when the mean values of two systems' characteristics are very near each other. Niizeki, Kawahara, & Miyamoto, (1993), on the other hand, defined coupling to be present when the SD of the phase difference between the onset of heartbeats and gait signals was below 0.1 (or 10% of the phase range). This suggests that synchronization occurs when the relative timing of events in each system becomes very consistent. Novak, Hu, Vyas, & Lipsitz (2007) used the coefficients of correlation (r) and

determination (R^2) to evaluate the coupling of heartbeat and stepping patterns. Because R-R intervals and step intervals do not occur simultaneously, the authors constructed continuous time series from the interval data to enable them to calculate r and R^2. It was unclear what method was used to construct the continuous time series. These are just three different methods that researchers have used to quantify the coupling of cardiac and locomotor systems. However, advancement has been made in recent decades to create methods that quantify the coupling within a dynamically changing system. The origin and development of those methods is outlined below.

Many techniques have been used to measure time series coupling and dynamics, each with their own strengths and weaknesses. Linear techniques such as quantifying the mean or variation of data are extremely informative when comparing to normative data, and is practical for use in clinically settings. However, physiological signals are nonlinear and chaotic, so these methods likely overlook phenomena that present themselves unpredictably or subtly. Fourier techniques provide great insight into the frequency domain characteristics of time series and can indicate directionality between coupled systems. However, this method does not account for when events actually occur. Phase angles or relative phase have been useful in identifying the onset of a coupling relationship, but again, this method is limited because it matches one event to another and does not allow for past events to have influence on future events. Entropy has been another promising measurement for studying the dynamics and coupling of time series. Specifically, it is possible to account for diverse types of data and look at the shared entropy between two signals. Combining entropy measures with recurrence plot analyses

ultimately will provide both a qualitative visualization of coupling as well as quantitative measurements with which to understand the measures the relationship of physiological subsystems. Recurrence plots deal with nonstationarity of data and can be symbolically transformed to account for differences in signal types and are therefore ideal in examining the coupling between cardiac and locomotor behaviors. Given the challenges described with other coupling methods, and the potential value of recurrence plots to examine cardiolocomotor coupling, manuscript 1 of this dissertation focuses on an evaluation of a coupling technique derived from recurrence plots. The general theory behind recurrence plots is described below, followed by description of how they can be used to quantify coupling between two systems.

Recurrence Plots

Beginning with a single time series, such as the stride interval time series, recurrence plots are constructed by marking points in time where values are within a certain radius of each other. However, this is accomplished through a process of embedding the time series in a *d*-dimensional state-space using time lag methods (Takens, 1981). Takens embedding theorem allows the derivation of underlying dynamical system characteristics from a single observable signal. That is, even though the control of the stride interval may require several degrees of freedom, the dynamics of its control behavior can be reconstructed and analyzed using a single observable signal derived from kinematics (e.g., stride interval time series). To reconstruct a phase space, a *d*-dimensional vector representation of a time series $x(i)$ can be created such that each component of $x(i)$ is the corresponding value of the time series at time point i and $i+k\tau$,

where k is all integers from 1 to d-1 and τ is the time lag constant. This process can then be repeated for another time point (j). The N x N matrix (or recurrence plot) can then be constructed by plotting i versus j and making points in which the vector $|x(i) - x(j)|$ (the distance between the points in a d-dimensional phase space) is within a certain radius. An example of the construction of a state-space from continuous knee angle data and a recurrence plot from stride interval data is shown in Figure 3a and 3b, respectively.

Figure 3. Illustration of Time Delay Embedding to Create a Phase Space and a Recurrence Plot. (a) The reconstruction of continuous knee angle time series (left) in two dimensions (center) and three dimensions (right). (b) A stride interval time series (left) and its resulting recurrence plot (right) using an embedding dimension of 5, time delay of 5, radius of 45 and line minimum of 2. (Adapted from Rhea & Kiefer, 2014).

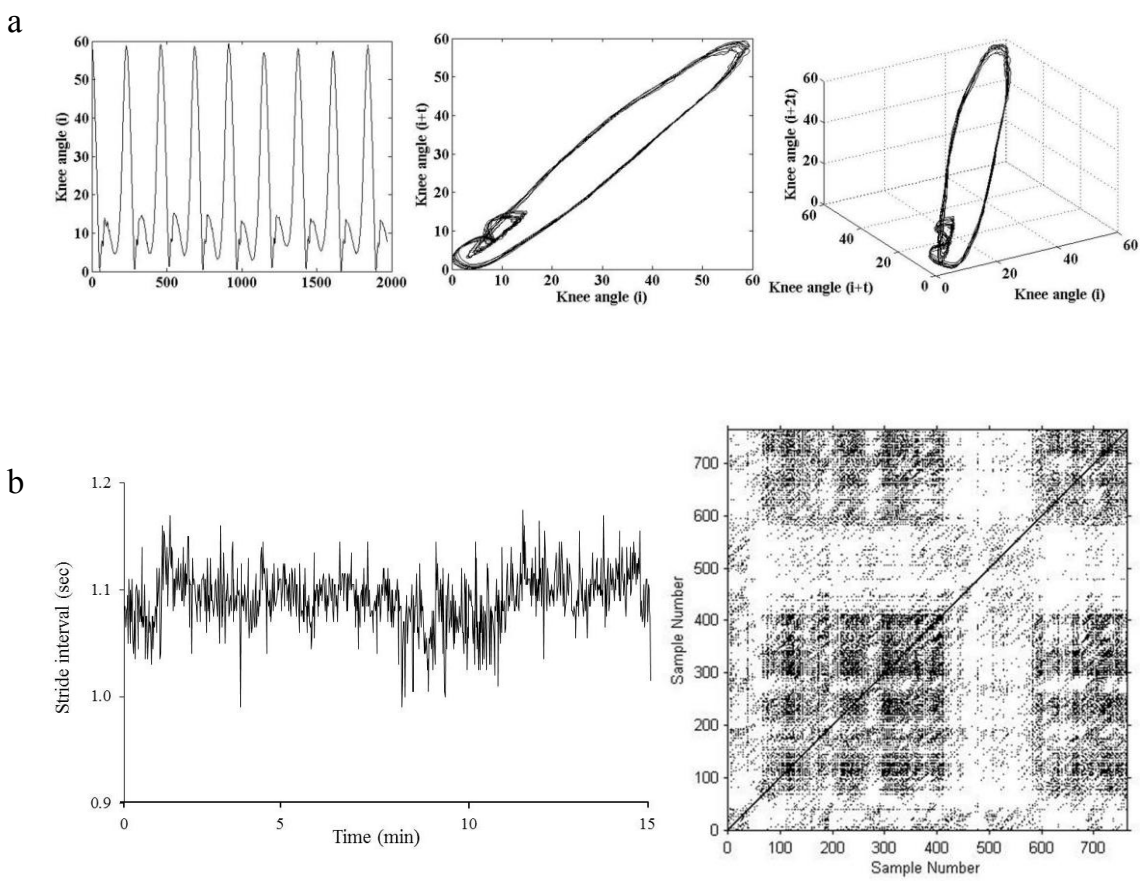

Eckmann, Kamphorst, and Ruelle (1987) first used recurrence plots to qualitatively assess the natural time correlation of a time series. This group original identified characteristics such as typology and texture to distinguish the large-scale and small-scale characteristics, respectively. Sparsely populated recurrence plots [i.e., "uniformly grey" (Eckmann, Kamphorst, & Ruelle, 1987, p. 974)] are indicative of homogenous dynamical systems. Conversely, long diagonal bands equally spaced from the line of identity (i.e., where $i = j$) indicate periodicity of the signal. The density of points as a function of time difference (i.e., the shading near to versus far from the line of identity) illustrates characteristics of drift or convergence of the signal. These qualitative observations of the recurrence plots eventually led to formalized quantitative methods to assess the dynamical characteristics of time series using recurrence plots.

Recurrence Quantification Analysis (RQA)

Webber and Zbilut (1994) developed RQA to quantify recurrence plots. They identified five measurable characteristics of the plots – percent recurrence (%REC), percent determinism (%DET), maximum line length (L_{max}), entropy (ENT), and trend (TND). Marwan et al. (2002) added two additional metrics – percent laminarity (%LAM) and trapping time (TT). %REC is simply the percentage of possible points in the N x N recurrence plot that are within the specified radius. To Eckmann, this would be identified as the darkness of the recurrence plot. %DET is the percentage of recurrent points that form diagonal lines, suggesting that a set of points reoccurred more than once within a time series. Diagonal lines must have a minimum length that is predefined and is often set to two points. L_{max} is the length of the longest diagonal line (excluding the line of identity

where $i = j$). This value is inversely related to the Lyapunov exponent and how chaotic, or unstable, a signal is. Thus, small values of L_{max} are associated with highly chaotic time series and large values with highly regular time series (e.g., a sine wave). ENT is the Shannon information entropy (Shannon, 1948) corresponding to the diagonal lines. It is important to note that ENT from RQA has an inverse relationship with more traditional entropy techniques (ApEn and SE) due to how it is mathematically derived (Rhea et al., 2011). In short, diagonal lines are placed into bins of a histogram based on their length. Individual probabilities for each bin can then be used to calculate the entropy of the signal (eq. 4), where H is the entropy, p is the probability of the bin and n is the total number of bins used.

$$H=\sum_{k=1\rightarrow n} p_i \cdot log(p_i) \quad \text{(eq. 4)}$$

TND can be used to quantify the stationarity of a time series and relates to Eckmann's identification of drift. It is calculated as the slope of the least squares regression of recurrence percentage as a function of distance from the line of identity. In other words, this maps the density of diagonal lines near and far from the center line. Values that deviate away from 0 (either positive or negative) suggest drift is present in the signal. %LAM and TT measure characteristics of vertical structures in the recurrence plots, percentage of points that create vertical structures and the average length of vertical structures, respectively. Vertical structures are indicative of the presence of a laminar state (i.e. transition from one chaotic behavior to another chaotic behavior), while diagonal lines are indicative of the transition between periodic and chaotic states.

RQA has been useful in understanding the dynamic characteristics of physiological signals including electromyograms (Farina, Fattorini, Felici, & Filligoi, 2002; Filligoi & Felici, 1999), cardiac signals (Marwan et al., 2002; Zbilut, Koebbe, Loeb, & Mayer-Kress, 1990), and kinematics of gait and posture (Labini, Meli, Ivanenko, & Tufarelli, 2012; Riley, Balasubramaniam, & Turvey, 1999; Riva, Toebes, Pijnappels, Stagni, & van Dieën, 2013). It is especially strong at detecting changes in the behavioral states of time series data. Specifically, by performing RQA with a sliding window, subtle changes in signal characteristics can be identified by changes in the RQA outcome measures as a function of time. This is of particular interest, because shifts in the behavioral state of a physiological system suggest that it is being stressed in some way and therefore attempting to operate in a more efficient manner. Features extracted from the RQA of R-R interval time series have been recently used to identify health status of hearts. Krishnan et al. (2012) proposed unique recurrence plot characteristics for atrial fibrillation, complete heart block, ischemic/dilated cardiac myopathy, sick sinus syndrome, and normal sinus rhythm. Using statistical models, RQA has the potential to automatically diagnose cardiac diseases. Laminar states associated with the onset of ventricular tachycardia have also been detected using RQA features (Marwan et al., 2002). Additionally, in the study of postural control, RQA has been able to distinguish between the distinct control strategies in aging (Seigle, Ramdani, & Bernard, 2009) and pathological (Schmit et al., 2006) populations, as well as when visual feedback is removed in a young, healthy population (Riley et al., 1999). Combined, these studies

demonstrate the success and potential of RQA in understanding physiological functioning across several different subsystems and observable signals.

Cross Recurrence Analyses

RQA was originally used to examine the dynamic characteristics of a single signal within a dynamical system. However, it is also possible to compare the dynamics of two different signals using a similar methodology. Cross recurrence quantification analysis (cRQA) was derived from recurrence quantification analysis (RQA) in order to study the shared dynamics of two signals. The state-spaces are constructed in the same way as described previously with RQA, except two separate time series are used. Then the N x N matrix can be constructed such that the distance vector $|x(i) - y(j)|$ [where $y(j)$ represents the second signal] will define the dark points of the recurrence plot. Importantly, this method is most appropriate for signals from the same process and ideally the same observable signal, such as comparing two cardiac signals (Marwan, Romano, Thiel, & Kurths, 2007). However, order patterns can be derived from cross recurrence plots and they allow for the assessment of common patterns between different observable signals (e.g., cardiac and gait signals) or of signals with dissimilar amplitudes (e.g., different channels of an EEG) (Groth, 2005). This is accomplished by applying the cross-recurrence plot concept to local ordinal patterns within two time series, disregarding the actual magnitude for each datum. Thus, in the case of identifying coupling between cardiac and locomotor rhythms, order patterns recurrence plots should be employed.

Order patterns are created using a symbolic transformation of a time series. Similar to RQA, a phase space can be reconstructed using time delay embedding of an

appropriate dimension, D. Next, the phase space can then be divided into equal regions such that each region is bounded by the locations within the space where the time series for each delayed embedding is equal to the time series at a different delayed embedding. For example, a three dimensional phase space can be split into six regions defined by the planes in which x(t) is equal to x(t+τ), x(t) is equal to x(t+2τ), or x(t+τ) is equal to x(t+2τ).Thus, for a given D, D! possible order patterns (π_x) will exist for the time series x(t) (Figure 4).

Figure 4. The Six Possible Order Patterns (π_x) of x(t) for Embedding Dimension D=3. Note that in application, when evaluating order patterns, < and ≥ are used to assess the locus of a point in phase space, negating potential equalities. (From Groth, 2005, p. 2).

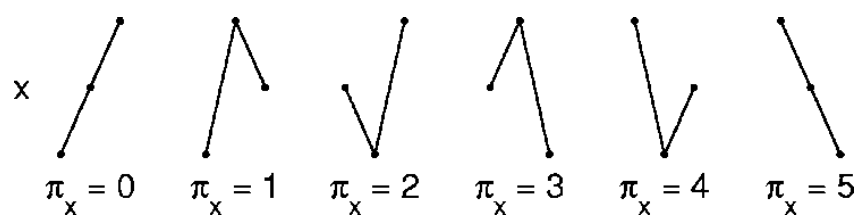

While it is more difficult to visualize a higher dimensional phase space, the mathematical process to identify the order patterns of a time series remains the same.

Once the order patterns for two separate time series have been identified, a recurrence plot can be constructed with points darkened when $\pi_x(t)=\pi_y(t')$. However, it is also possible to express this as a function of t and τ. As it is possible that time series $x(t)$ and $y(t')$ are on differing time scales, t' can be replaced by $t + \tau$. Thus, the order patterns can be visualized horizontally instead of diagonally, allowing easier analysis of longer

time periods. Figure 5 illustrates the order patterns recurrence plots in both forms for two channels of electroencephalography (EEG) data.

Figure 5. EEG Data Depicted as a Traditional Recurrence Plot (left) Using Order Patterns and as a Horizontal Recurrence Plot (right) from the Same Order Patterns. In the horizontal representation, bands represent time lags where similar dynamics were observed by both signals concurrently (and therefore, coupling). The left graph only shows a small time period near seizure onset, whereas the right graph shows a larger time period including periods immediately before, during, and after seizure offset. (Adapted from Groth, 2005).

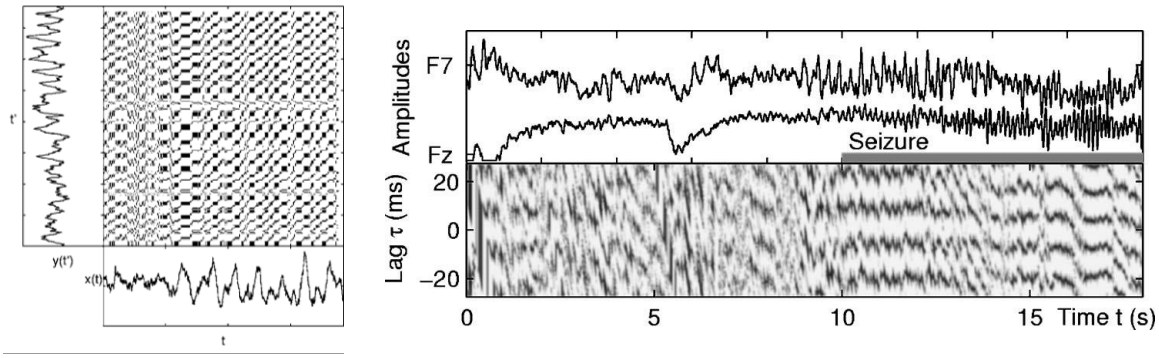

The utility of cRQA to evaluate coupling strength has been demonstrated with physically coupled oscillators (Shockley, Butwill, Zbilut, & Webber, Jr., 2002), the relationship between cognitive load to postural sway characteristics (Pellecchia & Shockley, 2005), interpersonal movement coordination (Riley, Richardson, Shockley, & Ramenzoni, 2011), and respirolocomotor coordination (Hessler, 2010). While it has not been used specifically to examine the relationship between cardiac and locomotor rhythms, the coupling index calculated from order patterns recurrence plots has been robust, and therefore, well-suited for the proposed research. It will be necessary,

however, to test this technique on cardiac and locomotor signals, as they will likely present unique challenges because they are two different observables (unlike EEG data).

The coupling index is measured by calculating the Shannon entropy of the normalized recurrence rate as a function of time lag. Equations 5, 6, and 7 show the series of required calculations.

$$RR(\tau)=\sum_t R(t,\tau) \text{ (eq. 5)}$$

$$rr(\tau)=RR(\tau)/\{\sum\tau[RR(\tau)]\} \text{ (eq. 6)}$$

$$\rho_\pi = 1-\{-\sum_{\tau\, min\rightarrow\tau\, max} rr(\tau)\cdot ln[rr(\tau)]\}/ln(\tau_{max}-\tau_{min}) \text{ (eq. 7)}$$

In summary, the recurrence rate, RR(τ), is defined by the total recurrent points at all times, *t*, for a given time lag (eq. 5). Next, it is normalized by dividing by the sum of the recurrence rate at each τ evaluated (eq. 6). Finally, the Shannon entropy can be calculated and use to define the coupling index, ρ_π, between two independent time series (eq. 7). The coupling index examines the distribution of recurrence rate at varying τ. Thus, ρ_π ranges from 0 (no coupling) to 1. Cutoff values have not yet been suggested to define strengths of coupled systems. However, between the qualitative assessment of banding and the quantification of coupling index, it will be apparent whether a younger or older population exhibit stronger coupled cardiac and locomotor rhythms. It is hopeful that this research will enlighten investigators as to the normative values and utility of coupling index for these particular time series.

Mechanisms for Coupling

Considering the above evidence, there are likely several mechanisms and explanations for the coupling of cardiac and locomotor patterns. Similar to the concept of movement variability being good to prevent overuse injury, but bad when you need consistent and reliable movement accuracy and performance, coupling can be viewed as having beneficial and detrimental pathways. Therefore coupling could occur under two distinct circumstances: (1) in the event that energetic efficiency is needed as during exercise or fatigue and (2) when aging or pathology results in a loss of neural connectivity, requiring interdependent control systems to then couple together more closely.

Improved efficiency has been suggested to occur through the optimization of blood flow to the muscles and therefore minimizing the energy needed for cardiac contractions (Kirby et al., 1989; Niizeki et al., 1993; Novak et al., 2007). Through exercise, muscle contractions may dynamically modulate venous return and therefore create a oscillating (and coupled) mechanical connection between the motor system and cardiac system (Blain, Meste, Blain, & Bermon, 2009). Previously, it had been proposed that vertical acceleration of the heart, due to impacts during walking or running, may impact the cardiac control networks (Kirby et al., 1989), but Blain et al. (2009) demonstrated that increased workload was associated with indications of increased coupling between the cardiac and locomotor systems during a cycling task.

In contrast, aging and pathological processes may result in deficits relating to the function and connectivity of neuronal networks. While muscle contractions will still aid

in venous return, other sensory loops within the cardiac control system may decline with aging and disease. Novak et al. (2007) suggested that attenuation of baroreflexes associated with aging may lead to enhanced coupling. While baroreflex sensitivity is increased, the stretch reflexes (Bainbridge reflex) become the primary source for sensory feedback in cardiac control. The increased blood volume associated with venous return and coupled with gait timing then drives the coupling between cardiac and locomotor systems.

Theoretical and Clinical Motivations

Coupling provides a framework in which to study how changes in one physiological subsystem affects another. Continued research using this framework will lead to better understanding of how healthy human function relates to systemic health and compensatory mechanisms when one subsystem is impaired. For example, by understanding the relationship between cardiac and motor rhythms, in addition to their relationships with health, we can begin to hypothesize the mechanisms and expected outcomes relating to aging and pathology. That is, when a patient presents with a heart attack, we'll have a better understanding of how this will influence their ability to ambulate. There are both theoretical and clinical implications of studying and implementing a coupling framework.

Dynamic systems theory allows us to consider how systems interact with each other to result in functional or dysfunctional behavior. Along with other groups, our research group has previously and consistently shown that gait patterns can be altered systematically in healthy individuals by asking them to synchronize their stepping

patterns with a blinking visual metronome (Bank, Roerdink, & Peper, 2011; Rhea, Kiefer, D'Andrea, et al., 2014; Rhea, Kiefer, Wittstein, et al., 2014). While this is a novel and important finding of its own, it is important to also consider how altering gait patterns may alter other characteristics of health. From a dynamic systems perspective, it is plausible that changing the gait timing patterns could also result in changes to cardiac dynamics. The potential changes across subsystems have not been prominently studied. By altering the timing patterns in gait, the baroceptor and Bainbridge reflexes allow a fractal stimulus to act within the cardiac control loops (Crystal & Salem, 2012; Novak et al., 2007). Similarly, walking faster or slower than the preferred walking speed has been shown to alter the fractal scaling of gait, which could also change cardiac behavior. Thus, how the heart responds to changes in the locomotor behavior may be very telling of the functional quality of the cardiac system.

From a more general perspective, considering system coupling along with individual system dynamics will help develop a framework to study the healthy (or unhealthy) function of the physiological system. By altering one subsystem's behavior intentionally, we can observe changes in other subsystems and then infer whether these dynamics are characteristics of healthy, aging, or pathological function of the individual subsystems and the whole person. Observations of the effects of altering gait patterns on cardiac patterns will guide empirical testing of the physiological mechanisms and theories that explain the phenomenon of cardiolocomotor coupling and its potential benefits to health sciences.

This method could then lead to an innovative application of theory to potentially change assessment and interventions of unhealthy behaviors. Once we understand how the cardiac and locomotor subsystems couple and interact with each other during walking we can apply this technique to develop either assessments or interventions. Regarding assessments, these findings will give us more detailed metrics to assess the health of an individual. By considering multiple subsystems, we can better assess the systemic quality of function related to aging or disease. Similarly, this method will allow us to identify non-invasive ways to alter cardiac dynamics through locomotor interventions. Specifically, by identifying variables of cardiac health that can be altered systematically through gait training, we can design interventions to improve these characteristics of heart health while also promoting healthy locomotor behavior. The potential of these applications is supported by recent studies that used intentional cardiolocomotor coupling to improve running performance (Phillips & Jin, 2013) and provided auditory or visual fractal stimuli to alter the complexity characteristics in gait (Hove, Suzuki, Uchitomi, Orimo, & Miyake, 2012; Rhea, Kiefer, D'Andrea, et al., 2014; Rhea, Wittstein, Kiefer, & Haran, 2013; Rhea, Kiefer, Wittstein, et al., 2014).

Thus, this dissertation contributes to the literature in three ways. Manuscript 1 explores the empirical value of a mathematical technique designed to quantify coupled systems, While this technique has proven useful in other domains, manuscript 1 uses synthetic signals to define coupling strength and then uses a cardiac single and a locomotor signal to empirically show the strength of cardiolocomotor coupling, which provides the foundation for future work in this area. Manuscript 2 then examines cardiac

and locomotor dynamics individually in two gait tasks in both younger and older adults. Finally, manuscript 3 employs the mathematical technique from manuscript 1 to examine cardiolocomotor coupling in younger and older adults during the two gait tasks. Collectively, these manuscripts help to better understand the interaction between the cardiac and locomotor systems, and how that interaction changes during different task demands and as a function of age.

CHAPTER III

METHODS

Participants

Two groups of twenty-five healthy adults of ages 18-35 and 63-80 yrs were recruited from the university population and local community to complete both experiments. To ensure that we would observe the desired changes in gait dynamics, a power analysis of the pilot data revealed that on the basis of observed effect size for phase (partial η^2=0.426), a sample size of 10 would be needed to obtain statistical power at the 0.8 level. Once significant changes in locomotor dynamics are observed (hypothesis 1), the purpose of this proposal was to examine concurrent changes in cardiac dynamics (hypothesis 2), and the coupling between locomotor and cardiac dynamics (hypothesis 3). Thus, the power analysis was run to ensure an adequate sample size with respect to hypothesis 1. While appropriate data is not currently available to conduct a power analysis for between-group effects, previous studies have successfully shown age-related differences in gait (Hausdorff et al., 1997; Herman et al., 2005; Kang & Dingwell, 2008) and cardiac (Iyengar, Peng, Morin, Goldberger, & Lipsitz, 1996; Kaplan et al., 1991) dynamics with sample sizes equal to or smaller than 50. Thus, a sample size of 50 (25 younger and 25 older adults) was selected. These age groups allowed for comparison to earlier studies that examined gait and/or cardiac dynamics. Healthy was defined as no pre-existing diagnoses of heart disease, neuromuscular dysfunction, or acute lower limb

injury, the ability to walk continuously on a treadmill without assistance for 45 minutes, and no other self-reported injuries or illness. All participants read and signed an informed consent form approved by the UNCG Institutional Review Board. Participants were requested not to exercise rigorously within 8 hours of their testing date(s) to limit the effect of acutely performed exercise on physiological subsystems. Participants were instructed to wear tight fitting, but comfortable walking clothes. Participants wearing clothing preventing the attachment of reflective markers on stable anatomical landmarks were asked to change into compression shorts and/or a tank top provided by the researchers.

Procedures

Upon arrival, participants provided informed consent and completed an intake questionnaire (APPENDIX A) to gather demographic, basic health, and exercise behavior information. The skin of the participant was cleaned using NuPrep® Skin Prep Gel (Weaver and Company, Aurora, CO, USA) inferior to the lateral clavicle on each side and superior the left ASIS. ECG electrodes were prepared with Signa Gel® (Parker Laboratories, Inc., Fairfield, NJ, USA) and placed on the cleaned sites. The ECG signal was collected at 1000 Hz using a MP-150 with a RSPEC wireless transmitter (Biopac Systems, Inc., Goleta, CA, USA) and viewed on a monitor to ensure signal fidelity. An 8-camera Qaulisys Oqus (Göthenberg, Sweden) system was used to track set of 34 markers at 200 Hz and identify the motions of both lower limbs. Individual markers were placed on the ASIS, PSIS, medial and lateral knee, medial and lateral malleolus, the first and fifth metatarsals, and the calcaneus of each limb. Additionally, 4-marker rigid bodies

were placed on each thigh and shank segment. A static image was recorded for two seconds to help develop a calibration model for motion tracking.

Upon placing the ECG electrodes and reflective markers, participants' blood pressure and 8-minutes of ECG signal were recorded while sitting. Next, participants identified their preferred walking speed. To find this speed, the treadmill was set to 0.5 meters per second and participants were asked to instruct the researchers to increase the speed until they feel they are at a comfortable walking pace similar to walking through a park. Next, the treadmill was set to 2.0 meters per second and participants were asked to instruct the researchers to decrease the speed until they again feel like they are at a comfortable walking speed. This process was repeated until the final speeds were within 0.2 meters per second. The average of the two speeds (starting slow and starting fast) was used for the rest of the study as the preferred walking speed.

Experimental Procedures

This study consisted of comparing the coupling index measurement between various synthetic and experimental signals and two experiments to be conducted on two separate days with at least 48 hours between testing sessions. The order of the experiments was counterbalanced. Both experiments used a similar structure consisting of three 15 minute phases. During the first and third phases of both experiments, participants walked with no cues or specific instructions at their preferred walking speed. This equates to a baseline phase (phase one) and retention phase (phase three). Phase two of both experiments was the experimental phase.

In the second phase of the first experiment, participants were instructed to synchronize their gait cycle to a visual metronome projected onto a screen in front of the treadmill. The metronome consisted of blinking left and right footprints presented at eye-height over a sliding textured floor, identical to a previous research project in our laboratory (Rhea, Kiefer, Wittstein, et al., 2014). The timing of the presentation of the footprints was fractal (DFA α = 0.98) and the participants were instructed to match the timing of their steps to the blinking footprints in front of them, such that when the right foot appears the participant should be making contact with their right heel (and left with left).

In the second phase of the second experiment, participants walked at 125% of their preferred walking speed, similar to the experiment by Jordan, Challis, & Newell (2007). This was accomplished by the researchers setting the treadmill speed to 100% of the preferred walking speed in phase one, increasing the treadmill speed to 125% in phase two, and then decreasing the treadmill speed back to 100% in phase three.

Data Reduction

The ECG data were reduced using custom written Matlab® scripts (Mathworks, Newton, MA). First, the data were filtered with a zero-lag 4th order Butterworth filter. Next, the R-peaks were identified by finding a local maximum above a cutoff threshold set to 2 SD of the mean value for each individual trial. R-R interval time series were constructed by calculating the time between consecutive R-peaks. Two artifacts are possible using this method: 1) identification of R-peaks where there is not a true event present and 2) missing the identification of R-peaks. Data was inspected for these two

artifacts manifesting as extremely small or long R-R intervals, respectively. In cases where a false positive was identified, the R-peak was removed and the time series was constructed without the removed R-peaks. In cases where a false negative was identified, an R-peak was manually placed at the visible peak of the missing heartbeat. If there was no clearly missed peak due to signal dropout or other artifacts, an R-peak was placed halfway between the nearest correctly identified R-peaks. In cases where several R-peaks were misidentified consecutively, the data was truncated to remove the suspect data as long as 400 consecutive heartbeats were identified. If these solutions were not possible, the data was removed from analysis completely or the subject rescheduled at a later date.

The kinematic data was reduced using custom Visual3D® scripts (C-Motion, Inc., Germantown, MD). The position of the calcaneus markers was used to identify the step length, step width, and stride interval during walking. First, the data was filtered with a zero-lag 4th order Butterworth filter. Next, the velocity of the calcaneus in the anterior-posterior (AP) direction was calculated by taking the derivative of the AP position data. During treadmill walking, when the AP velocity of the calcaneus markers goes from a positive velocity to a negative velocity, the foot is at heel contact (Zeni Jr, Richards, & Higginson, 2008). Events, labeled R_ON and L_ON, were placed at the positive to negative zero crossings of the AP velocity for the right and left foot, respectively. A third event, labeled STEP, was placed at each R_ON and L_ON event. The stride interval for each leg was calculated as the time between consecutive ON events for each respective leg. The step width was calculated as the medial-lateral (ML) distance between the calcaneus markers at the time of each step event. The step length was calculated as the

AP distance between the calcaneus markers at the time of each step event. Time series for stride interval, step width, and step length were then constructed from their calculated values. Each time series was inspected for false positive and false negative event identification using the stride interval time series. Similar to the cardiac signal, events were either manually placed at the most appropriate location or removed and the time series reconstructed.

For order patterns recurrence plot analysis, the R-R and stride interval time series was transformed into a continuous time series, each lasting 15-minutes in length. This was done by constructing a new time series using the time of events (as opposed to the event number) then filtering and resampling, such that each transformed time series consisted of 900 samples, reflecting a measurement of heart rate and stride interval each second. Each continuous time series was filtered with a low-pass bidirectional 2nd order Butterworth filter with a cutoff frequency of 5 Hz. As the continuous time series was constructed from discrete event series, this filter was selected to provide zero lag and eliminate high frequency oscillations that could not have been observed between heartbeats or step events from the original discrete time series. Researchers have reported using similar techniques to convert between discrete event series and continuous time series, however, their specific methodologies were not been clearly reported (Camm et al., 1996; Novak et al., 2007).

Mean, SD, CV, DFA α, and SE were calculated from the individual time series. Ordered recurrence plot analysis was used to calculate the coupling indices for stride time and R-R interval time series for each phase. For the calculation of DFA α, window sizes

of 4 through N/4 were used. An optimization process for the selection of parameters *m* and *r* (template length and radius, respectively) for the calculation of SE has been previously described by Lake et al. (2002). For this study, *m* and *r* was optimized based on a subset of our participants and set to 2 and 0.3 SD, respectively. The optimization process was done separately for cardiac and kinematic time series; however, the same parameters were selected based on the optimization for the stride interval time series and cardiac time series. In all, each phase of the experiment resulted in 5 measurements (mean, SD, CV, DFA α, and SE) for each individual time series (R-R interval, stride interval, step width, and step length) as well as a coupling index between the stride time and R-R interval time series.

To test the utility of coupling index, synthetic signals (four sinusoids with 90° phase shifts and two signals of Gaussian white noise) were constructed and reduced in the same manner as the experimental cardiac and locomotor data. Then, the coupling index was calculated for pairs of signals (e.g., a sinusoid with a random signal), allowing a comparison of the value of coupling index for theoretically highly coupled systems (sinusoids coupled to themselves or phase shifted sinusoids), weakly coupled systems (cardiac and locomotor coupling), and non-coupled systems (random signals with other signals).

Statistical Plan

In testing each hypothesis, alpha was set to .05 *a priori*. Any follow-up tests were appropriately adjusted.

Hypothesis 1: *As a group, young healthy adults will exhibit different variability characteristics of gait rhythms compared to older adults. Specifically, we hypothesized that the younger group would have greater mean, lesser SD and CV, greater DFA α, and greater SE of stride time, step length, and step width time series. We expected these predictions to persist through each phase of both experiments.* Separate 2 × 3 (group × phase) repeated measures MANOVAs were calculated and Hotelling's Trace was used to compare each variability characteristic (mean, SD, CV, DFA α, and SE) of the stride interval, step length, and step width time series between groups at each phase. A significant main effect for group, in the appropriate directions, indicated a correct hypothesis. When appropriate, follow-up analyses were used to determine how the groups' locomotor behaviors differed within each phase of the experiments and to assess interaction effects.

Hypothesis 2: *As a group, young healthy adults will exhibit different variability characteristics of cardiac rhythms compared to older adults. Specifically, we hypothesized that the younger group would have greater mean, greater SD and CV, greater DFA α, and greater SE of R-R intervals. We expected these predictions to persist through each phase of both experiments.* Separate 2 × 3 (group × phase) repeated measures MANOVAs were calculated and Hotelling's Trace was used to compare each variability characteristic (mean, SD, CV, DFA α, and SE) of the R-R interval time series between groups at each phase. A significant main effect for group, in the appropriate directions, indicated a correct hypothesis. When appropriate, follow-up analyses were

used to determine how the groups' cardiac behaviors differed within each phase of the experiments and to assess interaction effects.

Hypothesis 3: *We hypothesized that cardiolocomotor coupling, during the pre-test phase, would similar between the younger and older groups. When performing the gait synchronization task or increasing walking speed, we predicted the older group would demonstrate a larger increase in the coupling index. During the post-test phase, we predicted the younger group would return to pre-test phase values of the coupling index, while the older group would exhibit residual effects of the experimental condition*. A 2 × 3 (group × phase) repeated measures ANOVA was calculated and Hotelling's Trace was used to compare the coupling index between R-R interval time series and stride interval time series between groups at each phase. When appropriate, follow-up analyses were used to determine how the groups' cardiolocomotor coupling differed within each phase of the experiments and to assess interaction effects.

Hypothesis 4*: We hypothesized that highly coupled synthetic signals (sinusoids) would demonstrate markedly higher coupling index values than random signals or experimental data. Additionally, experimental data (i.e. cardiolocomotor coupling) would exhibit higher coupling index values than random signals.* Independent samples t-tests were used to test for significant differences between the coupling of pairs of signals.

Three manuscripts were developed to test these hypotheses. Manuscript I outlines a new technique to study cardiolocomotor coupling, testing Hypothesis 4. Hypotheses 1 and 2 are examined in Manuscript II, and hypothesis 3 is examined in Manuscript 3 using the new technique.

CHAPTER IV

MANUSCRIPT I

Introduction

Examining the dynamics of physiological subsystems has provided much insight into how systems change over time. For example, older adults exhibit cardiac rhythms that have weaker fractal organization compared to younger healthy adults (Iyengar et al., 1996). Likewise, too much or too little step width variability in gait has been associated with fall history in older adults (Brach et al., 2005). While this approach has been useful in understanding how a single subsystem fluctuates (e.g., the cardiac or loccomotor control system), it is generally recognized that many (if not all) subsystems work in conjunction with other subsystems. These connections are linked at the structural or functional level, and each connected subsystem may influence its connected partners. Thus, understanding how physiological subsystems are coupled may enhance our understanding of larger scale physiological functioning (i.e., across multiple subsystems), potentially leading to a stronger understanding of human health.

The coupling of physiological subsystems is not a new topic of research (Glass, 2001; Godin & Buchman, 1996; Kirby et al., 1989; Novak et al., 2007; Strogatz, Stewart, & others, 1993). Yet, breakthroughs in understanding the mechanisms and effects of coupling have been limited. For example, coupling of cardiac and locomotor rhythms have been demonstrated in running (Kirby et al., 1989), in aging populations (Novak et

al., 2007), and linked to improved performance in endurance running (Phillips & Jin, 2013). Many of the tools used to study physiological coupling stem from concepts in the physical sciences. The continued transition to applications in the biological and medical sciences may lead to new findings that demonstrate the utility of coupling to healthy function and to practical applications in health sciences (such as diagnostics, prognostics, and treatment advances). The coupling behavior of two interconnected systems (in this case, the cardiac and locomotor systems—termed cardiolocomotor coupling) may provide clues as to the quality of overall health and function of a person.

Prior research has generally characterized coupling as a common change in a specific or set of dynamics within two systems' measurements. For example, Niizeki and colleagues used heel contact times during treadmill running to define epochs of strides and then calculated the phase relationship between a stride and the cardiac beats within it (Niizeki et al., 1993). Then, the standard deviation of this phase relationship is calculated with a sliding window to identify periods when entrainment (or coupling) between the cardiac and locomotor systems is present. In an alternative approach, Novak and colleagues used correlations to identify the cardiolocomotor coupling in younger and older adults during walking at various speeds (Novak et al., 2007). They proposed that higher correlations in the time between these events (consecutive heartbeats or strides) indicated higher levels of coupling between the two systems. While these techniques provided new and interesting information about the relationship between cardiac and locomotor rhythms, there are more direct metrics to quantify the coupling between two independent signals.

Recurrence quantification analysis (RQA) measures patterns with recurrence plots and has become a popularly used technique to assess the dynamic characteristics of complex systems (Marwan et al., 2007; Marwan, 2008; Webber, Jr. & Zbilut, 1994). By nature, physiological systems are highly complex and dynamic. Thus, researchers have used RQA to analyze gait (Labini et al., 2012), electrocardiograms (ECG) (Krishnan et al., 2012; Naschitz et al., 2004; Zbilut, Thomasson, & Webber, Jr., 2002), electroencephalograms (EEG) (Groth, 2005), and electromyography (Farina et al., 2002), among many other physiological and non-physiological applications (e.g., financial data) (Marwan, 2008). Moreover, emerging theories suggest that the coupling relationship of physiological signals may play an important role in physiological function, especially in aging and pathological populations (Groth, 2005; Manor, Hu, Peng, Lipsitz, & Novak, 2012; Niizeki & Saitoh, 2014; Novak et al., 2007). Using RQA, it is possible to directly assess the coupling of two different signals over a finite amount of time.

In quantifying the coupling of signals from two different systems, three problems need to be addressed. First, the signals may be measured on different scales (i.e., have different magnitudes or different units). Transformation or normalization of the data, then, is necessary to observe the signals in the same space. Second, the signals of interest need to be collected at the same rate. When examining discrete events, such as the cardiac beat interval or stride interval, it is impossible to control event timing so that both occur simultaneously. Thus, data resampling can be used to model the signals for the duration of an experimental session. A third problem arises when working with complex systems or transient experimental conditions. Nonstationarity of data is especially

problematic for linear measurements, such as mean or standard deviation, but can also pose problems in several nonlinear measurements, such as entropy (Magagnin et al., 2011). To solve the nonstationarity problem, a symbolic transformation technique is often adopted (Marwan et al., 2007). Thus, it is possible to use signal processing techniques post-data collection to examine the coupling between two systems. Such steps make it possible to examine the coupling relationship between two nonlinear, independently observed, and chaotic signals such as those commonly found in physiological subsystems.

Mathematical methods, rooted in RQA, allow researchers to investigate more directly the coupling of two signals. Order pattern recurrence plots (ORPs), a specific type of recurrence plot, and their quantification have been previously used to demonstrate the coupling between separate channels of EEG signals (Groth, 2005). While theory suggests this method should also be able to be used on different signal types (e.g., one cardiac and one locomotor signal), it has not yet been demonstrated. The purpose of this paper is to demonstrate the utility of ORPs to quantify the coupling of two independent physiological signals while comparing its results to the coupling of synthetic signals (i.e., sinusoids and random noise). ORPs and the related coupling index (ρ_π) are calculated from pairs of diverse signal types ranging from simple sine waves to random Gaussian noise to cardiac inter-beat intervals and locomotor inter-stride intervals. Synthetic signals were constructed to convey varying levels of coupling, allowing this study to determine if this method is sensitive to changes in coupling between systems. It was hypothesized that

a larger ρ_π would be observed in signals that were coupled (i.e., comparing two sinusoid time series) relative to uncoupled signals (i.e., comparing two random time series)

Methods

Order Pattern Recurrence Plots

ORPs are a variation of recurrence plots in which a time series is symbolically transformed into a series of order patterns. Groth (2005) described this method and its value in assessing the coupling of EEG signals. By adjusting window size, lag, and window shift, it is possible to identify a relationship between time and coupling for the duration of a recording. Unlike EEGs, other physiological signals are discrete, such as the cardiac intervals and stride time intervals. Thus, the samples in a time series are taken at varying points in time (i.e., at the time when the event of interest occurs, such as R-wave in an ECG), and may not exhibit continuity from one measurement to the next.

Test Signals

Eight separate time series of 880 data points each were used to investigate the ability of ORPs to quantify coupling. First, four time series were created from a sine wave (x=sin(t) evaluated from 0 to 87.9 in 0.1 increments) with 90° phase shifts. As these signals are mathematically identical aside from the phase shift, we would expect them to exhibit a large degree of coupling. Because of the phase shift, the coupling will not be identical. However, it will, in all cases, be very high compared to other test signals.

Next, two random time series were created with the same statistical mean and standard deviation of the sine wave time series. These time series should show little to no coupling, both with any of the sine wave time series and with each other.

Last, a cardiac inter-beat interval time series, also called an R-R time series, and a stride interval time series were calculated from electrocardiogram and motion capture measurements, respectively, during 15-minutes of treadmill walking at a self-selected pace. As previously mentioned, measuring coupling between physiological subsystems requires the independent signals to be (1) normalized or transformed to account for differences in scale, (2) resampled to synchronize observations of each system, and (3) filtered or transformed to deal with nonstationarity. The raw signals were resampled to have a measurement of heart beat interval and stride interval every second from 0 to 900 seconds (901 data points), resolving the second issue. When resampling data near the endpoints, it is impossible to assume what the data prior to the first data point or after the last data point would have been. To account for this challenge, the first and last ten data points were truncated from each resampled time series. RQA using order patterns resolves the remaining issues, as magnitude of the signal is no longer relevant in the symbolically transformed data and recurrence quantification preserves characteristics of nonlinearity unique to the individual signals. Previous studies suggest that cardiolocomotor coupling should be more evident than random noise, but still quite low, in young healthy adults walking at a comfortable self-selected pace (Kirby et al., 1989; Niizeki et al., 1993; Novak et al., 2007). The participant from which the physiological signals were measured was a healthy, recreationally active adult male with no history of cardiac disease, no locomotor or neuromuscular dysfunction, and no lower limb injuries within the previous three months (21.4 yrs, 178.5 cm, 76.0 kg, 1.1 m/s walking speed, exercises on average 6 days a week for 30-60 minutes). The experimental data were

obtained from a larger study in which procedures were approved by the University of North Carolina at Greensboro Institutional Review Board.

Measurements of Coupling

As noted in the literature, there are several ways to quantify coupling of two signals. Thus, to examine the utility of ORP, we elected to examine the nature of coupling across a range of time series with defined dynamics. Thus, the following sets of signals, illustrated in Figure 6, were evaluated for coupling (listed in from greatest expected coupling to least):

1. the original sine wave with itself
2. the original sine wave with each of its 3 phase shifted signals
3. the random signal with itself
4. the original sine wave with a random Gaussian signal
5. The 1 Hz, resampled cardiac R-R interval and the stride interval time series.
6. the random signal with a separate random Gaussian time series

To quantify coupling in the signals, order pattern recurrence plots were constructed from the original time series. A limitation of traditional recurrence plots is that it requires signals to be on the same measurement scale. To solve this problem, order patterns are defined for each time series reflecting the magnitude relationship of consecutive data points (Keller & Lauffer, 2003). Setting the dimension, D, we can alter the number of points examined to define an order pattern. For the simple example of D=2, order patterns (π) can be defined as

$$\pi_x(t)=\{0, x(t) <(t+\vartheta); 1, x(t) \geq x(t+\vartheta). \quad (1)$$

The time-delay for embedding is denoted by ϑ. Thus, two possibilities exist, the first value of x is smaller (π=0) or larger (π=1) than the time delayed value of x. For any dimension, there exist D! possible order patterns (Figure 7). This symbolic transformation is robust to transient changes in amplitude, thus allowing the comparison of symbol sequences from different observed systems. Groth (2005) added to this technique by introducing order recurrence plots which examine the recurrence (or cross recurrence) of the local ordinal structure within time series, and making their characteristics quantifiable.

Next, with the order patterns defined for each time series, a cross recurrence analysis can be used to observe recurrent dynamics shared between two different observations. In this case, a recurrent point is identified when $\pi_x(t)= \pi_y(t')$ allowing us to create a recurrence plot and quantify its characteristics.

One measurement, recurrence rate (RR), represents a statistical measure of similarities between two dynamical systems and can be used to identify the coupling relationship between the time series of two systems. Specifically, we define RR(τ) as the total number of recurrence points over time (t) as a function of time lag (τ). Then, RR(τ) can be normalized by rr(τ)=RR(τ)/Σ_τRR(τ) to identify the relative amount of recurrence at a given time lag with respect to the total recurrence at all observed time lags.

Finally, the coupling index is calculated on windows ($\rho_{\pi,w}$) of data using Shannon entropy,

$$\rho_{\pi,w} = 1-\{-\sum_{\tau\, min \rightarrow \tau\, max} rr(\tau)\cdot ln[rr(\tau)]\}/ln(\tau_{max}-\tau_{min}) \quad (2)$$

and the average coupling index (ρ_π) can be reported for the entire time series. Coupling values can theoretically range from 0 (no coupling) to 1 (complete coupling), but are dependent on the values of τ_{max} and τ_{min} selected.

For each sinusoid evaluated, $\rho_{\pi,w}$ was calculated for 60 evenly spaced windows using varying lag lengths (±15 data points, ±30 data points, or ±60 data points) to calculate RR(τ) from the order recurrence plots. ρ_π for the entire time series was calculated as the average of the windowed calculations. Because a sinusoid should have much more coupling with itself (even with a phase shifted version of itself) than random or experimental data, and coupling should be relatively consistent across each 90° phase shift regardless of lag lengths observed, we calculated the standard deviation of $\rho_{\pi,w}$ for each lag length to identify which lag length demonstrated the most consistency. A lag length of ±15 data points was selected to report. However, it should be noted that the findings were consistent regardless of which lag length was used. The computational steps to create order pattern recurrence plots and calculate coupling are illustrated in Figure 8.

Independent samples t-tests were used to test for significant differences between the coupling index of pairs of signals. Alpha was set to 0.05 a priori.

Results

Figure 9 illustrates the order recurrence plots for each of the tested pairings of signals. Unlike traditional recurrence plots, these depict the recurrence in the diagonal

direction such that recurrence can be visualized as a function of time and lag. Therefore, the line of incidence for auto-recurrence plots is horizontal instead of diagonal.

The mean, standard deviation, and coefficient of variation of the coupling index for each pair of signals analyzed are presented in Table 2 and the inferential statistics are presented in Table 3.

Table 2. Coupling Index of Synthetic and Experimental Time Series. Mean, standard deviation (SD), and coefficient of variation (CV) of coupling index, $\rho_{\pi,w}$, for 60 evenly dispersed windows of test signals.

ORP Name	Time Series A	Time Series B	Mean	SD	CV
AA0	sin(x)	sin(x)	0.193443	0.258806	133.79%
AA1	sin(x)	sin(x+90)	0.178682	0.275402	154.13%
AA2	sin(x)	sin(x+180)	0.166237	0.276354	166.24%
AA3	sin(x)	sin(x+270)	0.179275	0.276011	153.96%
AR1	sin(x)	random(x)	0.000839	0.000390	46.56%
RR1	random(x)	random(x)	0.003698	0.002168	58.64%
RR2	random(x)	random(y)	0.001168	0.000463	39.62%
EXP	R-R interval	stride time	0.001574	0.000695	44.14%

Table 3. Inference Statistics of Difference of Coupling Index Between Pairs of Signals. Difference of average coupling index, ρ_π, for each possible pair of signals. Test signal codes are correspond to those designated in table 1. The signal indicated in **bold** had a significantly larger coupling index.

Test signals	**Difference**	**t**	***p*-value**
AA0 – AA1	0.01476	0.291	0.772
AA0 – AA2	0.02721	0.473	0.638
AA0 – AA3	0.01417	0.279	0.781
AR1 – **RR1**	- 0.00286	- 9.662	< 0.001
AR1 – **RR2**	- 0.00033	- 5.219	< 0.001
AR1 – **EXP**	- 0.00074	- 7.109	< 0.001
RR1 – RR2	0.00253	8.527	< 0.001
RR1 – EXP	0.00212	7.792	< 0.001
RR2 – **EXP**	- 0.00041	- 3.678	0.001

As predicted, the coupling of a sinusoid to itself or a 90° phase shifted version of itself was much stronger than the coupling between two dissimilar signals (the coupling between: sinusoid and a random signal, two random signals, two separate experimental signals). It was also much larger (approximately 50 times in magnitude) than a random signal's coupling with itself. Because coupling index is calculated over a range of lags, a completely coupled system ($\rho_\pi = 1$) would require two signals with matching order patterns at every time lag (i.e., two same-direction constant slopes). That was not the case for our signals, accounting for the relatively low mean coupling indices.

When looking more closely at the non-sinusoidal signals, ρ_π was significantly different than each other signal pair. Table 3 shows pairwise comparisons of ρ_π for each possible combination of pairings examined. While on one hand, the magnitude of this coupling appears to be very small, ρ_π did suggest there was more coupling between

cardiac and locomotor rhythms as compared to a sinusoid and random signal or two independent random signals. Yet, the cardiolocomotor coupling was less than the coupling exhibited by a random signal with itself.

Discussion

This study demonstrated how order pattern recurrence plots and their quantification can be used to calculate the coupling between two non-linear, independently observed, and chaotic signals. We showed that (1) coupling index, as calculated, has very different values for two sinusoids (an autorecurrence or cross recurrence of phase shifted sinusoids) as opposed to more random or chaotic signals that are often identified in nature, (2) by using order patterns to symbolically transform physiological data, coupling index can be calculated on diverse data types, and (3) coupling index is capable of identifying differences between two coupled physiological signals (cardiac and locomotor pattern) and two uncoupled random signals.

Each of these findings is important, as recurrence quantification may provide a new technique to assess the coupling between two seemingly independent physiological systems. There appears to be a trend in the literature, suggesting that the coupling of two physiological systems maybe be highly informative as to the mechanism and extent of dysfunction associated with pathology or aging (Censi, Calcagnini, & Cerutti, 2002; Godin & Buchman, 1996; Novak et al., 2007; Schulz et al., 2013). Thus, clearly demonstrating that this coupling index can distinguish the extent of coupling in different data types is a valuable contribution to better understanding coupling behavior. Moreover, the scale of coupling from this metric is more clear, as a self-coupled sinusoid

exhibited values more than 50 times greater than a self-coupled random signal, more than 100 times greater than that observed between cardiac and locomotor rhythms, and more than 150 times greater than the coupling of two separate random signals. Values of coupling indices were not reported by Groth (2005), and therefore it is valuable to report the scale of this metric in different conditions.

The coupling of physiological subsystems may indicate the overall quality of function of those subsystems and grander health issues. Considering the cardiac and locomotor systems, coupling may be increased to improve mechanical or metabolic efficiency (Kirby et al., 1989; Phillips & Jin, 2013) or as a necessity to accommodate increased constraints on these systems due to aging or other processes (Lipsitz & Goldberger, 1992; Novak et al., 2007). One reason for such low values in our experimental data is that our participant was very healthy and therefore his cardiac and locomotor rhythms were not very coupled. Thus, before this or other metrics can be used in a clinical setting, more research is necessary to discern the precision of coupling index, especially in varying populations that are believed to exhibit higher degrees of coupling. Developing a metric to quantify the coupling between diverse physiological subsystems will be an important step in understanding, diagnosing, and potentially even treating dysfunction that affects several physiological subsystems.

This research was limited to only the simple synthetic signals of sinusoids and random time series. Considering the raw values for coupling index, observables containing sinusoids (i.e. knee angle data) may be biased towards increased coupling index. Additional synthetic signals, specifically those of nonlinear coupled oscillators

should also be examined to better standardize the meaning of coupling values. In this study, a sinusoid only exhibited a coupling index with itself of approximately 0.2. While many may consider this a “perfectly coupled” system, it may suggest that 0.2 is on the upper extremes of coupling index (though it can theoretically be as large as 1).

The approach demonstrated in this study is one technique to overcome the challenges of recording, analyzing, and comparing diverse biological rhythms. However, it does pose some challenges that still need to be addressed. The recurrence of order patterns indicate some level of coupled dynamics between two systems. Yet, it is difficult to interpret the actual meaning of coupled behaviors. Similarly, because this technique is relatively new to physiological research, continued exploration of the magnitude of coupling and its relation to health is extremely important. This technique does require long time series and may lose accuracy towards the end-points of datasets. Experimentally, these issues can be controlled, but the technique needs to be refined to be of use in a clinical setting. Finally, as we embark into a new era of mathematical integrated physiology, challenges such as diverse types of data will need to be overcome. While this study demonstrated one technique to overcome cardiac and locomotor rhythms being recorded at different instances and having different magnitudes, other techniques should be explored to best identify a generalizable way to approach quantifying the coupling between two different observables.

Figure 6. 190 Data Points of Synthetic and Experimental Test Signals for Coupling Analyses. Panels A and B show the four synthetic sine waves and two synthetic random signals used for analyses, respectively. Panel C shows the sine wave and random signal tested for coupling. Panel D shows experimental RR interval and stride interval data tested for coupling. Coupling was calculated for the test signal in each panel (blue line) with each other signal. Self-coupling was also calculated for the sine wave and random Gaussian noise signals (blue lines in A and B, respectively). For clarity, signals are illustrated offset.

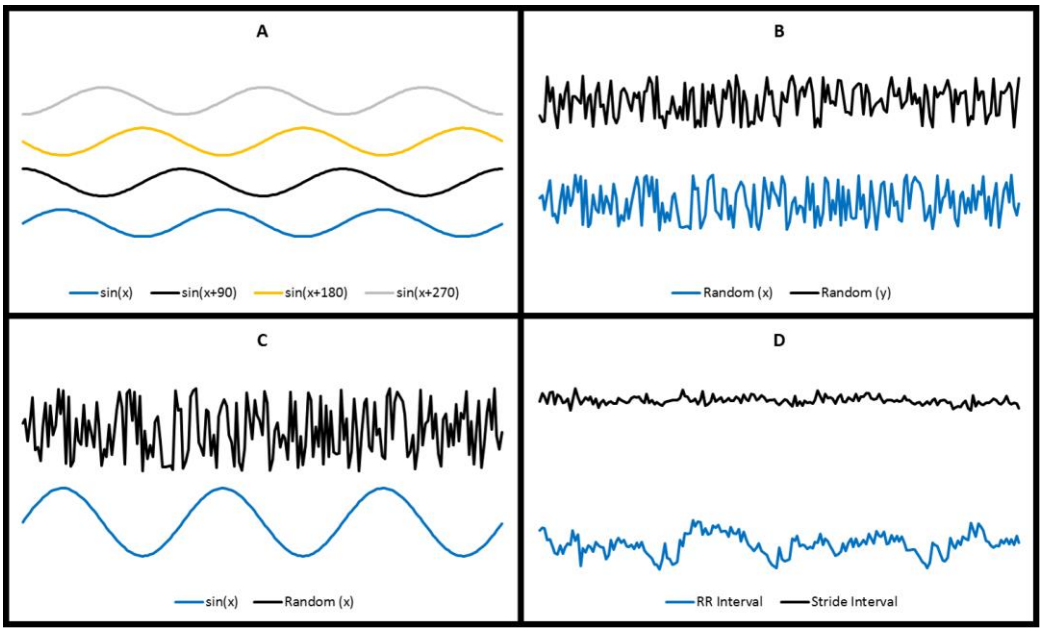

Figure 7. Possible Order Patterns for Dimension D=2 (top) and D=3 (bottom). Symbolic transformation of time series results in a sequence of order patterns which can then be used to implement cross recurrence analyses.

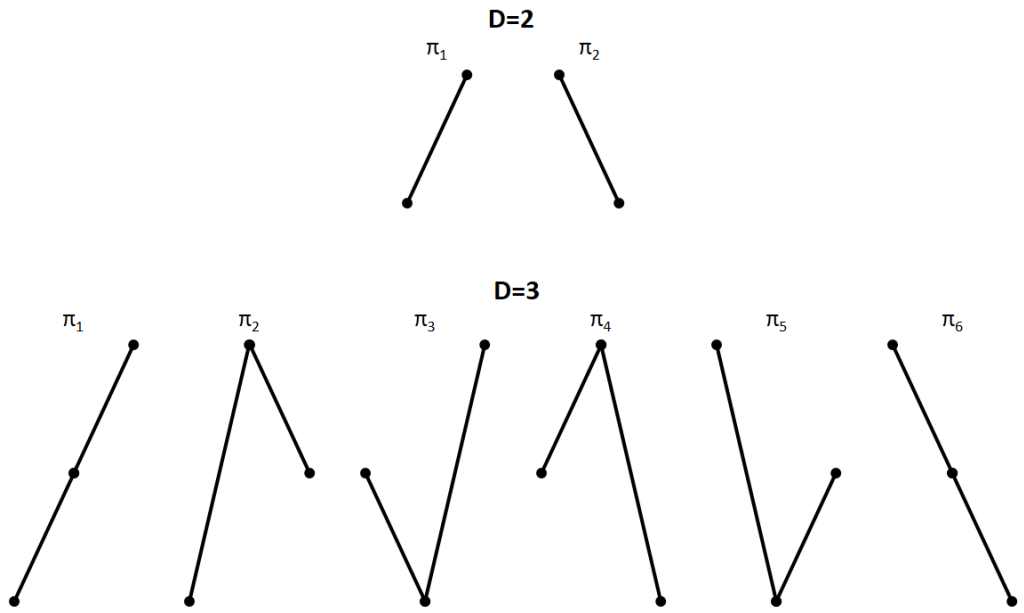

Figure 8. Visualization of the Process to Calculate Coupling Index (ρ_π) within One Window of Data (N=20, lag=±5). This processes is repeated using a sliding window to calculate the average coupling index for longer data sets. **A:** Twenty samples of cardiac and stride interval are shown with the first (red box), fifth (green box), and last (purple box) groupings of 3 samples highlighted to show how they were coded as order patterns (π_x). Examining 3 samples allows for 6 possible order patterns. The matching templates are shown in black at the bottom of each colored box. **B:** Cardiac (vertical axis) and stride interval (horizontal axis) order pattern series are highlighted with matching colors to those coded from **A**. Recurrent points are marked with a black square. The highlighted area (blue) shows the data in which data both ±5 samples were available to calculate coupling index. **C:** The recurrence plot is shown as a function of time and lag (τ). Calculation steps are shown to the right: (1) Calculate the recurrence rate for each lag time, (2) normalize the recurrence rate by dividing by the total number of recurrence points observed, and (3) calculate the Shannon Entropy of the normalized recurrence rates.

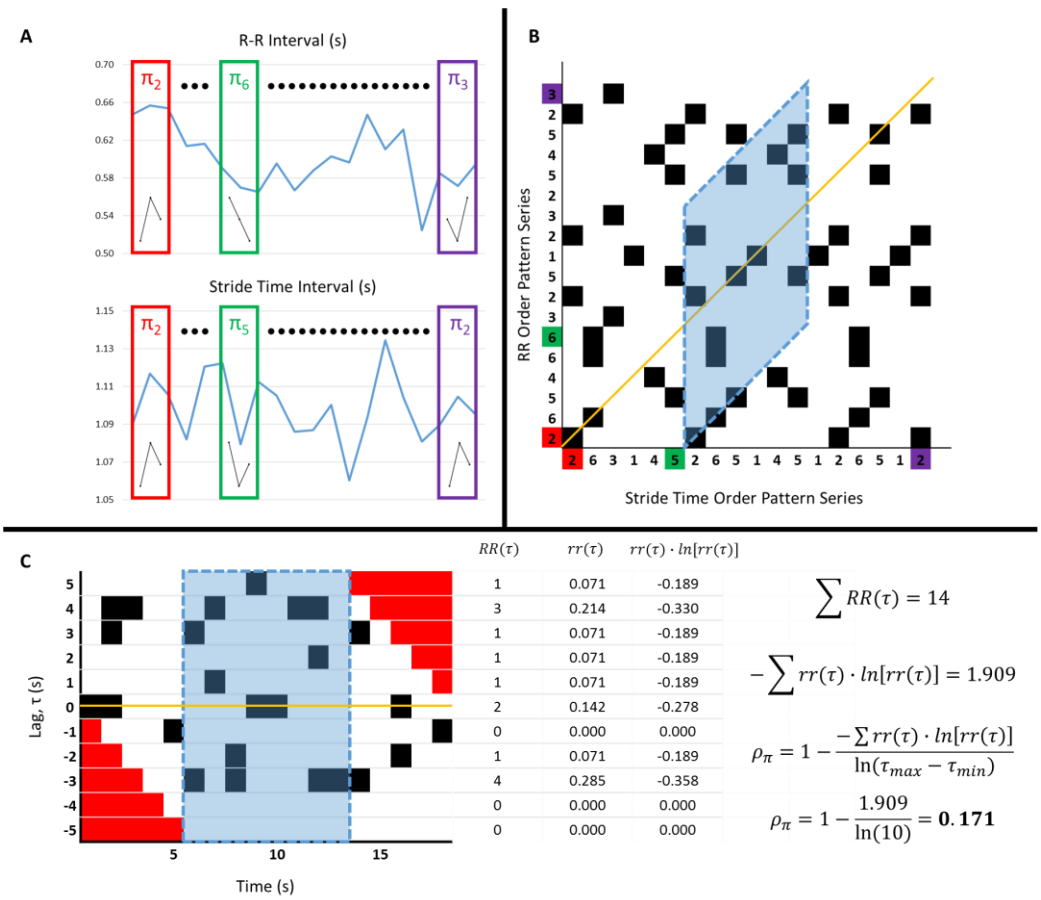

Figure 9. Diagonal-wise Order Pattern Recurrence Plots of Each Tested Pairing. Each recurrence plot is charted as time (x-axis) against lag (y-axis) ranging from 1 to 880 and -

15 to +15, respectively. The top panel shows the ORP of sin(x) with (A) itself, (B) sin(x+90), (C) sin(x+180), and (D) sin(x+270). The bottom panel shows the ORP of (E) sin(x) with random signal #1, (F) random signal #1 with itself, (G) random signal #1 with random signal #2, and (H) cardiac intervals with stride intervals in experimental data.

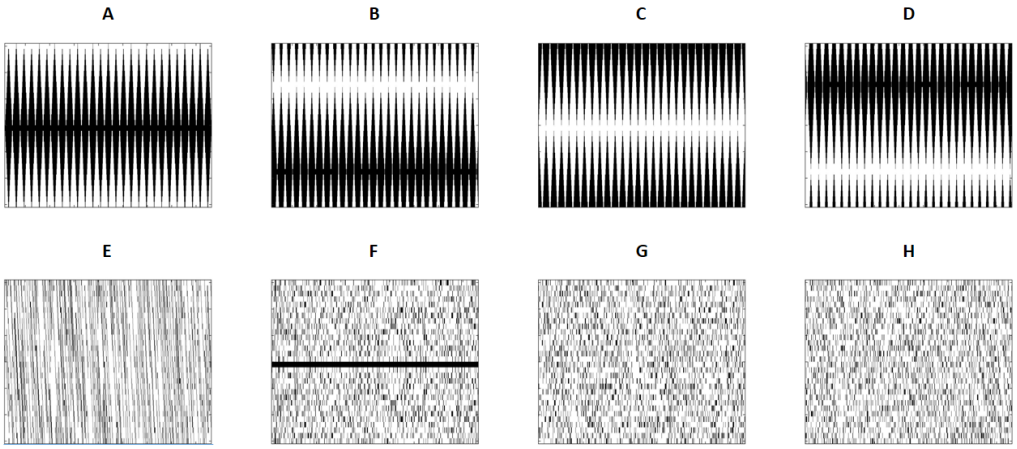

CHAPTER V

MANUSCRIPT II

Introduction

Individually, variation in cardiac and gait rhythms has been well-studied and is informative to understand the quality of their underlying control systems (Hausdorff et al., 2001; Jordan et al., 2009; Rhea, Kiefer, Wittstein, et al., 2014; Routledge, Campbell, McFetridge-Durdle, & Bacon, 2010; J. Zhang, 2007). For example, recurrence quantification analysis of cardiac beat intervals can be used to detect variation abnormalities in cardiac health (Krishnan et al., 2012), while fall-risk can be assessed by examining gait variability using inertial sensors (Riva et al., 2013). Even though physiological subsystems, such as the cardiac and locomotor systems, are often linked structurally and functionally, there has been an emphasis placed on studying individual subsystems. However, recent research has adopted a systems biology approach to examine multiple physiological subsystems concurrently (Wayne et al., 2013). By examining the variability in cardiac and locomotor subsystems together, it is possible to get a more complete understanding of the effects of aging and pathological processes (Schulz et al., 2013).

Both aging and pathology result in changes in the dynamics of several physiological subsystems. Often, these changes are concurrent, altering the shared dynamics between subsystems (Godin & Buchman, 1996; Seely & Christou, 2000). An

example of this is the observation that cardiolocomotor coupling is stronger in healthy older adults compared to healthy younger adults, which was postulated to reflect a decline in the complexity of neural networks and feedback loops in older adults (Novak et al., 2007). Thus, aging may require stronger coupling between physiological subsystems in order to maintain a certain level of function (i.e., to complete the given task). The cardiac and locomotor systems share structural and functional components, and, therefore, a change in one system is likely to result in an observable change in the other, which could ultimately influence the overall functional level of the person (Lipsitz, 2002). Thus, it is plausible that an altered cardiac system may lead to altered locomotor function and vice versa. It has also been suggested that altering one subsystem may have a holistic effect across multiple subsystems, potentially providing a new way to approach rehabilitation (Manor & Lipsitz, 2013). However, these are empirical questions that require observation of function across two or more physiological subsystems during a variety of tasks.

A starting point is to measure cardiac and gait rhythms when the dynamics of one system are predictably altered. Previous work in this area has shown at least two ways to experimentally alter gait dynamics. First, it has been demonstrated that the variability of gait rhythms can be altered intentionally and directionally using visual (Rhea, Kiefer, D'Andrea, et al., 2014; Rhea, Kiefer, Wittstein, et al., 2014) or auditory (Hove et al., 2012; Kaipust, McGrath, Mukherjee, & Stergiou, 2013; Marmelat, Torre, Beek, & Daffertshofer, 2014; Uchitomi, Ota, Ogawa, Orimo, & Miyake, 2013) fractal metronomes. Fractal metronomes provide a stimulus to which a participant can

synchronize their movement—often stride time—with the unique characteristic that the timing between visual or auditory beats is variable, and more specifically, exhibiting a self-similar and persistent pattern over time (i.e., the definition of a fractal). This fractal form of variation between stimulus beats reflects the non-uniform nature of human gait rhythms, which has been shown to be fractal in young healthy adults (Hausdorff et al., 1996), but typically becomes more random (i.e., less persistent) due to aging and pathology (Hausdorff, 2007; Rhea & Kiefer, 2014; Stergiou & Decker, 2011; Vaillancourt & Newell, 2002). By asking participants to synchronize their gait cycle to a metronome exhibiting either a random or persistent timing structure, gait dynamics are shifted toward the prescribed dynamic (Hove et al., 2012; Kaipust et al., 2013; Marmelat et al., 2014; Rhea, Kiefer, D'Andrea, et al., 2014; Rhea, Kiefer, Wittstein, et al., 2014; Uchitomi et al., 2013). Another way to alter gait dynamics is to alter walking speed. Increasing or decreasing speed from a preferred pace has demonstrated increases in fractal characteristics of stride times (Jordan et al., 2007b). Thus, either a fractal metronome or speed change can be used to predictably alter gait dynamics.

While these two methods have been shown to alter gait dynamics in a predictable way, it is unknown how cardiac rhythms are manipulated during these experimental manipulations. Since cardiac rhythms in their own right have been taken as a measure of cardiac health (Berntson et al., 1997; Iyengar et al., 1996; Pikkujämsä et al., 1999), understanding how cardiac rhythms are altered during these types of gait manipulations – which are becoming more commonplace in gait rehabilitation – would provide valuable information to ensure that an unintended consequence relative to cardiac health is not

occurring. The cardiac and locomotor systems are interconnected, and this interaction may change with increased age, so it is important to determine the effect of typical and experimental gait interventions on cardiac patterns in younger and older adults.

The purpose of this study was to simultaneously assess the variability in cardiac and locomotor rhythms in younger and older healthy adults during treadmill walking tasks. The two experimental conditions included: (1) walking while synchronizing to a fractal visual metronome and (2) walking at a fast speed, as well as a pre-test and post-test after each experimental manipulation to check for retention of the cardiac and locomotor patterns. Confirming the expected changes in gait patterns and observing the related changes in cardiac patterns may inform clinicians as to the potential value of these types of interventions as well as provide new considerations for prognostic, diagnostic, and treatment evaluation or aging (and potentially pathological) patients. It was hypothesized that the older group would exhibit a greater magnitude of variation [assessed with standard deviation (SD) and coefficient of variation (CV)] and an altered structure of variability [assessed with detrended fluctuation analysis (DFA) and sample entropy (SE)] in gait and cardiac patterns compared to the younger group across the pre-test, experimental conditions, and post-test.

Methods

Participants

A total of fifty-one healthy, physically active individuals participated in the study. Twenty-five younger adults (24.57±4.29 yrs, 1.76±0.09 m, 73.34±15.35 kg) and twenty-six older adults (67.67±4.70 yrs, 1.72±0.09 m, 70.13±14.30 kg) were recruited from a

convenience sample from the University of North Carolina at Greensboro and regional activity groups (i.e., hiking, running, and cycling). Volunteers were excluded from the study if they had any pre-existing diagnoses of heart disease, neuromuscular dysfunction, or acute lower limb injury. Additionally, all participants had to be classified as moderate to no risk of exercise according to the American College of Sports Medicine Guidelines for Exercise Testing and Prescription (Ehrman, 2010) and self-report an ability to walk unassisted for 45-minutes on a treadmill at a self-selected pace. Participant information is summarized in Table 4. All participants provided informed consent for the study. All procedures for the study were approved by the University of North Carolina Institutional Review Board.

Table 4. Participant Demographics by Group. Demographics [mean(SD)] for participants including age, mass, height, kinematic characteristics, blood pressure (BP), exercise descriptors, and time between testing sessions. Exercise duration corresponds to a categorical assessment of average time per session, (1 = less than 30 minutes, 5 = more than 120 minutes). Exercise intensity corresponds to a categorical assessment of average intensity during and exercise session (1 = very light, 5 = very hard).

Group	**Age (yrs)**	**Mass (kg)**	**Height (cm)**	**Avg. ST (s)**	**PWS (m/s)**	**125% PWS (m/s)**	**Systolic BP / Diastolic BP (mmHg)**	**Ex. Frequency (days/wk)**	**Ex. Duration (au)**	**Ex. Intensity (au)**	**Time btwn. Sessions (hrs)**
Older	67.67 (4.70)	70.13 (14.30)	1.72 (0.09)	1.08 (0.09)	1.18 (0.23)	1.48 (0.29)	136.77 (15.91) / 80.23 (10.94)	6.27 (1.00)	2.88 (1.07)	3.38 (0.64)	184.02 (63.15)
Younger	24.57 (4.29)	73.34 (15.35)	1.76 (0.09)	1.15 (0.08)	1.10 (0.17)	1.38 (0.22)	119.48 (8.73) / 76.76 (8.91)	5.32 (1.38)	2.52 (0.92)	3.36 (0.56)	216.95 (154.68)

Experimental Design

The experiment was conducted during two sessions, at least 96 hours apart (200.8 ± 119.0 hours between). During the first session only, participants completed an intake questionnaire about health history and lifestyle, the SF-36 Health Survey (Optum, Eden Prairie, MN), and had their height and mass recorded. Additionally, only during the first session, each participant's preferred walking speed (PWS) was identified. PWS was identified by asking the participants to walk on the treadmill at a slow speed (0.5 m/s) and inform the researcher to increase the speed until they felt they were at a "natural and comfortable walking pace". Participants were then asked to start walking at a fast pace (2.0 m/s) and inform the researcher to decrease the speed of the treadmill until they felt they were at a "natural and comfortable walking pace". If the two speeds were within 0.2 m/s of each other, the average was recorded as the participant's PWS. Otherwise, the process was repeated until a PWS was identified.

In both sessions, the experimental procedures included, in order, measurement of blood pressure, 8-minutes of electrocardiogram (ECG) measurement while sitting, 15 minutes of treadmill walking at a self-selected pace, 15 minutes of treadmill walking in one of two experimental conditions (i.e., gait synchronization or fast walking), and 15 additional minutes of treadmill walking at their preferred pace. These phases are referred to as the sitting, pre-test, experimental, and post-test phases, respectively. During walking, both ECG and kinematics were recorded.

The two experimental conditions were a gait synchronization task (matching heel strike timing to a visual metronome projected in front of the participant at their PWS) and

fast walking (walking at 125% of their PWS). The visual metronome consisted of two flashing footprints projected at eye-level on a screen in front of the treadmill (Figure 10). The footprints prescribed the desired timing between heel strikes for the left and right feet, with the timing between the appearance of the footprints exhibiting a fractal pattern (DFA $\alpha = 0.98$, indicating persistence) and the same mean stride time as that of the participant at their PWS (Table 4). The experimental walking trial condition was counterbalanced such that half of each group completed the visual metronome task on their first visit followed by the fast walking task on their second visit, whereas the other half of the group performed the opposite task order.

Instrumentation

Thirty-six retroreflective markers were placed on anatomical landmarks to define a model consisting of the foot, knee, thigh, and pelvis. Markers were placed bilaterally on the anterior superior iliac spine, posterior superior iliac spine, greater trochanter of the femur, medial and lateral condyle of the femur, medial and lateral malleoli, calcaneus, and first and fifth metatarsal heads. Additionally, rigid plates consisting of 4 markers were placed on each thigh and shank segment. An 8-camera motion capture system (Qualisys AB, Gothenburg, Sweden) collected movement data at 200 Hz for each 15-minute walking trial.

ECG data were recorded using an MP-150 Data Acquisition System (Biopac Systems, Inc., Goleta, CA) at 1000 Hz. Three Ag/AgCl electrodes were place on the torso of each participant – below the clavicle on the right and left side of the participant and

above the left anterior superior iliac spine – to form an Einthoven's triangle. Lead I (right shoulder to left shoulder) electrical activity was recorded.

Data Reduction

Data reduction consisted of converting raw ECG signal to beat-to-beat interval time series (R-R time series) and position data from motion capture into stride interval, step width, and step length time series. The three variables selected to quantify locomotor behavior allowed for an examination of both temporal (stride interval) and spatial (step width and step length) characteristics, which are commonly reported in the gait literature (Brach et al., 2005, 2008; Gabell & Nayak, 1984; Jordan et al., 2007b). Measurements of variability could then be extracted from the cardiac and locomotor time series from each variable.

ECG data were reduced to a beat-to-beat interval time series. First, the raw ECG data were detrended and filtered. A 6th order polynomial was fit to and subtracted from the data to remove nonlinear trends in the raw ECG signal. Next, a 7th order Savitzky-Golay filter was applied to sliding windows of 21 data points to remove high frequency noise from the raw signal. R-peaks and S-peaks (or troughs) were then identified as any local maxima or minima more than three standard deviations from the mean signal (Hargittai, 2005). Traditionally, the beat-to-beat interval is calculated as the time between R-peaks. However, in some cases due to axis deviation of the ECG signal, identifying R-peaks was problematic with several false peaks being identified. In cases in which the average distance away from the mean ECG signal was smaller for the R-peak than that of the S-peak, the R-peaks were reidentified by finding the local maxima within 0.1 seconds

prior to the S-peak. Beat-to-beat interval time series were constructed from the time between R-peaks after the detrending, filtering, and R-peak identification were completed. Finally, data were examined for outliers – R-R intervals greater than two standard deviations from the average R-R interval for the 10 beats before and after it. Outliers (< 5% of the data) were replaced with the median of the ten beat-to-beat intervals before and after the outlier. In cases at the beginning and end of the trial where there were not 10 intervals before or after, a total of 20 intervals was still used to calculate the median replacement and local mean.

Visual 3-D (C-Motion, Bethesda, MD) was used to calculate each time series from position data recorded with motion capture. Position data were first smoothed using a bidirectional 2nd order butterworth filter with lowpass cutoff frequency of 6 Hz. Heel contact time of each foot was identified using the velocity (derivative of position) of each calcaneus marker (Zeni Jr et al., 2008). The time between consecutive heel contacts was used to construct left and right stride interval time series. Because previous research has indicated no difference between limbs for these variables, only the right limb stride interval data is reported (Rhea, Kiefer, D'Andrea, et al., 2014). Similarly, using the timing of consecutive steps (right heel contact to left heel contact), step width and length were identified as the medial-lateral and anterior-posterior distances, respectively, of the calcaneus markers at heel contact time. Step width and step length time series were then constructed from these data.

The mean, SD, CV, DFA scaling exponent alpha (DFA α), and SE were calculated from each time series to quantify characteristics of data variability. SD and CV

provide a measurement of the magnitude of variability, while DFA α and SE provide a measurement of the structure of variability. DFA α and SE calculation methods are provided in detail in other publications (Peng et al., 1994; Richman & Moorman, 2000). In short, DFA α quantifies the self-similarity of a time series on multiple scales (i.e., we used window sizes ranging from 4 data points to one-fourth of the data length) by establishing a relationship between fluctuations in the time series at each scale and the scale size. Values typically range on a spectrum from 0.5 (Gaussian white noise) to 1.0 (pink noise or 1/f noise) in physiological subsystems. In healthy individuals stride interval time series DFA α exhibits values near 0.75, while R-R interval time series exhibits values near 1.0. This difference is thought to be due to the voluntary control that can override gait rhythms but are less prevalent for control of cardiac rhythms (Jordan et al., 2007a). SE quantifies the complexity of a time series by using a pattern matching algorithm, dependent on *m* (template length for counting matches) and *r* (radius within which two vectors must be to be considered a match). Parameters *m* and *r* were set to 2 and 30% of the SD of the time series, respectively. These values were selected based upon previous use of SE in the literature for cardiac and gait data (Eduardo Virgilio Silva & Otavio Murta, 2012; Lake et al., 2002; Porta et al., 2013; Richman & Moorman, 2000; Yentes et al., 2013). Highly regular time series (e.g. a sinusoid) will exhibit a SE of 0, while random time series will exhibit a value near 2.

Statistical Approach

The two experimental conditions were tested as separate experiments. That is, separate MANOVAs were used for data collected on the gait synchronization day and on

the fast walking day. Hotelling's Trace was used as the test criterion for both experiments. For gait data, a 2 x 3 (GROUP x PHASE) MANOVA was used to examine the mean, SD, CV, DFA α, and SE for stride interval, step length, and step width time series. Because the cardiac data also included a sitting phase, a 2 x 4 (GROUP x PHASE) MANOVA was used. Follow-up Bonferroni adjusted t-tests were used to compare the experimental and post-test phases to the pre-test phase. Significant difference from the pre-test for the experimental condition would indicate a change due to the condition. Additionally, if the post-test was also significantly different from the pre-test and in the same direction, there is some evidence of retention. Alpha was set a priori to 0.05.

Results

Gait Synchronization Task

All findings for the gait synchronization experiment are summarized in Table 5.

For gait variables, a PHASE x GROUP interaction was identified during the gait synchronization experiment ($F_{30,162}$=2.353, $p<0.001$, partial η^2=.303). Specifically, step length mean, stride time mean, stride time SD, stride time CV, and stride time entropy demonstrated the interaction effect.

Table 5. Summary of Results [Mean(SD)] from the Gait Synchronization Task Experiment. Significant main effects of GROUP are indicated by * (p<0.05). Significant difference from pre-test phase indicated by † (p<0.05. Note, this is a main effect for the collapsed groups.

		Group	Pre-Test	Synchronization	Post-Test
Step Length (m)	*mean*	Older	0.60(0.10)	0.59(0.10)†	0.62(0.09)†
		Younger	0.57(0.09)	0.56(0.09)	0.58(0.09)
	*SD**	Older	0.02(0.01)	0.05(0.01)†	0.02(0.01)
		Younger	0.02(0.01)	0.04(0.01)	0.02(0.01)
	*CV**	Older	0.04(0.03)	0.09(0.03)†	0.04(0.03)
		Younger	0.03(0.01)	0.08(0.01)	0.03(0.01)
	DFA α	Older	0.64(0.11)	0.80(0.09)†	0.67(0.12)†
		Younger	0.65(0.11)	0.86(0.05)	0.70(0.10)
	SE	Older	1.41(0.24)	1.16(0.19)†	1.40(0.32)
		Younger	1.49(0.24)	1.22(0.15)	1.46(0.23)
Step Width (m)	*mean*	Older	0.09(0.03)	0.11(0.03)†	0.09(0.03)
		Younger	0.11(0.03)	0.12(0.03)	0.11(0.03)
	*SD**	Older	0.02(0.01)	0.02(0.01)†	0.02(0.00)†
		Younger	0.02(0.01)	0.02(0.01)	0.02(0.01)
	*CV**	Older	0.26(0.10)	0.24(0.09)†	0.29(0.10)†
		Younger	0.18(0.06)	0.17(0.05)	0.20(0.07)
	DFA α	Older	0.64(0.06)	0.70(0.09)†	0.64(0.08)
		Younger	0.66(0.06)	0.74(0.08)	0.64(0.09)
	SE	Older	1.68(0.05)	1.62(0.07)†	1.68(0.07)
		Younger	1.67(0.05)	1.59(0.01)	1.67(0.05)
Stride Interval (s)	*mean**	Older	1.10(0.09)	1.09(0.08)†	1.14(0.09)†
		Younger	1.17(0.08)	1.16(0.07)	1.18(0.08)
	SD	Older	0.03(0.02)	0.08(0.02)†	0.02(0.01)
		Younger	0.02(0.01)	0.08(0.01)	0.02(0.01)
	CV	Older	0.02(0.01)	0.07(0.02)†	0.02(0.01)
		Younger	0.02(0.01)	0.07(0.01)	0.02(0.01)
	DFA α	Older	0.80(0.09)	0.86(0.07)†	0.81(0.11)
		Younger	0.78(0.09)	0.88(0.05)	0.81(0.10)
	*SE**	Older	1.32(0.26)	0.96(0.18)†	1.41(0.19)
		Younger	1.47(0.15)	0.99(0.15)	1.45(0.15)

		Group	Pre-Test	Synchronization	Post-Test
R-R interval (s)	*mean**	Older	0.72(0.08)	0.68(0.10)†	0.71(0.08)
		Younger	0.65(0.12)	0.64(0.13)	0.68(0.20)
	SD	Older	0.05(0.06)	0.04(0.07)	0.05(0.06)
		Younger	0.04(0.02)	0.04(0.05)	0.14(0.50)
	CV	Older	0.07(0.08)	0.06(0.07)	0.07(0.09)
		Younger	0.06(0.03)	0.07(0.08)	0.13(0.35)
	DFA α	Older	0.80(0.19)	0.86(0.17)†	0.79(0.19)
		Younger	0.82(0.12)	0.86(0.12)	0.82(0.11)
	*SE**	Older	0.85(0.31)	0.77(0.27)	0.87(0.35)
		Younger	1.12(0.35)	1.09(0.32)	1.11(0.32)

Multivariate main effects were identified for both GROUP ($F_{15,34}$=2.720, p=0.008, partial η^2=.545) and PHASE ($F_{30,19}$=31.498, p<0.001, partial η^2=.980). Pairwise comparisons revealed significant differences between groups for stride interval mean (F=6.891, p=0.012, partial η^2=.126), stride interval SE (F=4.269, p=0.044, partial η^2=.082), step width SD (F=11.272, p=0.002, partial η^2=.190), step width CV (F=12.789, p=0.001, partial η^2=.210), step length SD (F=14.106, p<0.001, partial η^2=.227), and step length CV (F=5.246, p=0.026, partial η^2=.099). Specifically, the older group exhibited shorter stride times and less complexity in the stride time data, as well as less step width and step length variability. Significant main effects for PHASE were identified for all gait kinematics variables (mean, SD, CV, DFA α, and SE for stride interval, step width, and step length time series). Pairwise comparisons by phase indicated that all gait kinematics variables were significantly different between the pre-test and experimental phases (all p<0.01). Significant differences were also identified between the pre-test and post-test phases for stride interval mean, step width SD, step width CV, step length mean, and step length DFA α (all p<0.01). Of the variables with both post-test and experimental phases

being different than the pre-test phase, only step width SD and step length DFA α were in the same direction (in both cases these variables increased after the pre-test).

For cardiac variables, a PHASE x GROUP interaction was identified during the gait synchronization experiment ($F_{15,407}$=2.579, p=0.001, partial η^2=.087). Specifically, mean R-R interval demonstrated the interaction effect. Multivariate main effects were identified for both GROUP ($F_{5,43}$=889, p<0.001, partial η^2=.508) and PHASE ($F_{15,33}$=50.394, p<0.001, partial η^2=.958) of cardiac variables as well. The older group exhibited significantly slower R-R intervals (F=5.313, p=0.026, partial η^2=.102) and less complex (lower SE) R-R interval patterns (F=21.181, p<0.001, partial η^2=.311) than the younger group. Follow-up testing also showed that R-R interval mean was shorter (faster heart beat) (F=11.454, p=0.001, partial η^2=.196) and DFA α was elevated (F=4.085, p=0.049, partial η^2=.080) during the experimental phase compared to the pre-test phase. However, neither of these changes in cardiac behavior were retained during the post-test phase.

Fast Walking Task

All findings for the fast walking experiment are summarized in Table 6.

No interaction effects were identified for gait variables ($F_{30,162}$=1.268, p=0.177, partial η^2=.190) or cardiac variables ($F_{15,407}$=1.165, p=0.297, partial η^2=.041) during the fast walking experiment.

Table 6. Summary of Results [Mean(SD)] from the Fast Walking Task Experiment. Significant main effects of GROUP are indicated by * ($p<0.05$). Significant difference from pre-test phase indicated by † ($p<0.05$). Note, this is a main effect for the collapsed groups.

		Group	***Pre-Test***	***Fast Walking***	***Post-Test***
Step Length (m)	mean	Older	0.60(0.10)	0.69(0.10)	0.62(0.09)
		Younger	0.59(0.08)	0.67(0.08)	0.60(0.08)
	SD*	Older	0.02(0.01)	0.02(0.01)	0.02(0.01)
		Younger	0.02(0.01)	0.02(0.01)	0.02(0.01)
	CV*	Older	0.04(0.03)	0.03(0.02)	0.04(0.02)
		Younger	0.03(0.01)	0.02(0.01)	0.03(0.01)
	DFA α	Older	0.65(0.16)	0.67(0.12)	0.65(0.11)
		Younger	0.67(0.10)	0.68(0.12)	0.69(0.08)
	SE	Older	1.39(0.31)	1.42(0.26)	1.44(0.21)
		Younger	1.51(0.21)	1.45(0.27)	1.49(0.22)
Step Width (m)	mean	Older	0.09(0.03)	0.09(0.03)†	0.09(0.03)
		Younger	0.11(0.03)	0.11(0.03)	0.10(0.03)
	SD*	Older	0.02(0.01)	0.02(0.01)†	0.02(0.01)
		Younger	0.02(0.00)	0.02(0.00)	0.02(0.01)
	CV*	Older	0.26(0.09)	0.28(0.08)†	0.29(0.09)
		Younger	0.19(0.06)	0.19(0.07)	0.21(0.08)
	DFA α	Older	0.65(0.07)	0.61(0.06)†	0.65(0.06)
		Younger	0.66(0.07)	0.63(0.07)	0.65(0.06)
	SE	Older	1.67(0.06)	1.70(0.06)†	1.67(0.06)
		Younger	1.65(0.08)	1.69(0.05)	1.68(0.05)
Stride Interval (s)	mean*	Older	1.10(0.09)	1.02(0.08)†	1.14(0.10)
		Younger	1.17(0.08)	1.07(0.07)	1.18(0.08)
	SD	Older	0.07(0.24)	0.02(0.01)	0.02(0.01)
		Younger	0.02(0.01)	0.01(0.01)	0.02(0.01)
	CV	Older	0.06(0.20)	0.02(0.01)	0.02(0.01)
		Younger	0.02(0.01)	0.01(0.01)	0.02(0.01)
	DFA α	Older	0.80(0.11)	0.77(0.11)	0.76(0.10)
		Younger	0.80(0.08)	0.79(0.10)	0.81(0.09)
	SE	Older	1.33(0.38)	1.43(0.29)	1.46(0.14)
		Younger	1.45(0.14)	1.52(0.14)	1.43(0.17)

		Group	*Pre-Test*	*Fast Walking*	*Post-Test*
R-R interval (s)	mean	Older	0.71(0.10)	0.68(0.21)	0.68(0.11)
		Younger	0.67(0.12)	0.65(0.16)	0.74(0.32)
	SD	Older	0.05(0.07)	0.09(0.18)	0.05(0.08)
		Younger	0.05(0.08)	0.13(0.37)	0.13(0.41)
	CV	Older	0.07(0.07)	0.11(0.14)	0.06(0.09)
		Younger	0.06(0.08)	0.18(0.57)	0.10(0.20)
	DFA α	Older	0.79(0.17)	0.80(0.18)	0.81(0.19)
		Younger	0.84(0.13)	0.84(0.15)	0.83(0.13)
	SE*	Older	0.76(0.37)	0.69(0.34)	0.83(0.31)
		Younger	1.13(0.31)	1.09(0.30)	1.14(0.22)

For gait variables, the fast walking experiment also exhibited main effects for both GROUP ($F_{15,34}$=3.439, p=0.001, partial η^2=.630) and PHASE ($F_{30,19}$=262.162, p<0.001, partial η^2=.998). Significant differences between groups were identified for stride interval mean (F=5.981, p=0.018, partial η^2=.070), step width SD (F=10.329, p=0.001, partial η^2=.177), step width CV (F=13.951, p<0.001, partial η^2=.225), step length SD (F=8.294, p=0.006, partial η^2=.147), and step length CV (F=4.943, p=0.031, partial η^2=.093). The older group demonstrated shorter stride time intervals and more variability of both step width and step length (both SD and CV). Differences across phases of the experiment were identified for stride interval mean, step width mean, step width SD, step width CV, step width DFA α, step width SE, step length mean, step length SD, and step length CV (all p<0.05). The pre-test and experimental phase were significantly different for each of these variables, with the exception of step width mean. Additionally, changes in gait kinematics were persistent during the post-test phase for step width variability (both SD and CV increased during fast walking and remained elevated during the post-test as compared to the pre-test phase) and step length mean

(longer step lengths were used during fast walking and the post-test than during pre-test walking).

For cardiac variables, the fast walking experiment also identified significant main effects for both GROUP ($F_{5,43}$=11.599, p<0.001, partial η^2=.574) and PHASE ($F_{15,33}$=40.668, p<0.001, partial η^2=.949). The older group exhibited significantly less complexity (lower SE) in their R-R interval patterns (F=28.591, p<0.001, partial η^2=.378) than the younger group. Follow-up testing revealed that differences in phase were only found between the sitting phase and pre-test phase. There was no effect of phase on any cardiac variables when comparing the experimental and post-test phases to the pre-test phase.

Discussion

This study demonstrated that both older and younger healthy adults alter gait patterns similarly when presented with a gait synchronization task. During the gait synchronization experiment, main effects for phase were exhibited for all gait pattern variables, but none were shown during the fast walking task. This might suggest that a gait synchronization task has greater potential to alter gait and cardiac rhythms than fast walking. Moreover, R-R interval changed only during the synchronization condition (decreased mean and increased DFA α). These are important findings because it suggests that it may be possible to alter gait and cardiac rhythms simultaneously.

Manor and Lipsitz (2013) suggest that by modifying a single component of a system, such as gait timing, it may holistically alter the dynamics across several physiological subsystems, a postulate that is supported by our data. One theory to

facilitate this is a diminishing of baroreflex sensitivity associated with aging. Adaptive, healthy people may not experience this deficit, while others will necessarily rely more heavily on the information that is available and shared between subsystems, ultimately resulting in elevated cardiolocomotor coupling. In the future, it may be possible to take advantage of this phenomenon by targeting one subsystem for intervention and observing improvements across other subsystems. For example, it may be possible to strategically prescribe gait interventions that predictably alter cardiac dynamics.

It has been demonstrated that a gait synchronization task can be used to change gait rhythm dynamics in a prescribed direction and that there is some retention of these changes once a stimulus is removed (Hove et al., 2012; Rhea, Kiefer, Wittstein, et al., 2014; Uchitomi et al., 2013). In this study, a concurrent increase of R-R interval, step width, step length, and stride interval DFA α during the gait synchronization task supports the likelihood that cardiolocomotor synchronization occurs during walking. Coupling may be enhanced to account for natural aging processes that decrease the redundancy in neurological pathways (Manor & Lipsitz, 2013) or to accommodate external constraints during walking as demonstrated during the gait synchronization task. It should be noted that no retention was observed after the gait synchronization task in the post-test with respect to the gait dynamics. This likely occurred due to the fact that the mean of each participants' prescribed fractal time series was normalized to their preferred walking speed, whereas previous research used a single time series across all participants (Rhea & Kiefer, 2014; Rhea, Kiefer, Wittstein, et al., 2014). Recent work has begun to characterize how altering characteristics of a fractal stimulus can affect synchronization

(Marmelat et al., 2014), so future work should continue to examine the nature of human synchronization to a variety of stimulus signal characteristics.

Much of the literature supports a loss of physiological complexity (i.e., moving toward more patterned behavior) associated with aging, illness, and dysfunction (Goldberger, Peng, et al., 2002; Lipsitz & Goldberger, 1992; Vaillancourt & Newell, 2002). It is suggested that these changes in complexity arise due to reduced connectivity between components of the system, such as degraded neural connections, which may lead to lower functionality (Lipsitz, 2002). This study supports previous findings with the observation that older healthy adults exhibited lower sample entropy of R-R intervals and stride intervals than younger healthy adults. Combined with evidence of cardiolocomotor coupling (Novak et al., 2007), it becomes more important, now, to consider the interaction of physiological rhythms across different systems (i.e. cardiac and locomotor systems).

The population examined included a convenience sample of healthy college students and very active, healthy older adults from the community. As the burden to participate was likely higher on the older adults (traveling to campus, busier schedules, etc.), and these adults had to exhibit the same healthy characteristics as the younger adults, it is likely that these older adults were exceptionally healthy and motivated and were not experiencing many of the hallmarks common to aging, a notion supported by their exercise frequency and duration as well as their PWS (i.e., it was faster than the younger group's PWS). Examining a more diverse population that has exhibited more

common signs of aging, it is likely that our findings would be more pronounced, supporting the case for gait synchronization to modify gait rhythms and cardiac rhythms.

Future studies should be designed to understand the mechanisms of coupling between physiological subsystems. This will lead to creating new interventions designed to restore healthy system dynamics in older or unhealthy individuals, ultimately leading to more adaptive and functional improvements in these populations (Manor & Lipsitz, 2013). It is important to link experimental findings with theoretical and mechanical underpinnings, such as loss of complexity theory and physiological coupling, to further progress our understanding of how healthy (and unhealthy) physiological function emerges. Physiological coupling has been previously examined by measuring the correlation between coinciding cardiac and step intervals (Novak et al., 2007), identifying periods in which heart rate and step rate are very near equal (Kirby et al., 1989), identifying time periods in which the relative timing of physiological events (cardiac, locomotor, and respiratory) remained consistent (Niizeki et al., 1993), and quantifying the recurring patterns present across cardiac and respiratory rhythms (Censi et al., 2002). These studies demonstrate that there is a natural phenomenon of coupling in physiological subsystems. It has further been suggested that uncoupling of physiological subsystems may help explain the pathogenesis of multiple organ dysfunction (Godin & Buchman, 1996). Future work could expand upon these studies by introducing more challenging or constraining tasks with well-defined dynamic characteristics to understand how interventions could be designed to improve physiological rhythms across multiple systems. Continuing to understand individual subsystem dynamics and response to

constraints (i.e., interventions) combined with a foundational understanding of how systems couple in varying tasks will lead to improved intervention design that can be more selective in changing physiological subsystems' dynamics.

In conclusion, this study showed that younger and older healthy adults exhibited similar changes in gait rhythms when synchronizing their step timing to a visual metronome, but no changes during a fast walking task. Similarly, cardiac dynamics changed during only the gait synchronization task. This suggests the potential for specific walking tasks to be designed to alter cardiac and gait dynamics simultaneously and in a specified manner.

Figure 10. Experimental Setup Illustrating Gait Synchronization Task. Alternating left and right footprints were presented to the participant on a projection screen during treadmill walking. The timing between steps exhibited fractal characteristics. Adapted from Rhea et al. (2014).

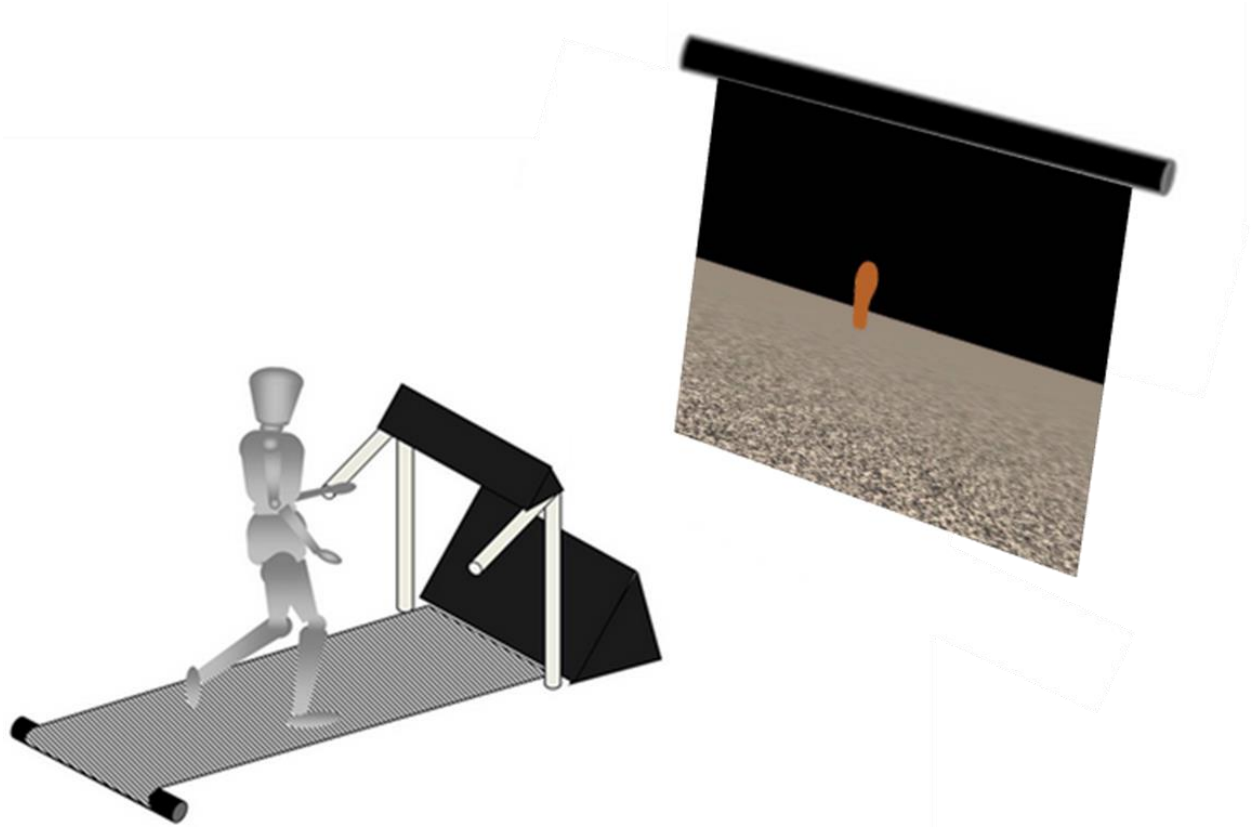

CHAPTER VI

MANUSCRIPT III

Introduction

Aging throughout adulthood leads to changes in the rhythmicity of the cardiac system. Average and maximum heart rate becomes slower with age, leading to lower cardiac reserve to complete strenuous tasks. Moreover, the variability in time between heart beats changes as we age, which has been associated with decreased functional ability in the cardiac system (Amaral, Goldberger, Ivanov, & Stanley, 1998; Iyengar et al., 1996; Pikkujämsä et al., 1999). For example, congestive heart failure is often characterized by overly regular timing between heart beats (i.e., very low variability), whereas myocardial infarction exhibits highly variable and complex patterns between heart beats (Costa et al., 2005; Glass, 2001; Y.-L. Ho et al., 2011; Mourot, 2014). Collectively, research on the rhythmicity of heart beat behavior has been informative about cardiac health. However, very little research has examined how cardiac factors influence fundamental movement patterns, such as walking.

Similar to cardiac behavior, gait rhythmicity changes throughout adulthood. The parallels between cardiac and gait behavior are strikingly similar. Gait speed slows and stride time variability changes with age; both of which area associated decreased functional ability, leading to an increase in fall rate (Hausdorff, 2007; Herman et al.,

2005; Morrison & Newell, 2012; Öberg et al., 1993). It is no surprise that these indicators of dysfunction derived from rhythmicity occur across physiological subsystems, as each system plays a role in maintaining the overall function of a larger biological system (i.e., the human), sharing functional and structural components (Bailon, Garatachea, De La Iglesia, Casajus, & Laguna, 2013; Niizeki & Saitoh, 2014; Novak et al., 2007). Thus, behaviors of physiological subsystems in humans are inevitably coupled and observed changes in movement rhythms will likely coincide with changes in cardiac rhythms, and vice versa (Blain et al., 2009; Kirby et al., 1989; Niizeki & Saitoh, 2014; Novak et al., 2007). Despite the interconnected nature of cardiac and locomotor rhythms, directly quantifying the coupling between two physiological subsystems has rarely been done. Yet, as a framework, coupling across subsystems provides additional, important information about the current state (or level of function) of a complex system (i.e., a system with many interacting parts, such has human physiology). It is likely that coupling is enhanced when physiological demands are placed on an organism. With aging, declines in strength or stroke volume make it more necessary for the body's physiological subsystems to work in concert to maintain adequate function. Therefore, quantifying the coupling between the cardiac and locomotor system as a function of aging could lead to a more holistic understanding of how the subsystems are linked, potentially opening up new pathways for assessment and rehabilitation.

The notion of cardiolocomotor coupling has been previously examined. Kirby et al. (1989) identified the consistency between heart and step rates during walking and running on a treadmill, as well as when cycling on an ergometer. Similarly, Niizeki et al.

(1993) observed consistency in the relative timing of steps within a cardiac cycle and classified this as coupling of the two systems. Novak, et al. (2007) found enhanced correlation between cardiac and step intervals in elderly individuals and provided a simple model to explain how cardiac and locomotor rhythms may be coupled and increased in relation to aging. Together, these papers suggest that cardiolocomotor coupling may be related to the functional capacity of the physiological system, which is dependent on the integration of its subsystems. Thus, coupling may increase as needed in order to complete the task demands. While previous research in this area has contributed to our understanding of cardiolocomotor coupling, most work in this area has examined concurrent changes in both systems using linear statistical methods (e.g., correlations between systems, relative phase of events, etc.).

One issue that must be navigated in this area is selecting an appropriate measurement from the wealth of techniques available to assess dynamic behaviors of complex systems, synchronization, and coupling. Cardiac and locomotor control systems are nonlinear in their behaviors, and therefore, it is likely that their coupling characteristics will also exhibit nonlinear properties. Recurrence quantification analysis offers a unique way to quantify the coupling relationship between physiological systems by considering the each signal's completely in relation to the other. It is also important to note that cardiolocomotor coupling may change when task demands are altered, which would provide further insight into the holistic nature of the system. Thus, taking advantage of advances in measurement and analytic techniques, in conjunction with

altered task demands may provide novel information about cardiolocomotor coupling as a function of aging.

The purpose of this study was to quantify the coupling of cardiac and locomotor rhythms in younger and older healthy adults during two treadmill walking tasks, each with a different task demand. We hypothesized that older adults would exhibit higher levels of cardiolocomotor coupling than younger adults. Moreover, this coupling relationship would increase in both groups when task demands are increased in each treadmill walking task.

Methods

Participants

Fifty-one healthy, physically active participants provided informed consent to participate in the study. A convenience sample of twenty-five younger adults (24.57±4.29 yrs, 1.76±0.09 m, 73.34±15.35 kg) and twenty-six older adults (67.67±4.70 yrs, 1.72±0.09 m, 70.13±14.30 kg) were recruited from the University of North Carolina at Greensboro and regional activity groups (i.e., hiking, running, and cycling). This data was collected as part of a larger study (Wittstein, Starobin, et al., n.d.-a) and participant characteristics are summarized in Table 4. All procedures for the study were approved by the University of North Carolina at Greensboro Institutional Review Board.

Experimental Design

The experiment was conducted during two sessions on separate days with at least 96 hours apart (200.8±119.0 hours between). During the first session only, participants completed an intake questionnaire about health history and lifestyle, the SF-36 Health

Survey (Optum, Eden Prairie, MN), and had their height and mass recorded. The intake questionnaire included questions to assess participants' risk of exercise. Participants classified as high risk according to the American College of Sports Medicine Guidelines for Exercise Testing and Prescription (Ehrman, 2010) were excluded from the study. Additionally, each participant's preferred walking speed (PWS) was identified during the first testing session. PWS was identified using an iterative process in which participants were instructed to request increases or decreases in treadmill speed until they felt like they were at a comfortable pace. Participants started with slow walking (0.5 m/s) and asked for increases in speed then repeated the process starting with fast walking (2.0 m/s) and asking for decreases in speed. This process was repeated until consecutive trials were within 0.2 m/s of each other. PWS was recorded as the average of the two speeds the participants settled upon.

Each testing session consisted of three 15-minute phases: (1) pre-test phase, (2) experimental phase, and (3) post-test phase. During the pre-test and post-test phases, participants walked on the treadmill at their PWS without any instructions. During the experimental phase, participants were asked to perform a gait synchronization task while walking or walk at a faster speed. These experimental conditions were counterbalanced such that half the participants completed the gait synchronization and fast walking tasks during their first and second sessions, respectively. While walking on the treadmill, electrocardiographs and gait kinematics were recorded simultaneously.

In the gait synchronization task, participants walked on the treadmill at their PWS while matching the timing of their heel strike to a visual metronome projected before

them. The metronome showed blinking left and right feet on a moving ground and black background (Figure 10). A fractal time series (DFA $\alpha = 0.98$) was constructed with the same mean stride time as the participant and was used to define the time between footprint appearance on the screen. In the fast walking task, participants walked at 125% of their PWS without any visual cues. The gait synchronization task and the fast walking task were selected as experimental manipulations because both task have been previously shown to increase task demands during walking, hereby altering gait variability in a specific and predictable manner (Jordan et al., 2007b; Rhea, Kiefer, D'Andrea, et al., 2014). Thus, cardiolocomotor coupling could be examined in this context to investigate the concurrent behavior of the cardiac and locomotor systems when task demands are increased.

Instrumentation

A model of the lower limbs (i.e., pelvis, thigh, shank, foot) was constructed from retroreflective markers placed bilaterally on the anterior superior iliac spine, posterior superior iliac spine, greater trochanter of the femur, medial and lateral condyle of the femur, medial and lateral malleoli, calcaneus, and first and fifth metatarsal heads, along with rigid plates consisting of 4 markers on each thigh and shank segment. An 8-camera motion capture system (Qualisys AB, Gothenburg, Sweden) recorded movement data at 200 Hz during each 15-minute phase. An MP-150 Data Acquisition System (Biopac Systems, Inc., Goleta, CA) was used to record ECG data at 1000 Hz. Three Ag/AgCl electrodes were place on the torso of each participant (below the left and right clavical

and just above the left anterior superior iliac spine) to form an Einthoven's triangle. Lead I electrical activity was recorded from the right shoulder to left shoulder.

Data Reduction

Raw ECG signals were converted to beat-to-beat interval time series (R-R time series) and position data into stride interval time series. The coupling of the two time series could then be calculated during each phase using order pattern recurrence plots (Wittstein, Starobin, et al., n.d.-b).

To reduce the raw ECG data to R-R time series, data were detrended and filtered. Nonlinear trends were removed by subtracting a best fit 6th order from the signal. Likewise, high frequency noise was removed using a 7th order Savitzky-Golay filter applied to sliding windows of 21 data points (Hargittai, 2005). R-peaks and S-peaks (or troughs) were then identified as any local maxima or minima more than three standard deviations from the mean signal. Traditionally, R-R interval is calculated as the time between R-peaks. However, in some cases due to axis deviation of the ECG signal, identifying R-peaks was problematic with several false peaks being identified. In cases in which the average distance away from the mean ECG signal was smaller for the R-peak than that of the S-peak, the R-peaks were reidentified by finding the local maxima within 0.1 seconds prior to the S-peak. R-R interval time series were constructed from the time between R-peaks after the detrending, filtering, and R-peak identification were completed. Finally, outliers greater than 2 SD from the local (±10 epochs) mean of R-R intervals were identified and replaced with the local median. In cases at the beginning

and end of the trial where there were not 10 intervals before or after, a total of 20 intervals was still used to calculate the median replacement and local mean.

Visual 3-D (C-Motion, Bethesda, MD) was used to calculate stride interval time series from position data. Position data were first smoothed using a bidirectional 2nd order butterworth filter with lowpass cutoff frequency of 6 Hz. The velocity (derivative of position) of the calcaneus marker in the sagittal plane was used to identify heel contact times (Zeni Jr et al., 2008). The time between consecutive heel contacts of the same foot was used to construct left and right stride interval time series. Only the right stride interval time series was used for analysis because previous research has indicated no difference in stride interval dynamics between legs during walking (Rhea, Kiefer, D'Andrea, et al., 2014).

R-R interval and stride interval time series were resampled to have a measurement of heart beat at each second from 0 to 900 seconds (901 data points). To account for issues with resampling the data near the end points, the first and last ten data points were truncated from each time series. Order pattern recurrence plots were constructed by symbolically transforming each time series into local ordinal structures then identifying recurrent patterns between the two time series. Specific details of this methodology were described by Groth (2005) with electroencephalograms. These methods were refined for use with cardiac and locomotor signals (Wittstein, Starobin, et al., n.d.-b). In short, the order patterns represent the local transition data points and are coded to uniquely represent a patter. For an order of two consecutive data points there are only two possible patterns (a positive slope or negative slope). By examining three or more consecutive

data points to define order patterns, the patterns become more complex. Order patterns were defined using sets of three consecutive data points. To quantify the coupling between the time series, recurrent points (identical order patterns) were identified for the entire time series. The relative recurrence rate was calculated as the amount of recurrence at a given time lag with respect to the total recurrence at all observed time lags. Last, the coupling index is calculated as the Shannon entropy of relative recurrence rate within a window. Coupling index was calculated for 60 evenly spaced windows using lag lengths of ±15 data points. The average coupling index and heart rate for the entire time series was reported, representing the overall level of coupling during each 15-minute walking trial.

Statistical Approach

The dependent variable was the average coupling index and the independent variables were group (younger or older), experiment condition (gait synchronization task or fast walking task), and phase (pre-test, experimental, or post-test). A three way (GROUP x EXPERIMENT x PHASE) repeated measures ANOVA was used to test for statistical significance. Hotelling's Trace was used as the test criterion. Follow-up Bonferroni adjusted t-tests were used where appropriate. Alpha was set a priori to 0.05. Effects sizes (Cohen's *d*) were calculated $[(\mu_{a} - \mu_{b})/\sigma_{pooled}]$ and interpreted to examine the magnitude of differences between and within groups (Cohen, 1992).

Results

A repeated measures ANOVA indicated a main effect of PHASE for the heart rate of participants ($F_{2,46}$=16.739, p<0.001, partial η^2=.421). No other effects were identified.

The average heart rate for the older group ranged from 84.3±9.2 beats per minute (bpm) during the pre-test on the synchronization day to 93.2±19.8 bpm during the fast walking phase. Meanwhile, the younger group exhibited average heart rates ranging from 88.7±20.5 bpm during the post-fast walking test to 97.6±18.0 bpm during the gait synchronization test.

A main effect was identified for PHASE ($F_{2,46}$=6.605, p=0.003, partial η^2=.223). Specifically, the experimental conditions exhibited a 14.8% increase in cardiolocomotor coupling compared to the pre-test (p=0.002, Cohen's d = 0.692) and was 13.3% higher than the post-test phase (p=0.007, Cohen's d = 0.608). The pre-test and post-test phases were not significantly different. Results are illustrated in Figure 11. A GROUP x PHASE interaction neared significance ($F_{2,46}$=2.439, p=0.098, partial η^2=.098). To explore this interaction, the between and within group effect sizes were calculated and are presented in Table 7.

Table 7. Effect Sizes (Cohen's d) for Between and Within Group Comparisons.

Between group effect sizes						
	Gait synchronization task			Fast walking task		
	Younger adults vs older adults			Younger adults vs older adults		
	pre-test	exp	post-test	pre-test	exp	post-test
	0.686	0.117	0.455	0.510	0.244	0.046
Within group effect sizes						
	Gait synchronization task			Fast walking task		
	pre-test vs. exp	pre-test vs. post-test	exp vs. post-test	pre-test vs. exp	pre-test vs. post-test	exp vs. post-test
younger	0.153	0.017	0.143	0.255	0.167	0.326
older	0.755	0.220	0.608	0.771	0.259	0.668

Discussion

This study quantified cardiolocomotor coupling in younger and older adults during treadmill walking tasks where the demands were increased. The data demonstrate that both older and younger healthy adults exhibit enhanced cardiolocomotor coupling when tasked with a step timing constraint or increased speed during treadmill walking. However, comparing the effect size between the pre-test to experimental phases within each group, enhanced coupling appeared to more pronounced in the older population, suggesting that aging alters the coordination between the cardiac and locomotor systems in order to adapt to increased task demands. The age group by phase interaction neared significance, so we elected to use effects sizes to continue exploring this observation. Since both populations were able to successfully complete both waking tasks, this highlights the notion that increased cardiolocomotor coupling develops with aging in order to get the same motor output (treadmill task completion). This supports the possibility to use cardiolocomotor coupling to assess the physiological demand placed on a system by either task, environment, or even aging and pathology. Additionally, this could be used to quantify the ability of a person to adapt to cardiac or locomotor tasks and constraints.

Previous research on cardiolocomotor coupling has led to two, seemingly antithetical interpretations about the nature of the coupling. An increase in cardiolocomotor coupling was shown to relate to improved performance of motor tasks (Blain et al., 2009; Phillips & Jin, 2013), suggesting that increased coupling reflects enhanced functional ability. However, increased cardiolocomotor coupling has also been

observed in older adults and pathological populations (Kirby et al., 1989; Novak et al., 2007), suggesting that increased coupling reflects decreased functional ability. It could be argued, however, that these two observations are simply different mechanisms by which the demands on the system are increased. Therefore, a common theme between previous cardiolocomotor coupling research – supported by data in the current paper – is that coupling may be used by an organism when it has a need for more efficiency as in a more difficult task.

In the current study, we demonstrated a similar increase in cardiolocomotor coupling between our two experimental conditions. Although the nature of the task demands were different, both experimental conditions altered the task demands relative to the pre-test phase and led to an increase in cardiolocomotor coupling to adapt to the tasks. When the task constraints were removed (i.e. during the post-test phase) the cardiolocomotor coupling decreased. Looking more closely, the older population experienced at 17.6% increase during gait synchronization and 31.2% increase during fast walking, large effect sizes (Cohen's d = 0.755 and 0.771, respectively). Meanwhile, the younger group only experienced 3.2% and 8.9% increases during gait synchronization and fast walking conditions, respectively.

It is logical that a younger, and likely healthier neural network would allow a younger participant to couple less and still complete the fast walking and gait synchronization tasks successfully. Likewise, less complex neural networks that may be common in older adults could force coupling to play a more prominent role in adapting control systems to task demands. Our results suggest that both older and younger adults

were able to adapt to an increase in walking task demands, but they used different pathways to complete the task. The older adults increased their coupling as a survival mechanism, per se, while the younger adults did not. This highlights the flexible nature of our cardiac and locomotor systems as we age in order maintain functional ability when new task demands are presented or removed.

A limitation of this study is that it only included healthy younger and older adults. Because of the health quality of these groups, it may have led to smaller coupling index values – though larger than the coupling observed between a random signal and a sinusoid (Wittstein, Starobin, et al., n.d.-b). However, this is a necessary first step to understand the typical behavior of cardiolocomotor coupling. Future work should expand this methodology to incorporate pathological populations across a wider range of physiological subsystems and experimental conditions. For example, Groth (2005) demonstrated increased coupling of electroencephalogram channels is associated with the onset of epileptic seizures. However, it is unclear whether coupling caused the seizure or if coupling was a result of another neurological deficit. This brings up the importance to consider that coupling likely plays a role in both healthy and unhealthy function. It is therefore imperative to continue to examine coupling in healthy and pathological populations under varying task demands. Finally, associating individual system dynamics in addition to coupling of systems to other markers of health function and decline may provide new evidence and possibilities to develop diagnostics, assessments, and treatments for a wide range of ailments.

In conclusion, it is becoming increasingly important to consider the implication of one physiological subsystem's function on another (Lipsitz, 2002; Manor & Lipsitz, 2013). By examining coupling, we can get stronger insight into an individual's functional health status. This study demonstrated that older adults may have developed a pathway of relying more heavily on coupling physiological subsystems to adapt to challenging physical demands compared to younger adults.

Figure 11. Cardiolocomotor Coupling in Older (blue) and Younger (yellow) Healthy Adults. Results are illustrated with both numerical values for coupling (bars with standard error) and as a percentage of the pre-test value (at 100% in green) of coupling (lines).

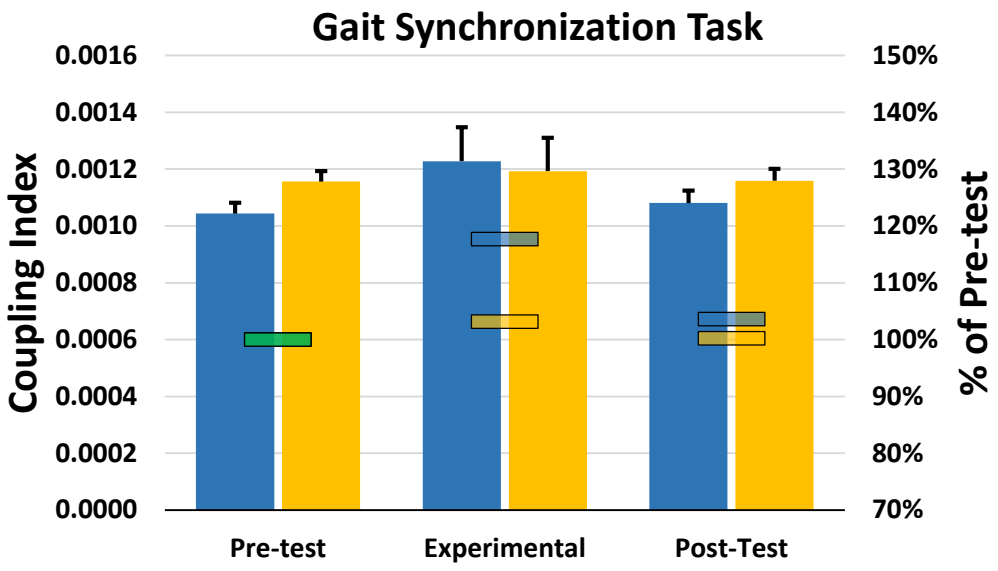

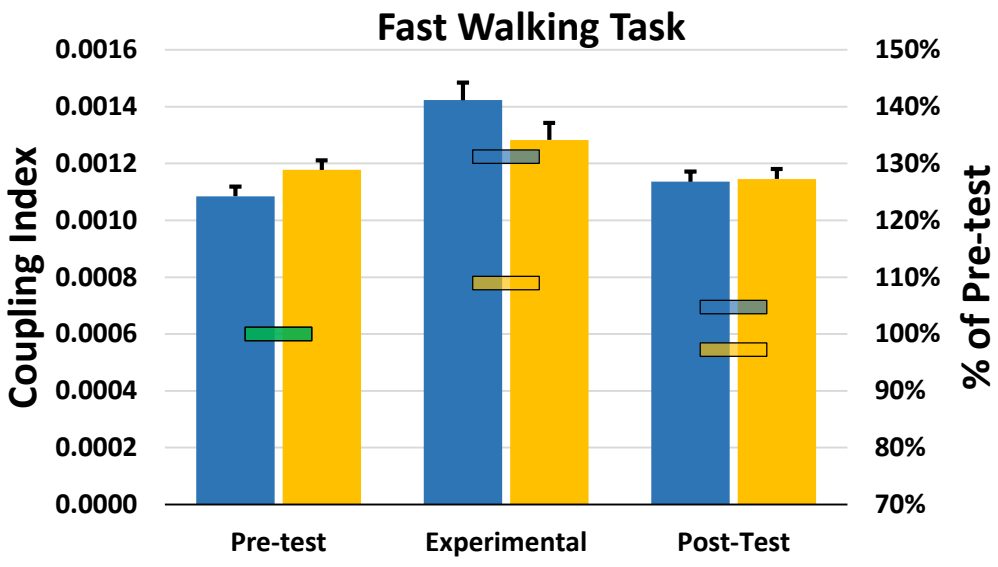

CHAPTER VII

DISCUSSION

This dissertation research was designed to quantify the coupling of cardiac and locomotor rhythms in younger and older healthy adults. It has been previously suggested that the dynamics within and between (i.e., coupling) physiological subsystems is a marker of both individual system function and overall health of an individual (Lipsitz, 2002; Manor & Lipsitz, 2013; Schulz et al., 2013). To this end, better understanding the natural rhythms as they relate to healthy aging will lead to deeper understanding of how functional and dysfunctional health evolves. To accomplish this, first, a technique to study cardiac and locomotor coupling was refined and tested on synthetic (i.e., sine waves and Gaussian noise) and experimental data. Second, an experiment was conducted to measure the cardiac and locomotor rhythms in healthy adults during normal treadmill walking, during a gait synchronization task, and during a fast walking task. The data from this experiment support previous research indicating that changes in gait rhythms are task dependent. Importantly, it adds to this body of research by concurrently observing cardiac dynamics and quantifying the coupling between the two systems.

Many studies in physiological variability are limited to studying each physiological subsystem separately (Acharya et al., 2002; Faust & Bairy, 2012; Hausdorff, 2005; Stergiou & Decker, 2011). However, this approach hinders the ability to consider human health more holistically. Humans are complex organisms composed of an

untold number of components interconnected through common neuronal pathways, shared resources (e.g., oxygen, sodium, etc.), and ultimately the functional purpose to maintain life. This massive network only exacerbates the importance of considering health a function of how systems work together, as opposed to how one system is failing. Examining the common dynamics and coupling between physiological signals is an entry point to accomplishing this task.

Conducting novel and meaningful research requires the application of analytical techniques to new applications. Groth (2005) presented a method of quantifying the coupling of time series using recurrence patterns applied to the analysis of EEG signals. Not only did these findings demonstrate the utility of order pattern recurrence plots, it also demonstrated how the coupling of EEG signals may relate to the onset of epileptic seizure. However, this method had not yet been used to examine the coupling of two different physiological susbsystems. The first part of this dissertation aimed to extend this work to examine cardiolocomotor coupling and compare its measurement to the coupling of known synthetic signals of theoretically (but qualitatively) known amounts of coupling. The present data demonstrated that phase shifted sinusoids (theoretically highly coupled) exhibit coupling on a much larger scale than uncoupled signals (i.e., two random signals or a sinusoid to a random signal) or than cardiolocomotor coupling. Interestingly, however, cardiolocomotor coupling was also significantly greater than the sets of uncoupled signals. This provides a starting point to understand the meaning of coupling index as calculated from recurrence plots and supports previous literature

describing physiological subsystems as coupled (Diab, Hassan, Boudaoud, Marque, & Karlsson, 2013; Schulz et al., 2013; Strogatz et al., 1993)

The second part of this dissertation used gait tasks to predictably manipulate gait dynamics while observing the accompanying modifications of cardiac dynamics as well as the coupling between the two systems. Gait characteristics were altered using a visual metronome with fractal characteristics (Rhea, Kiefer, D'Andrea, et al., 2014) as well as a fast walking task (Jordan et al., 2007b). Pre-test and post-test phases of the experiment also allowed for comparison to normal walking and an assessment of short-term retention.

The first two hypotheses of this dissertation concerned the relationship of cardiac and locomotor dynamics to aging in healthy populations. The findings suggest that both younger and older healthy adults alter gait similarly when presented with a gait synchronization task or fast walking task. More importantly, the data revealed a PHASE x GROUP interaction effect during the gait synchronization experiment that may suggest control mechanisms differ with age. This study also demonstrated that cardiac dynamics are also altered during these tasks. This is important because it may allow clinicians to identify specific gait tasks to intervene and predictably alter cardiac dynamics in addition to gait dynamics.

The second hypothesis of this dissertation examined the coupling between cardiac and locomotor rhythms in relation to aging. Only a main effect for PHASE was identified for coupling, suggesting that younger and older adults exhibit similar changes in coupling due to increased task constraints. Though there were not clear group differences, the data

was suggestive of older adults demonstrating greater increases in cardiolocomotor coupling during gait synchronization and fast walking. This was supported by moderate to large effect sizes of coupling within the older group and smaller effect sizes in the younger group due to change from the pre-test to experimental phase.

Limitations to these findings should be considered. A convenience sample of healthy older and healthy younger adults may not illicit as diverse populations as desired. The older population was more active than the younger population, did not exhibit many of the hallmarks common of aging (such as sowed preferred walking speed) and may be more motivated to maintain or improve their physical health. Additionally, increasing the demands of the tasks would likely help identify a critical point in which a change in control strategy (i.e. changed dynamics or changed coupling) needs to occur in order to complete the task. Walking tasks with only moderate workload and little motivation for success may have limited these findings.

In all, this research supports the following conclusions: (1) the coupling between diverse pairs of physiological signals (in this case, cardiac and locomotor) can be quantified using order pattern recurrence plots, (2) a gait synchronization task and a fast walking task alter both gait and cardiac dynamics in both healthy younger and older adults, (3) task related changes in cardiac and gait dynamics may also be age dependent, (4) and cardiolocomotor coupling appears to manifest when task constraints or increased workload are placed on an individual, regardless of their age. Continued study in this area should test these phenomena on more diverse populations, especially those that exhibit known deficits to one physiological subsystem of interest. Additionally, future work

should try to empirically test mechanisms, such as baroceptor reflex, thought to be responsible for coupling relationships between physiological subsystems.

REFERENCES

Aboy, M., Cuesta-Frau, D., Austin, D., & Micó-Tormos, P. (2007). Characterization of sample entropy in the context of biomedical signal analysis. In *Annual International Conference of the IEEE Engineering in Medicine and Biology - Proceedings* (pp. 5942–5945). http://doi.org/10.1109/IEMBS.2007.4353701

Acharya, R. U., Joseph, K. P., Kannathal, N., Lim, C. M., & Suri, J. S. (2006). Heart rate variability: a review. *Medical and Biological Engineering and Computing*, *44*(12), 1031–1051.

Acharya, R. U., Lim, C. M., & Joseph, P. (2002). Heart rate variability analysis using correlation dimension and detrended fluctuation analysis. *ITBM-RBM*, *23*(6), 333–339.

Amaral, L. A. N., Goldberger, A. L., Ivanov, P. C., & Stanley, H. E. (1998). Scale-independent measures and pathologic cardiac dynamics. *Physical Review Letters*, *81*(11), 2388.

Angelini, L., Maestri, R., Marinazzo, D., Nitti, L., Pellicoro, M., Pinna, G. D., … Tupputi, S. A. (2007). Multiscale analysis of short term heart beat interval, arterial blood pressure, and instantaneous lung volume time series. *Artificial Intelligence in Medicine*, *41*(3), 237–250.

Bailon, R., Garatachea, N., De La Iglesia, I., Casajus, J. A., & Laguna, P. (2013). Influence of running stride frequency in heart rate variability analysis during treadmill exercise testing. *IEEE Transactions on Biomedical Engineering*, *60*, 1796–1805. http://doi.org/10.1109/TBME.2013.2242328

Bank, P. J., Roerdink, M., & Peper, C. E. (2011). Comparing the efficacy of metronome beeps and stepping stones to adjust gait: steps to follow! *Exp Brain Res*, *209*(2), 159–169. http://doi.org/10.1007/s00221-010-2531-9

Beckers, F., Ramaekers, D., & Aubert, A. E. (2001). Approximate entropy of heart rate variability: validation of methods and application in heart failure. *Cardiovascular Engineering: An International Journal*, *1*(4), 177–182.

Berntson, G. G., Bigger Jr, J. T., Eckberg, D. L., Grossman, P., Kaufmann, P. G., Malik, M., … others. (1997). Heart rate variability: Origins, methods, and interpretive caveats. *Psychophysiology*.

Blain, G., Meste, O., Blain, A., & Bermon, S. (2009). Time-frequency analysis of heart rate variability reveals cardiolocomotor coupling during dynamic cycling exercise in humans. *American Journal of Physiology-Heart and Circulatory Physiology*, *296*(5), H1651–H1659.

Brach, J. S., Berlin, J. E., VanSwearingen, J. M., Newman, A. B., & Studenski, S. A. (2005). Too much or too little step width variability is associated with a fall history in older persons who walk at or near normal gait speed. *J Neuroeng Rehabil*, *2*, 21. http://doi.org/10.1186/1743-0003-2-21

Brach, J. S., Studenski, S. A., Perera, S., VanSwearingen, J. M., & Newman, A. B. (2008). Stance time and step width variability have unique contributing impairments in older persons. *Gait Posture*, *27*(3), 431–439. http://doi.org/10.1016/j.gaitpost.2007.05.016

Bravi, A., Longtin, A., & Seely, A. J. E. (2011). Review and classification of variability analysis techniques with clinical applications. *BioMedical Engineering OnLine*, *10*(1), 90. http://doi.org/10.1186/1475-925X-10-90

Bryan, W. L., & Harter, N. (1897). Studies in the Physiological and Psychology of the Telegraphic Language. *Psychological Review*, *4*(1), 27–53.

Buzzi, U. H., & Ulrich, B. D. (2004). Dynamic Stability of Gait Cycles as a Function of Speed and System Constraints. *Motor Control*, *8*(3), 241–254.

Camm, A. J., Malik, M., Bigger Jr, J. T., Breithardt, G., Cerutti, S., Cohen, R. J., … others. (1996). Heart rate variability: standards of measurement, physiological interpretation and clinical use. Task Force of the European Society of Cardiology and the North American Society of Pacing and Electrophysiology. *Circulation*, *93*(5), 1043–1065. http://doi.org/10.1161/01.CIR.93.5.1043

Censi, F., Calcagnini, G., & Cerutti, S. (2002). Coupling patterns between spontaneous rhythms and respiration in cardiovascular variability signals. *Computer Methods and Programs in Biomedicine*, *68*(1), 37–47.

Cohen, J. (1992). Statistical Power Analysis. *Current Directions in Psychological Science (Wiley-Blackwell)*, *1*, 98–101. http://doi.org/10.1111/1467-8721.ep10768783

Costa, M. D., Goldberger, A. L., & Peng, C.-K. (2002). Multiscale Entropy Analysis of Complex Physiologic Time Series, 6–9. http://doi.org/10.1103/PhysRevLett.89.068102

Costa, M. D., Goldberger, A. L., & Peng, C.-K. (2005). Multiscale entropy analysis of biological signals. *Phys Rev E Stat Nonlin Soft Matter Phys*, *71*(2 Pt 1), 21906. Retrieved from http://www.ncbi.nlm.nih.gov/pubmed/15783351

Costa, M. D., Peng, C.-K., & Goldberger, A. L. (2008). Multiscale analysis of heart rate dynamics: entropy and time irreversibility measures. *Cardiovasc Eng*, *8*(2), 88–93. http://doi.org/10.1007/s10558-007-9049-1

Crystal, G. J., & Salem, M. R. (2012). The Bainbridge and the “reverse” Bainbridge reflexes: history, physiology, and clinical relevance. *Anesthesia & Analgesia*, *114*(3), 520–532.

Davids, K., Bennett, S., & Newell, K. M. (2006). *Movement System Variability*. Human Kinetics. Retrieved from http://books.google.com/books?id=IAamvxsVlGAC

Davids, K., Glazier, P., Araújo, D., & Bartlett, R. (2003). Movement systems as dynamical systems. *Sports Medicine*, *33*(4), 245–260.

Diab, A., Hassan, M., Boudaoud, S., Marque, C., & Karlsson, B. (2013). Nonlinear estimation of coupling and directionality between signals: Application to uterine EMG propagation. In *Proceedings of the Annual International Conference of the IEEE Engineering in Medicine and Biology Society, EMBS* (pp. 4366–4369). http://doi.org/10.1109/EMBC.2013.6610513

Diniz, A., Wijnants, M. L., Torre, K., Barreiros, J., Crato, N., Bosman, A. M. T., … Delignières, D. (2011). Contemporary theories of 1/f noise in motor control. *Human Movement Science*, *30*(5), 889–905. http://doi.org/10.1016/j.humov.2010.07.006

Eckmann, J., Kamphorst, S. O., & Ruelle, D. (1987). Recurrence plots of dynamical systems. *EPL (Europhysics Letters)*, *4*(9), 973.

Eduardo Virgilio Silva, L., & Otavio Murta, L. (2012). Evaluation of physiologic complexity in time series using generalized sample entropy and surrogate data analysis. *Chaos (Woodbury, N.Y.)*, *22*(4), 043105. http://doi.org/10.1063/1.4758815

Ehrman, J. K. (2010). *ACSM Guidelines for Exercise Testing and Prescription, 8th Edition*. *Medicine & Science in Sports & Exercise* (Vol. 37). http://doi.org/9781609136055

Fabris, C., De Colle, W., & Sparacino, G. (2013). Voice disorders assessed by (cross-) Sample Entropy of electroglottogram and microphone signals. *Biomedical Signal Processing and Control*, *8*(6), 920–926. http://doi.org/10.1016/j.bspc.2013.08.010

Farina, D., Fattorini, L., Felici, F., & Filligoi, G. (2002). Nonlinear surface EMG analysis to detect changes of motor unit conduction velocity and synchronization. *Journal of Applied Physiology (Bethesda, Md. : 1985)*, *93*(5), 1753–63. http://doi.org/10.1152/japplphysiol.00314.2002

Faust, O., & Bairy, M. G. (2012). Nonlinear analysis of physiological signals: a review. *Journal of Mechanics in Medicine and Biology*, *12*(04).

Filligoi, G., & Felici, F. (1999). Detection of hidden rhythms in surface EMG signals with a non-linear time-series tool. *Medical Engineering & Physics*, *21*(6-7), 439–48. Retrieved from http://www.ncbi.nlm.nih.gov/pubmed/10624740

Frenkel-Toledo, S., Giladi, N., Peretz, C., Herman, T., Gruendlinger, L., & Hausdorff, J. M. (2005). Treadmill walking as an external pacemaker to improve gait rhythm and stability in Parkinson's disease. *Movement Disorders*, *20*(9), 1109–1114.

Gabell, A., & Nayak, U. S. (1984). The effect of age on variability in gait. *J Gerontol*, *39*(6), 662–666. Retrieved from http://www.ncbi.nlm.nih.gov/pubmed/6491179

Gates, D. H., & Dingwell, J. B. (2007). Peripheral neuropathy does not alter the fractal dynamics of stride intervals of gait. *Journal of Applied Physiology*, *102*(3), 965–971.

Georgoulis, A. D., Moraiti, C., Ristanis, S., & Stergiou, N. (2006). A novel approach to measure variability in the anterior cruciate ligament deficient knee during walking: the use of the approximate entropy in orthopaedics. *Journal of Clinical Monitoring and Computing*, *20*(1), 11–18. http://doi.org/10.1007/s10877-006-1032-7

Glass, L. (2001). Synchronization and rhythmic processes in physiology. *Nature*, *410*(6825), 277–284. http://doi.org/10.1038/35065745

Glass, L., & Mackey, M. C. (1988). *From clocks to chaos: the rhythms of life*. Princeton University Press.

Glazier, P. S., Davids, K., & Bartlett, R. (2003). Dynamical systems theory: a relevant framework for performance-oriented sports biomechanics research. *Sportscience*, *7*(retrieved from sportsci. org/jour/03/psg. htm).

Godin, P. J., & Buchman, T. G. (1996). Uncoupling of biological oscillators: a complementary hypothesis concerning the pathogenesis of multiple organ dysfunction syndrome. *Critical Care Medicine*, *24*(7), 1107–16. Retrieved from http://www.ncbi.nlm.nih.gov/pubmed/8674321

Goldberger, A. L. (1990). Chaos and fractals in human physiology. *Scientific American*. Retrieved from http://eric.ed.gov/?id=EJ409296

Goldberger, A. L., Amaral, L. A. N., Hausdorff, J. M., Ivanov, P. C., Peng, C.-K., & Stanley, H. E. (2002). Fractal dynamics in physiology: alterations with disease and aging. *Proceedings of the National Academy of Sciences of the United States of America*, *99 Suppl 1*, 2466–72. http://doi.org/10.1073/pnas.012579499

Goldberger, A. L., Peng, C.-K., & Lipsitz, L. A. (2002). What is physiologic complexity and how does it change with aging and disease? *Neurobiology of Aging*, *23*(1), 23–6. Retrieved from http://www.ncbi.nlm.nih.gov/pubmed/11755014

Gomez-Garcia, J. A., Martinez-Vargas, J. D., & Castellanos-Dominguez, G. (2011). Complexity-based analysis for the detection of heart murmurs. In *Engineering in Medicine and Biology Society, EMBC, 2011 Annual International Conference of the IEEE* (pp. 2728–2731).

Grassberger, P. (1991). Information and complexity measures in dynamical systems. In *Information dynamics* (pp. 15–33). Springer.

Grassberger, P. (2012). Randomness, information, and complexity. *arXiv Preprint arXiv:1208.3459*.

Groth, A. (2005). Visualization of coupling in time series by order recurrence plots. *Physical Review E*, *72*(4), 46220.

Grubaugh, J., & Rhea, C. K. (2014). Gait performance is not influenced by working memory when walking at a self-selected pace. *Experimental Brain Research*, *232*(2), 515–525.

Guzzetti, S., Magatelli, R., Borroni, E., & Mezzetti, S. (2001). Heart rate variability in chronic heart failure. *Autonomic Neuroscience*, *90*(1), 102–105.

Hales, S. (2000). Foundations of anesthesiology. *Journal of Clinical Monitoring and Computing*, *16*(1), 45–47.

Hargittai, S. (2005). Savitzky-Golay least-squares polynomial filters in ECG signal processing. In *Computers in Cardiology* (Vol. 32, pp. 763–766). http://doi.org/10.1109/CIC.2005.1588216

Hausdorff, J. M. (2005). Gait variability : methods , modeling and meaning Example of Increased Stride Time Variability in Elderly Fallers Quantification of Stride-to-Stride Fluctuations, *9*, 1–9. http://doi.org/10.1186/1743-Received

Hausdorff, J. M. (2007). Gait dynamics, fractals and falls: finding meaning in the stride-to-stride fluctuations of human walking. *Human Movement Science*, *26*(4), 555–89. http://doi.org/10.1016/j.humov.2007.05.003

Hausdorff, J. M., Mitchell, S. L., Firtion, R., Peng, C.-K., Cudkowicz, M. E., Wei, J. Y., & Goldberger, A. L. (1997). Altered fractal dynamics of gait: reduced stride-interval correlations with aging and Huntington's disease. *Journal of Applied Physiology*, *82*(1), 262–269.

Hausdorff, J. M., Purdon, P. L., Peng, C.-K., Ladin, Z., Wei, J. Y., & Goldberger, A. L. (1996). Fractal dynamics of human gait: stability of long-range correlations in stride interval fluctuations. *Journal of Applied Physiology*, *80*(5), 1448–1457.

Hausdorff, J. M., Rios, D. a, & Edelberg, H. K. (2001). Gait variability and fall risk in community-living older adults: a 1-year prospective study. *Archives of Physical Medicine and Rehabilitation*, *82*(8), 1050–6. http://doi.org/10.1053/apmr.2001.24893

Herman, T., Giladi, N., Gurevich, T., & Hausdorff, J. M. (2005). Gait instability and fractal dynamics of older adults with a "cautious" gait: why do certain older adults walk fearfully? *Gait & Posture*, *21*(2), 178–185.

Hessler, E. E. (2010). *Relative Phase Dynamics in Motor-Respiratory Coordination*. Arizona State University.

Ho, K. K. L., Moody, G. B., Peng, C.-K., Mietus, J. E., Larson, M. G., Levy, D., & Goldberger, A. L. (1997). Predicting survival in heart failure case and control subjects by use of fully automated methods for deriving nonlinear and conventional indices of heart rate dynamics. *Circulation*, *96*(3), 842–848.

Ho, Y.-L., Lin, C., Lin, Y.-H., & Lo, M.-T. (2011). The prognostic value of non-linear analysis of heart rate variability in patients with congestive heart failure—a pilot study of multiscale entropy. *PloS One*, *6*(4), e18699.

Hove, M. J., Suzuki, K., Uchitomi, H., Orimo, S., & Miyake, Y. (2012). Interactive rhythmic auditory stimulation reinstates natural 1/f timing in gait of parkinson's patients. *PLoS ONE*, *7*. http://doi.org/10.1371/journal.pone.0032600

Iyengar, N., Peng, C.-K. K., Morin, R., Goldberger, A. L., & Lipsitz, L. A. (1996). Age-related alterations in the fractal scaling of cardiac interbeat interval dynamics. *The American Journal of Physiology*, *271*(4 Pt 2), R1078–R1084.

Jordan, K., Challis, J. H., Cusumano, J. P., & Newell, K. M. (2009). Stability and the time-dependent structure of gait variability in walking and running. *Human Movement Science*, *28*(1), 113–128.

Jordan, K., Challis, J. H., & Newell, K. M. (2007a). Speed influences on the scaling behavior of gait cycle fluctuations during treadmill running. *Hum Mov Sci*, *26*(1), 87–102. http://doi.org/10.1016/j.humov.2006.10.001

Jordan, K., Challis, J. H., & Newell, K. M. (2007b). Walking speed influences on gait cycle variability. *Gait & Posture*, *26*(1), 128–134.

Kaipust, J. P., McGrath, D., Mukherjee, M., & Stergiou, N. (2013). Gait variability is altered in older adults when listening to auditory stimuli with differing temporal structures. *Annals of Biomedical Engineering*, *41*(8), 1595–1603. http://doi.org/10.1007/s10439-012-0654-9

Kang, H. G., & Dingwell, J. B. (2008). Separating the effects of age and walking speed on gait variability. *Gait & Posture*, *27*(4), 572–577.

Kaplan, D. T., Furman, M. I., Pincus, S. M., Ryan, S. M., Lipsitz, L. A., & Goldberger, A. L. (1991). Aging and the complexity of cardiovascular dynamics. *Biophysical Journal*, *59*(4), 945–949.

Keller, K., & Lauffer, H. (2003). Symbolic Analysis of High-Dimensional Time Series. *International Journal of Bifurcation and Chaos*, *13*(9), 2657–2668. http://doi.org/10.1142/S0218127403008168

Kirby, R. L., Nugent, S. T., Marlow, R. W., MacLeod, D. A., & Marble, A. E. (1989). Coupling of cardiac and locomotor rhythms. *Journal of Applied Physiology (Bethesda, Md. : 1985)*, *66*, 323–329.

Kleiger, R. E., Miller, J. P., Bigger Jr, J. T., & Moss, A. J. (1987). Decreased heart rate variability and its association with increased mortality after acute myocardial infarction. *The American Journal of Cardiology*, *59*(4), 256–262.

Kreuz, T., Mormann, F., Andrzejak, R. G., Kraskov, A., Lehnertz, K., & Grassberger, P. (2007). Measuring synchronization in coupled model systems: A comparison of different approaches. *Physica D: Nonlinear Phenomena*, *225*(1), 29–42.

Krishnan, M. M. R., Sree, S. V., Ghista, D. N., Ng, E. Y. K., Swapna, Ang, A. P. C., … Suri, J. S. (2012). Automated diagnosis of cardiac health using recurrence quantification analysis. *Journal of Mechanics in Medicine and Biology*, *12*(04).

Kyriazis, M. (2003). Practical applications of chaos theory to the modulation of human ageing: nature prefers chaos to regularity. *Biogerontology*, *4*(2), 75–90. Retrieved from http://www.ncbi.nlm.nih.gov/pubmed/12766532

Labini, F. S., Meli, A., Ivanenko, Y. P., & Tufarelli, D. (2012). Recurrence quantification analysis of gait in normal and hypovestibular subjects. *Gait & Posture*, *35*(1), 48–55.

Lake, D. E., Richman, J. S., Griffin, M. P., & Moorman, J. R. (2002). Sample entropy analysis of neonatal heart rate variability. *American Journal of Physiology-Regulatory, Integrative and Comparative Physiology*, *283*(3), R789–R797.

Lin, A., Shang, P., & Zhong, B. (2014). Hidden cross-correlation patterns in stock markets based on permutation cross-sample entropy and PCA. *Physica A: Statistical Mechanics and Its Applications*, *416*, 259–272. http://doi.org/10.1016/j.physa.2014.08.064

Lipsitz, L. A. (2002). Dynamics of stability: the physiologic basis of functional health and frailty. *The Journals of Gerontology. Series A, Biological Sciences and Medical Sciences*, *57*(3), B115–25. Retrieved from http://www.ncbi.nlm.nih.gov/pubmed/11867648

Lipsitz, L. A., & Goldberger, A. L. (1992). Loss of complexity and aging. *The Journal of the American Medical Association*, *267*(13), 1806–1809. Retrieved from http://reylab.bidmc.harvard.edu/pubs/1992/jama-1992-267-1806.pdf

Liu, L. Z., Qian, X. Y., & Lu, H. Y. (2010). Cross-sample entropy of foreign exchange time series. *Physica A: Statistical Mechanics and Its Applications*, *389*(21), 4785–4792. http://doi.org/10.1016/j.physa.2010.06.013

Magagnin, V., Bassani, T., Bari, V., Turiel, M., Maestri, R., Pinna, G. D., & Porta, A. (2011). Non-stationarities significantly distort short-term spectral, symbolic and entropy heart rate variability indices. *Physiological Measurement*, *32*(11), 1775–86. http://doi.org/10.1088/0967-3334/32/11/S05

Manor, B. D., Hu, K., Peng, C.-K., Lipsitz, L. A., & Novak, V. (2012). Posturo-respiratory synchronization: effects of aging and stroke. *Gait Posture*, *36*(2), 254–259. http://doi.org/10.1016/j.gaitpost.2012.03.002

Manor, B. D., & Lipsitz, L. A. (2013). Physiologic complexity and aging: implications for physical function and rehabilitation. *Prog Neuropsychopharmacol Biol Psychiatry*, *45*, 287–293. http://doi.org/10.1016/j.pnpbp.2012.08.020

Marmelat, V., Torre, K., Beek, P. J., & Daffertshofer, A. (2014). Persistent fluctuations in stride intervals under fractal auditory stimulation. *PloS One*, *9*(3), e91949.

Marwan, N. (2008). A historical review of recurrence plots. *The European Physical Journal-Special Topics*, *164*(1), 3–12.

Marwan, N., Romano, M. C., Thiel, M., & Kurths, J. (2007). Recurrence plots for the analysis of complex systems, *438*, 237–329. http://doi.org/10.1016/j.physrep.2006.11.001

Marwan, N., Wessel, N., Meyerfeldt, U., Schirdewan, A., & Kurths, J. (2002). Recurrence-plot-based measures of complexity and their application to heart-rate-variability data. *Physical Review E*, *66*(2), 26702.

Molina-Picó, A., Cuesta-Frau, D., Aboy, M., Crespo, C., Miró-Martínez, P., & Oltra-Crespo, S. (2011). Comparative study of approximate entropy and sample entropy robustness to spikes. *Artificial Intelligence in Medicine*, *53*(2), 97–106. http://doi.org/10.1016/j.artmed.2011.06.007

Morrison, S., & Newell, K. M. (2012). Aging, neuromuscular decline, and the change in physiological and behavioral complexity of upper-limb movement dynamics. *Journal of Aging Research*, *2012*.

Mourot, L. (2014). Could Non-Linear Heart Rate Variability Analysis of Short RR Intervals Series Give Clinically Valuable Information in Heart Disease. *J Clin Exp Res Cardiol*, *1*(1), 104.

Mrowka, R., Cimponeriu, L., Patzak, A., & Rosenblum, M. G. (2003). Directionality of coupling of physiological subsystems: age-related changes of cardiorespiratory interaction during different sleep stages in babies. *American Journal of Physiology. Regulatory, Integrative and Comparative Physiology*, *285*(6), R1395–401. http://doi.org/10.1152/ajpregu.00373.2003

Naschitz, J. E., Rosner, I., Rozenbaum, M., Fields, M., Isseroff, H., Babich, J. P., … others. (2004). Patterns of cardiovascular reactivity in disease diagnosis. *Qjm*, *97*(3), 141–151.

Niizeki, K., Kawahara, K., & Miyamoto, Y. (1993). Interaction among cardiac, respiratory, and locomotor rhythms during cardiolocomotor synchronization. *Journal of Applied Physiology (Bethesda, Md. : 1985)*, *75*, 1815–1821.

Niizeki, K., & Saitoh, T. (2014). Cardiolocomotor phase synchronization during rhythmic exercise. *The Journal of Physical Fitness and Sports Medicine*, *3*(1), 11–20.

Norris, P. R., Stein, P. K., & Morris Jr, J. A. (2008). Reduced heart rate multiscale entropy predicts death in critical illness: a study of physiologic complexity in 285 trauma patients. *Journal of Critical Care*, *23*(3), 399–405.

Novak, V., Hu, K., Vyas, M., & Lipsitz, L. A. (2007). Cardiolocomotor coupling in young and elderly people. *The Journals of Gerontology. Series A, Biological Sciences and Medical Sciences*, *62*, 86–92.

Öberg, T., Karsznia, A., & Öberg, K. (1993). Basic gait parameters: reference data for normal subjects, 10-79 years of age. *Journal of Rehabilitation Research and Development*, *30*, 210.

Öberg, T., Karsznia, A., & Öberg, K. (1994). Joint angle parameters in gait: reference data for normal subjects, 10-79 years of age. *Journal of Rehabilitation Research and Development*, *31*(3), 199–213.

Pellecchia, G. L., & Shockley, K. (2005). Application of recurrence quantification analysis: Influence of cognitive activity on postural fluctuations. In *Tutorials in Contemporary Nonlinear Methods for the Behavioral Sciences*.

Peng, C.-K., Buldyrev, S. V, Havlin, S., Simons, M., Stanley, H. E., & Goldberger, A. L. (1994). Mosaic organization of DNA nucleotides. *Physical Review E*, *49*(2), 1685.

Peng, C.-K., Havlin, S., Stanley, H. E., & Goldberger, A. L. (1995). Quantification of scaling exponents and crossover phenomena in nonstationary heartbeat time series. *… Interdisciplinary Journal of …*. Retrieved from http://link.aip.org/link/?cha/5/82/1

Phillips, B., & Jin, Y. (2013). Effect of Adaptive Paced Cardiolocomotor Synchronization during Running: A Preliminary Study. *Journal of Sports Science & Medicine*, *12*(3), 381.

Pikkujämsä, S. M., Mäkikallio, T. H., Sourander, L. B., Räihä, I. J., Puukka, P., Skyttä, J., … Huikuri, H. V. (1999). Cardiac interbeat interval dynamics from childhood to senescence comparison of conventional and new measures based on fractals and chaos theory. *Circulation*, *100*(4), 393–399.

Pincus, S. M. (1994). Greater signal regularity may indicate increased system isolation. *Mathematical Biosciences*, *122*(2), 161–181.

Pincus, S. M., Gladstone, I. M., & Ehrenkranz, R. A. (1991). A regularity statistic for medical data analysis. *Journal of Clinical Monitoring*, *7*(4), 335–345.

Porta, a, Castiglioni, P., Bari, V., Bassani, T., Marchi, a, Cividjian, a, … Di Rienzo, M. (2013). K-nearest-neighbor conditional entropy approach for the assessment of the short-term complexity of cardiovascular control. *Physiological Measurement*, *34*(1), 17–33. http://doi.org/10.1088/0967-3334/34/1/17

Rhea, C. K., & Kiefer, A. W. (2014). Patterned variability in gait behavior: How can it be measured and what does it mean. In L. (Georgia S. U. Li & M. (Georgia S. U. Holmes (Eds.), *Gait Biometrics: Basic Patterns, Role of Neurological Disorders and Effects of Physical Activity* (pp. 17–44). Hauppauge, NY: Nova Science Publishers.

Rhea, C. K., Kiefer, A. W., D'Andrea, S. E., Warren, W. H., & Aaron, R. K. (2014). Entrainment to a real time fractal visual stimulus modulates fractal gait dynamics. *Human Movement Science*, *36*, 20–34.

Rhea, C. K., Kiefer, A. W., Wittstein, M. W., Leonard, K. B., MacPherson, R. P., Wright, W. G., & Haran, F. J. (2014). Fractal gait patterns are retained after entrainment to a fractal stimulus. *PloS One*, *9*(9), e106755. http://doi.org/10.1371/journal.pone.0106755

Rhea, C. K., Silver, T. A., Hong, S. L., Ryu, J. H., Studenka, B. E., Hughes, C. M. L., & Haddad, J. M. (2011). Noise and Complexity in Human Postural Control : Interpreting the Different Estimations of Entropy, *6*(3), 1–9. http://doi.org/10.1371/journal.pone.0017696

Rhea, C. K., Wittstein, M. W., Kiefer, A. W., & Haran, F. J. (2013). Retaining fractal gait patterns learned in virtual environments. In *International Conference on Virtual Rehabilitation*.

Richman, J. S., & Moorman, J. R. (2000). Physiological time-series analysis using approximate entropy and sample entropy. *Am J Physiol Heart Circ Physiol*, *278*(6), H2039–49. Retrieved from http://www.ncbi.nlm.nih.gov/pubmed/10843903

Riley, M. A., Balasubramaniam, R., & Turvey, M. T. (1999). Recurrence quantification analysis of postural fluctuations. *Gait & Posture*, *9*(1), 65–78.

Riley, M. A., Richardson, M. J., Shockley, K., & Ramenzoni, V. C. (2011). Interpersonal synergies. *Frontiers in Psychology*, *2*.

Riva, F., Toebes, M. J. P., Pijnappels, M., Stagni, R., & van Dieën, J. H. (2013). Estimating fall risk with inertial sensors using gait stability measures that do not require step detection. *Gait & Posture*, *38*(2), 170–174.

Rosano, C., Brach, J. S., Studenski, S. A., Longstreth Jr., W. T., & Newman, A. B. (2008). Gait variability is associated with subclinical brain vascular abnormalities in high-functioning older adults. *Neuroepidemiology*, *29*(3-4), 193–200. http://doi.org/10.1159/000111582

Rosenberg, J., Amjad, A., Breeze, P., Brillinger, D., & Halliday, D. (1989). The Fourier approach to the identification of functional coupling between neuronal spike trains. *Prog Biophys Molec Biol*, *53*(1980), 1–31.

Routledge, F. S., Campbell, T. S., McFetridge-Durdle, J. A., & Bacon, S. L. (2010). Improvements in heart rate variability with exercise therapy. *Canadian Journal of Cardiology*, *26*(6), 303–312.

Saul, J. P. (1990). Beat-to-beat variations of heart rate reflect modulation of cardiac autonomic outflow. *News Physiol Sci*, *5*(1), 32–37.

Scafetta, N., Marchi, D., & West, B. J. (2009). Understanding the complexity of human gait dynamics. *Chaos: An Interdisciplinary Journal of Nonlinear Science*, *19*(2), 26108.

Schmit, J. M., Riley, M. A., Dalvi, A., Sahay, A., Shear, P. K., Shockley, K. D., & Pun, R. Y. K. (2006). Deterministic center of pressure patterns characterize postural instability in Parkinson's disease. *Experimental Brain Research*, *168*(3), 357–367.

Schreiber, T. (2000). Measuring information transfer. *Physical Review Letters*, *85*(2), 461–464. http://doi.org/10.1103/PhysRevLett.85.461

Schulz, S., Adochiei, F., Edu, I., Schroeder, R., Costin, H., Bär, K., & Voss, A. (2013). Cardiovascular and cardiorespiratory coupling analyses: a review. *Philosophical Transactions. Series A, Mathematical, Physical, and Engineering Sciences*, *371*, 20120191. http://doi.org/10.1098/rsta.2012.0191

Schumacher, A. (2004). Linear and nonlinear approaches to the analysis of RR interval variability. *Biological Research for Nursing*, *5*(3), 211–221.

Seely, A. J. E., & Christou, N. V. (2000). Multiple organ dysfunction syndrome: exploring the paradigm of complex nonlinear systems. *Crit Care Med*, *28*(7), 2193–2200. Retrieved from http://www.ncbi.nlm.nih.gov/pubmed/10921540

Seigle, B., Ramdani, S., & Bernard, P. L. (2009). Dynamical structure of center of pressure fluctuations in elderly people. *Gait & Posture*, *30*(2), 223–226.

Shannon, C. E. (1948). A Mathematical Theory of Communication. *Bell Systems Technical Journal*, *27*, 379–423 & 623–656.

Shockley, K., Butwill, M., Zbilut, J. P., & Webber, Jr., C. L. (2002). Cross recurrence quantification of coupled oscillators. *Physics Letters A*, *305*(1), 59–69.

Stergiou, N., & Decker, L. M. (2011). Human movement variability, nonlinear dynamics, and pathology: is there a connection? *Hum Mov Sci*, *30*(5), 869–888. http://doi.org/10.1016/j.humov.2011.06.002

Stergiou, N., Harbourne, R. T., & Cavanaugh, J. (2006). Optimal movement variability: a new theoretical perspective for neurologic physical therapy. *Journal of Neurologic Physical Therapy : JNPT*, *30*(3), 120–9. Retrieved from http://www.ncbi.nlm.nih.gov/pubmed/17029655

Strogatz, S. H., Stewart, I., & others. (1993). Coupled oscillators and biological synchronization. *Scientific American*, *269*(6), 102–109.

Takens, F. (1981). Detecting strange attractors in turbulence. *Dynamical Systems and Turbulence, Warwick 1980*. Retrieved from http://link.springer.com/content/pdf/10.1007/BFb0091924.pdf

Thorndike, E. L. (1927). The Law of Effect. *The American Journal of Psychology*, *39*, 212–222.

Thorndike, E. L., Lay, W., & Dean, P. R. (1909). The Relation of Accuracy in Sensory Discrimination to General Intelligence. *The American Journal of Psychology*, *20*, 364–369.

Tochigi, Y., Segal, N. A., Vaseenon, T., & Brown, T. D. (2012). Entropy analysis of tri-axial leg acceleration signal waveforms for measurement of decrease of physiological variability in human gait. *Journal of Orthopaedic Research*, *30*(6), 897–904.

Uchitomi, H., Ota, L., Ogawa, K. ichiro, Orimo, S., & Miyake, Y. (2013). Interactive Rhythmic Cue Facilitates Gait Relearning in Patients with Parkinson's Disease. *PLoS ONE*, *8*(9). http://doi.org/10.1371/journal.pone.0072176

Vaillancourt, D., & Newell, K. M. (2002). Changing complexity in human behavior and physiology through aging and disease. *Neurobiology of Aging*, *23*(1), 1–11.

Van Orden, G. C., Kloos, H., & Wallot, S. (2009). Living in the pink: Intentionality, wellbeing, and complexity. *Philosophy of Complex Systems. Handbook of the Philosophy of Science*, *10*.

von Vierordt, K. (1881). Ueber das Gehen des Menschen in Gesunden und Kranken Zustaenden nach Selb-stregistrireden Methoden. *Tubingen: Laupp*.

Wayne, P. M., Manor, B., Novak, V., Costa, M. D., Hausdorff, J. M., Goldberger, A. L., … Lipsitz, L. A. (2013). A systems biology approach to studying Tai Chi, physiological complexity and healthy aging: Design and rationale of a pragmatic randomized controlled trial. *Contemporary Clinical Trials*, *34*(1), 21–34. http://doi.org/10.1016/j.cct.2012.09.006

Webber, Jr., C. L., & Zbilut, J. P. (1994). Dynamical assessment of physiological systems and states using recurrence plot strategies. *Journal of Applied Physiology*, *76*, 965–973. Retrieved from http://jap.physiology.org/content/76/2/965.short

West, B. J., & Griffin, L. (1998). Allometric control of human gait. *Fractals*, *6*(02), 101–108.

Willson, K., Francis, D. P., Wensel, R., Coats, A. J. S., & Parker, K. H. (2002). Relationship between detrended fluctuation analysis and spectral analysis of heart-rate variability. *Physiological Measurement*, *23*(2), 385.

Winter, D. A. (1991). *Biomechanics and motor control of human gait: normal, elderly and pathological*.

Wittstein, M. W., Day, T. J., Wang, H.-M., Shultz, S. J., Schmitz, R. J., & Rhea, C. K. (n.d.). The association between multi-planar knee joint laxity and dynamic patterns in gait. *Gait & Posture*.

Wittstein, M. W., & Rhea, C. K. (2015). The effect of a gait synchronization task on dynamic characteristics of cardiac and gait rhythms. In *International Society for Posture and Gait Research*. Seville, Spain.

Wittstein, M. W., Starobin, J. M., Haran, F. J., Shultz, S. J., Schmitz, R. J., & Rhea, C. K. (n.d.-a). Gait and cardiac rhythms during treadmill walking.

Wittstein, M. W., Starobin, J. M., Haran, F. J., Shultz, S. J., Schmitz, R. J., & Rhea, C. K. (n.d.-b). Use of order pattern recurrence plots to quantify coupling of two independently observed physiological systems.

Xie, H. B., Zheng, Y. P., Guo, J. Y., & Chen, X. (2010). Cross-fuzzy entropy: A new method to test pattern synchrony of bivariate time series. *Information Sciences*, *180*, 1715–1724. http://doi.org/10.1016/j.ins.2010.01.004

Yentes, J. M., Hunt, N., Schmid, K. K., Kaipust, J. P., McGrath, D., & Stergiou, N. (2013). The appropriate use of approximate entropy and sample entropy with short data sets. *Annals of Biomedical Engineering*, *41*(2), 349–365.

Zbilut, J. P., Koebbe, M., Loeb, H., & Mayer-Kress, G. (1990). Use of recurrence plots in the analysis of heart beat intervals. In *Computers in Cardiology 1990, Proceedings.* (pp. 263–266).

Zbilut, J. P., Thomasson, N., & Webber, Jr., C. L. (2002). Recurrence quantification analysis as a tool for nonlinear exploration of nonstationary cardiac signals. *Medical Engineering & Physics*, *24*(1), 53–60.

Zeni Jr, J. A., Richards, J. G., & Higginson, J. S. (2008). Two simple methods for determining gait events during treadmill and overground walking using kinematic data. *Gait & Posture*, *27*(4), 710–714.

Zhang, J. (2007). Effect of age and sex on heart rate variability in healthy subjects. *Journal of Manipulative and Physiological Therapeutics*, *30*(5), 374–379.

Zhang, T., Yang, Z., & Coote, J. H. (2007). Cross-sample entropy statistic as a measure of complexity and regularity of renal sympathetic nerve activity in the rat. *Experimental Physiology*, *92*(4), 659–669. http://doi.org/10.1113/expphysiol.2007.037150

APPENDIX A

INTAKE QUESTIONS

Intake Questions

All information will be collected and/or recorded electronically using Qualtrics software.

These questions are to screen you for participation in the study, gather basic demographic information, and record a basic health history.

1. What is your sex?

2. What is your date of birth?

3. Do you have any general health problems or illnesses (e.g., diabetes, respiratory disease, concussion, etc.)?

4. Do you have any vestibular (inner ear) or balance disorders?

5. Have you ever been diagnosed with a cardiac condition or disease or have you ever suffered a cardiac event (such as a heart attack)?

6. Have you ever been diagnosed with, or are you currently aware of any neuromuscular or movement dysfunction?

7. Please list any surgeries you have had, including a description and date (approximate if necessary).

8. Are you able to walk at a comfortable pace for 45 minutes without stopping and without assistance?

9. Please list all medications (including dosage) you are currently taking. This includes over the counter medications, vitamins, or supplements that you take regularly, in addition to medication prescribed by a physician.

10. Please list all lower extremity injuries that you have experienced in the last 10 years. List the location of the injury, a description of the injury, and the date the injury occurred (approximate if necessary).

11. Please list any activities you participate in for exercise. Estimate the total number of hours per week you participate in each activity.

12. When was the last time you exercised? What activity were you doing?